

# Synergies in the offshore domain

-a case study of the  
WINWIN concept

Mats Mowinckel Giovannoni

# **Synergies in the offshore domain - a case study of the WINWIN concept**

**Mats Mowinckel Giovannoni**

## **Abstract**

Since the ratification of and commitments made under the COP 21 summit, we have witnessed an increase towards implementing and utilizing renewable technologies in our energy mix. The global cumulative installed wind energy capacity in 2017 surpassed 540 GW, which is an increase of over 173% compared to 2010 levels. At the same time, Solar PV technology has also experienced a significant cost reduction, and the global installed capacity was 500 GW in 2018. Despite rapid development and growth, the overall contribution on the global energy scene is still limited. Fossil fuels still dominates the global energy supply, and are likely to do so in the coming years. This thesis explores the potential upside of considering synergies in the offshore domain, in order to further expand the diffusion of renewable technologies. First, we considered the effects of combining offshore wind technology with wave technology through a quantitative research. Through synergies, several advantages were identified, where the cumulative results could lower the expected LCOE costs of a combined wave- and floating wind farm compared to if these technologies were operated individually. The second research objective considers the feasibility of DNV GL's WINWIN concept. The intention behind the WINWIN concept is that a floating offshore wind turbine autonomously runs and powers the water injection processes required in oil production. Our results show that the WINWIN concept is able to deliver water injection rates in line with industry expectations (<44 000 BBL/day) at a competitive cost estimate, compared to conventional water injection technologies.

## **Disclaimer**

The author re-iterates that the findings and views presented in the thesis are attributed to the author alone and does not necessarily

represents DNV GLs view.

# Contents

<b>List of Figures</b>	<b>7</b>
<b>List of Tables</b>	<b>11</b>
<b>1 Introduction</b>	<b>1</b>
1.1 Introduction	1
1.1.1 DNV GL’s WINWIN concept	5
1.2 Objectives	5
1.2.1 Limitations and assumptions in the thesis.	6
1.2.2 Methodology	7
1.2.3 Report Layout	8
<b>2 Synergies in the offshore domain</b>	<b>9</b>
2.1 Synergies in offshore environment.	9
2.1.1 Wave and wind synergy	10
2.1.2 Electrification of platforms through wind technology	15
2.2 Introduction to the WINWIN concept	17
2.2.1 Description of the WINWIN	17
2.2.2 Advantages with WINWIN	20
2.2.3 Other applications of the WINWIN unit	20
2.2.4 Comparison with the DOT	21
<b>3 Oil companies and Renewables</b>	<b>23</b>
3.1 Oil companies and their renewable energy portfolio	23
3.1.1 Integration of renewables in the value chain.	25
3.2 Introduction to water injection	28
3.3 Water injection today	30
3.3.1 Waterinjection on Ekofisk.	31
3.3.2 Emission from oil and gas production.	32
3.3.3 Concluding remarks	35
<b>4 WINWIN system modeling and technical aspects</b>	<b>37</b>
4.1 Establishing the base case design	37
4.1.1 Modelling considerations	38
4.1.2 Water injection levels	39
4.1.3 Reservoir depth and water depth	39
4.1.4 Wind resources	40
4.1.5 Lift pumps	40
4.1.6 Water treatment options	41
4.1.7 Wind Turbine	41

4.1.8	Pumping system . . . . .	42
4.1.9	System curve . . . . .	44
4.2	Technical description of the pump systems . . . . .	45
4.2.1	Pump solution 1 (P1). . . . .	45
4.2.2	Pump solution 2 (P2). . . . .	47
4.2.3	Power requirements of P1 and P2 . . . . .	48
4.3	Reservoir and safe injection levels . . . . .	48
4.4	Methodology for modeling the pump system . . . . .	53
4.4.1	Application of the pump modeling methodology. . . . .	56
4.4.2	Limitations and assumptions . . . . .	59
4.5	Summary . . . . .	59
4.5.1	Flowchart of the modeling process . . . . .	60
<b>5</b>	<b>Site assessment and considerations</b>	<b>63</b>
5.1	Introduction . . . . .	63
5.2	Possible scenario's where WINWIN should be considered . . . . .	64
5.3	Definition of the selection criteria . . . . .	67
5.3.1	Site selection for North Sea . . . . .	67
5.3.2	Site selection for the Gulf of Mexico . . . . .	69
5.3.3	Site Selection for West Africa . . . . .	70
5.3.4	Site selection for Brazil . . . . .	70
5.4	Summary of Site Selection . . . . .	72
<b>6</b>	<b>WINWIN Performance results</b>	<b>75</b>
6.1	A guide to the results presented. . . . .	75
6.2	North Sea . . . . .	77
6.2.1	Wind conditions . . . . .	77
6.2.2	Injection performance for North sea location . . . . .	77
6.3	Brazil . . . . .	79
6.3.1	Wind conditions in Brazil . . . . .	79
6.3.2	Injection performance for Brazil location . . . . .	79
6.4	GoM. . . . .	81
6.4.1	Wind conditions in GoM. . . . .	81
6.4.2	Injection performance for GoM location . . . . .	81
6.5	West Africa . . . . .	83
6.5.1	Wind conditions in West Africa. . . . .	83
6.5.2	WIN-WIN performance in West-Africa . . . . .	83
6.6	Analysis of the WINWIN performance results . . . . .	85
6.7	Sensitivity analysis on performance-major repair. . . . .	86
<b>7</b>	<b>Economic analysis and preliminary design.</b>	<b>89</b>
7.1	Background . . . . .	89
7.2	LC-Method. . . . .	89
7.2.1	Discount Rate. . . . .	90
7.2.2	Assumptions and specifications . . . . .	91

7.3	Capex Breakdown and choice of technology . . . . .	91
7.3.1	Choice of Substructure . . . . .	91
7.3.2	Cost of substructure . . . . .	92
7.3.3	Mooring lines . . . . .	93
7.3.4	Anchors . . . . .	95
7.3.5	Rotor,turbine and tower. . . . .	96
7.3.6	Pump systems and auxiliaries . . . . .	96
7.3.7	Battery and electrical infrastructure . . . . .	97
7.3.8	Control Systems . . . . .	98
7.3.9	Injection Well and riser . . . . .	98
7.3.10	Development cost. . . . .	99
7.3.11	Installation and assembly. . . . .	99
7.3.12	Summary Of CAPEX . . . . .	102
7.4	Operation and maintenance . . . . .	103
7.4.1	Sea states . . . . .	103
7.4.2	Maintenance philosophy . . . . .	104
7.4.3	Scheduled maintenance. . . . .	104
7.4.4	Unscheduled maintenance . . . . .	105
7.4.5	Summary of O&M expenses for WINWIN unit . . . . .	106
7.4.6	Decommissioning of WINWIN. . . . .	107
7.5	Summary and results of the economic analysis. . . . .	107
7.5.1	Sensitivity analysis. . . . .	108
7.6	Alternative solution with gas turbines . . . . .	109
7.7	Topside alternative: . . . . .	110
7.7.1	Pump capacity and cost. . . . .	110
7.7.2	Fuel and emission costs. . . . .	110
7.7.3	Calculation methodology . . . . .	111
7.7.4	Results Topside. . . . .	111
7.8	Subsea Solution . . . . .	112
7.9	Retrofit case . . . . .	113
<b>8</b>	<b>Conclusion and reflection</b>	<b>115</b>
8.1	Objective 1. . . . .	115
8.2	Objective 2. . . . .	116
8.2.1	Objective 3. . . . .	117
8.3	Future Work. . . . .	118
<b>A</b>	<b>Appendix A</b>	<b>119</b>
A.1	Intermezzo-Consideration when applying the affinity laws . . . . .	121
A.2	Hall-plot equations constants . . . . .	124
<b>B</b>	<b>Appendix B</b>	<b>125</b>
B.1	WIN WIN performance North Sea, sensitivity analysis . . . . .	126
B.2	Brazil. . . . .	129
B.3	GoM. . . . .	132
B.4	West- Africa . . . . .	135
	References. . . . .	138



# List of Figures

1.1	Primary energy supply by source (DNV-GL, 2018).	2
1.2	Energy scenarios and corresponding CO <sub>2</sub> emissions (Boxern et al., 2016).	3
1.3	Oil demand by sector (DNV-GL, 2018).	4
2.1	Wind-wave farm	12
2.2	Layout of the Alpha Ventus wind farm and the alternative layout (A-D) of the wave farm (Astariz et al., 2015a). Squares represent the layout of the wave farm and the blue dots represent the wind turbines.	13
2.3	Levelised cost of floating wind, wave and co-located wind wave farm (Clark et al., 2019).	14
2.4	Hywind-Tampen project overview (Equinor, 2018).	16
2.5	Artistic impression of WINWIN concept (DNV GL, 2018).	18
2.6	Overview and schematic working principles of the DOT (Diepeveen, 2004).	21
3.1	Funds allocated to renewable energy by major oil companies (\$ bn) (Vaughan, 2018)	24
3.2	Coalinga oil field and solar thermal tower (BrightSource, 2011)	26
3.3	Comparison of recovered oil with steady rate injection (blue) and intermittent (red) (Sandler et al., 2014)	28
3.4	Schematic overview of waterflooding process (Shah et al., 2010)	29
3.5	Capillary effects (Muggeridge et al., 2014)	29
3.6	Oil production before and after onset of water injection. (NDP, 2018)	32
3.7	Produced water as result of water breakthrough, note that measurements started in 2001. (NDP, 2018)	32
3.8	Global CO <sub>2</sub> emissions from Oil and Gas production (IOGP, 2017)	33
3.9	Energy usage per tonne production (IOGP, 2017)	34
3.10	Ekofisk oil production data and related emissions per unit (Gavenas et al., 2015)	35
4.1	Representation of the WINWIN concept. The floating turbine is located above the water injection well. The wind generates power to drive the systems on board, and the pumps are responsible for injecting water into the reservoir.	41
4.2	Power curve for the 6 MW wind turbine.	42
4.3	A comparative overview of centrifugal pumps against positive displacement pumps (Petersen and Jacoby, 2007).	43

4.4	Required pump head plotted against flow rate for the WINWIN system, from equation 4.2. . . . .	46
4.5	Operational envelope of pump solution 1 and the system head curve. Operational envelope is provided by pump manufacturer. . . . .	47
4.6	Operational envelopes for the pumps described and system curve for the WINWIN system. Operational envelope is provided by pump manufacturer. . . . .	48
4.7	Power requirements for P1 and P2 at full capacity obtained from pumps data sheet. . . . .	49
4.8	Hall Plot representation and fault detection modes (IHS Inc., 2014) .	51
4.9	Predicted bottom-hole pressure plotted against barrels injected according to equation 4.8. . . . .	52
4.10	Example of a variable speed pump curve system and system curve, please note that GPM stands for Gallons per minute (1 GPM= 0,23 $m^3/h$ ) (C. Edmondson et al., 2016). . . . .	54
4.11	Typical representation of the required pump power, rotational speed, and flow (Zhang et al., 2012). . . . .	54
4.12	Relationship between the dimensionless pump speed $\lambda$ and flow of pump (Equation 4.19). . . . .	55
4.13	Flow power relationship for a variable speed drive pump, curve derived from equation 4.21. . . . .	56
4.14	Power requirements and operation range of the two pump systems, P1 and P2 based upon variables presented in table 4.7 applied in equation 4.22. . . . .	58
4.15	Flowchart for WINWIN performance modeling. . . . .	61
5.1	Njord A being assisted to shore by towing vessel KL Sandefjord (Equinor, 2016) . . . . .	65
5.2	Schematic overview of oil field Maria (Molde, 2015) . . . . .	66
5.3	Chosen location for WINWIN case study . . . . .	68
5.4	Significant oil and gas activity in immediate location (Norsk Petroleum, 2018) . . . . .	68
5.5	Overview over oil and gas fields in GoM. Yellow markers indicate fields in water depths below 1000 feet, and red markers indicate fields in waters more than 1000 feet (Nixon et al., 2016). . . . .	69
5.6	Wind resource data over the US offshore domain at 100 meters (NREL, 2018). . . . .	70
5.7	Chosen location for WINWIN case study . . . . .	70
5.8	Hydrocarbon production overview . . . . .	71
5.9	Site selection for West Africa. . . . .	71
5.10	Overview of the Campos basin with location and associated field names (Offshore Technology, 2018) . . . . .	73
6.1	Monthly average wind speed . . . . .	77
6.2	WIN-WIN performance with P1 configuration for North Sea site. . . . .	78
6.3	WIN-WIN performance with P2 configuration for North Sea site. . . . .	78

6.4	Brazil wind speed . . . . .	79
6.5	WIN-WIN performance with P1 configuration for Brazil site. . . . .	80
6.6	WIN-WIN performance with P2 configuration for Brazil site. . . . .	80
6.7	Mean wind speed GoM . . . . .	81
6.8	WIN-WIN performance with P1 configuration for GoM site. . . . .	82
6.9	WIN-WIN performance with P2 configuration for GoM site. . . . .	82
6.10	Mean wind speed in West Africa on a monthly basis . . . . .	83
6.11	WIN-WIN performance with P1 configuration for West-Africa site. . . . .	84
6.12	WIN-WIN performance with P2 configuration for West-Africa site. . . . .	84
7.1	Cost of capital as a percentage share of LCOE (Hundleby, 2016) . . . . .	91
7.2	Mooring costs predictions as a function of water depth, where the price per ton is 2000€(Campanile et al., 2018). . . . .	95
7.3	Proposed Gant chart of assembly line process for the WINWIN unit. . . . .	100
7.4	Mating of the tower-nacelle assembly with floating substructure (Håkonsen, 2017). Day rate for Saipem 7000 is around 630k€ (Bjørheim, 2015) . . . . .	101
7.5	Levelized cost per injected barrel . . . . .	108
7.6	Sensitivity analysis of the WINWIN unit . . . . .	109
7.7	Cost of subsea and topside solution . . . . .	113
A.1	Available water injection pumps found in the market today. For the topside water injection solution, the head (mlc) at a pipe-length of 15000 meters was found to be approximately 3800 meters. If the flow rate are kept constant at 331 $m^3/hr$ we are outside the operational envelope of the pump. . . . .	120
A.2	Figure depicts how wrongful use of the affinity curves underestimates pump performance. Adapted from Carlson (2000) . . . . .	123
A.3	The correct way of applying the affinity laws. Adapted version from Carlson (2000) . . . . .	123
B.1	WIN-WIN performance 3 hr operational strategy with P1 system . . . . .	127
B.2	WIN-WIN performance 3 hr operational strategy with P2 system . . . . .	127
B.3	WIN-WIN performance 8 hr operational strategy with P1 system . . . . .	128
B.4	WIN-WIN performance 8 hr operational strategy with P2 system . . . . .	128
B.5	WIN-WIN performance 3 hr operational strategy with P1 system . . . . .	130
B.6	WIN-WIN performance 3 hr operational strategy with P2 system . . . . .	130
B.7	WIN-WIN performance 8 hr operational strategy with P1 system . . . . .	131
B.8	WIN-WIN performance 8 hr operational strategy with P2 system . . . . .	131
B.9	WIN-WIN performance 3 hr operational strategy with P1 system, GoM . . . . .	133
B.10	WIN-WIN performance 3 hr operational strategy with P2 system . . . . .	133
B.11	WIN-WIN performance 8 hr operational strategy with P1 system, GoM . . . . .	134
B.12	WIN-WIN performance 8 hr operational strategy with P2 system, GoM . . . . .	134
B.13	WIN-WIN performance 3 hr operational strategy with P1 system, West Africa . . . . .	136

---

B.14 WIN-WIN performance 3 hr operational strategy with P2 system, West Africa . . . . .	136
B.15 WIN-WIN performance 8 hr operational strategy with P1 system, West Africa . . . . .	137
B.16 WIN-WIN performance 8 hr operational strategy with P2 system, West Africa . . . . .	137

# List of Tables

2.1	Fuel and emissions savings due to the integration of wind power as reported in Korpås et al. (2012).	16
3.1	Classification of how major oil companies include renewable energy in it's portfolio (Zhong and Bazilian, 2018)	25
3.2	Enhanced oil recovery methods and oil requirements (Taber et al., 1997)	30
3.3	Emissions by source for the Norwegian Shelf (Norwegian Petroleum Directorate, 2018)	34
4.1	Overview of the largest oilfields discovered in the North Sea, and corresponding water production rates.	40
4.2	Relevant K values for WINWIN case study. Adapted from (Johnson, 1998).	45
4.3	Original reservoir pressure for Snorre and Ekofisk	49
4.4	System curve in figure 4.4 represented by d, e and f coefficients found from data fitting tools.	57
4.5	Coefficient values for the head-flow relationship, as stated in equation 4.13.	57
4.6	Pump power coefficients as referred to in equation 4.15.	57
4.7	Coefficients that yield the final power at flow rate $q$ .	57
4.8	Parameters for base case 1.	60
5.1	Overview of number of platforms and corresponding depths (Bureau of Safety and Environmental Enforcement, 2018)	69
5.2	Overview of selected areas for further analysis of the WINWIN system.	72
6.1	Comparison of P1 and P2 in North Sea location	77
6.2	Comparison of P1 and P2 in Brazil location	79
6.3	Comparison of P1 and P2 in GoM location	81
6.4	Comparison of P1 and P2 in West-Africa location	83
6.5	Summary of performance results and capacity factor of wind turbine.	85
6.6	Modelled sensitivity analysis	87
7.1	Evaluation of floating technology concepts, adapted from IRENA (2016).	92
7.2	Hywind-Scotland 6 MW turbine parameters, water depth 90-120 meters. Please note that mass given represents total mass required. (Equinor, 2015)	93

7.3	Substructure cost estimates . . . . .	93
7.4	Properties of Li-ion and Lead acid batteries. Adapted from IRENA (2017) . . . . .	97
7.5	Comparison of lead acid and Li-ion batteries. . . . .	98
7.6	Expected transportation costs. Day rates include fuel and personnel costs, and are provided by Fairstar NV (2011) . . . . .	100
7.7	Cost estimate for for the assembly process. . . . .	101
7.8	Float out and hook up costs. . . . .	102
7.9	Summary of CAPEX costs. . . . .	102
7.10	Seastate and significant wave height ( $H_s$ ) of the North Atlantic ocean. Adapted from Faltinsen (1990). . . . .	103
7.11	Expected cost for preventive maintenance and the five year scheduled hull and mooring line inspection. . . . .	105
7.12	Reliability and expected downtime due to failure for offshore turbines. Adapted from Faulstich et al. (2010). Pump reliability is found in Shao (2009) . . . . .	105
7.13	Cost breakdown of minor and major failures on a yearly basis. . . . .	106
7.14	Expected yearly cost of operation and maintenance for the WINWIN unit. . . . .	106
7.15	Expected decommissioning costs. Note that the towing by the ATHS vessel takes 2.5 days, half a day is added to accommodate for travel to destination. . . . .	107
7.16	Value of scrap steel. . . . .	107
7.17	Cost of subsea flowline, adapted from OilFieldWiki (2018) . . . . .	110
7.18	Summary of input values. . . . .	111
A.1	Parameters and values used in equation 4.8 . . . . .	124
B.1	Comparison of P1 and P2 in North Sea site, 3 hr operational strategy	126
B.2	Comparison of P1 and P2 in North Sea site, 8 hr operational strategy	126
B.3	Comparison of P1 and P2 in Brazil, 3 hr operational strategy . . . . .	129
B.4	Comparison of P1 and P2 in Brazil, 8 hr operational strategy . . . . .	129
B.5	Comparison of P1 and P2 in GoM, 3 hr operational strategy, GoM . . . . .	132
B.6	Comparison of P1 and P2 in GoM, 8 hr operational strategy . . . . .	132
B.7	Comparison of P1 and P2 in West-Africa, 3 hr operational strategy . . . . .	135
B.8	Comparison of P1 and P2 in West-Africa, 8 hr operational strategy . . . . .	135

# 1

## Introduction

### 1.1. Introduction

Many countries have agreed to limit global greenhouse gas emissions as per the Paris agreement (COP21). Through this effort, signing members are committed to limit the increase in global temperature by 2 °C compared to pre-industrial times. To achieve this, a profound transition must take place. Already, we are witnessing a rapid development and implementation of renewable energy technologies. The global cumulative installed wind energy capacity in 2017 surpassed 539 GW, which is an increase of over 173% compared to 2010 levels (GWEC, 2017). Solar PV technology has also experienced a significant cost reduction, and the global installed capacity was 500 GW in 2018 (IEA, 2018). However, in the global energy picture, the contribution from renewable energy technologies is limited. In fact, energy produced from renewable technologies today only contributes to a few percent of the primary energy supply, where the major contribution comes from fossil fuels (DNV-GL, 2018). Thus, it is likely that the dependency on hydrocarbons will continue in the coming decades.

In figure 1.1, the expected development of the primary energy supply up to the year 2050 is outlined. Here it can be observed that the world's energy demand is predicted to grow towards 2030, before a reduction in demand can be seen. Currently, oil supplies 28% of the energy demand, and this will increase towards 2030 before being surpassed by natural gas (DNV-GL, 2018). Furthermore, it can be seen that despite the active mobilization of renewable energy technologies, the total impact in the global energy supply is marginal. Thus, the global greenhouse gas emissions are expected to grow in line with the growth in hydrocarbon supply towards 2030. The current trajectory is in strong contrast to the recommendations in the recently published IPCC report. In the IPCC report, it is recommended to cut the global GHG emissions with 30-40% compared to 2010 levels to avoid an

increase in temperature of 1.5 °C, and a reduction of 20 % by 2030 to limit the increase to 2 °C (IPCC, 2018). Furthermore, depending on the temperature limit set, society should by 2050 or by 2075 become a net zero emitter to limit the temperature increase to 1.5-2 °C respectively.

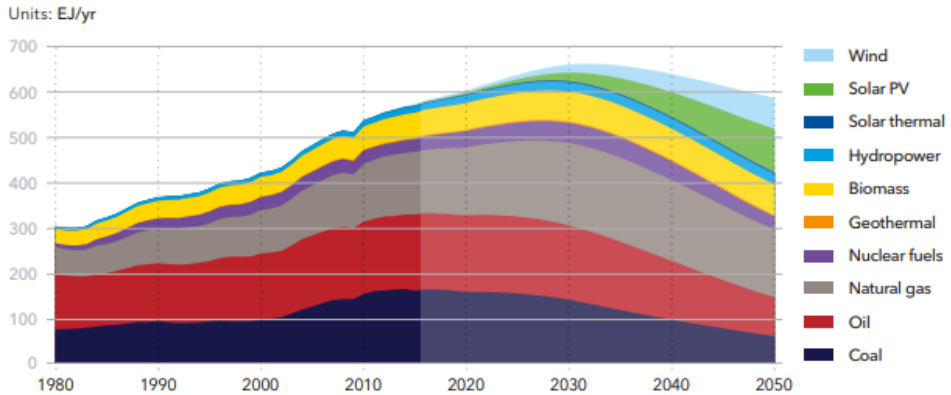


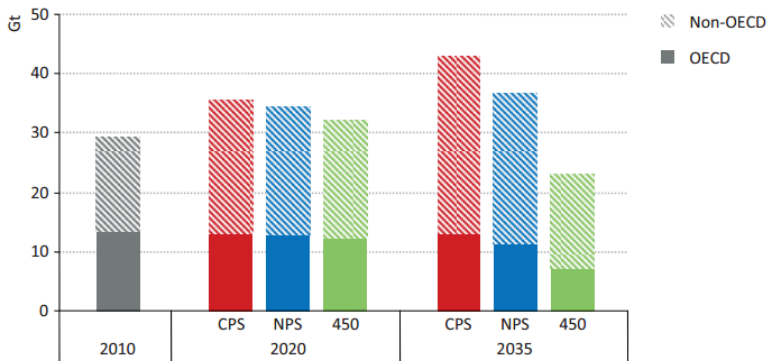
Figure 1.1: Primary energy supply by source (DNV-GL, 2018).

The International Energy Agency (IEA) analyzed the current, expected, and required climate policy scenarios, and coupled them with GHG emissions. The three scenarios are as follows:

- The current policy scenario describes legislative policies and measures that have been implemented as of mid-2017.
- The new policy scenario tries to encompass and account for the political ambitions towards the likely future energy sector. It is important to note that these measures are not yet implemented.
- The 450-scenario is based upon the IPCC conclusion that carbon dioxide concentrations should be limited to 450 parts per million in the atmosphere, to have a 50% chance to prevent the global temperature increase to 2 °C, with reference to pre-industrial levels.

In figure 1.2 we can again conclude that as a society, the targets set in the COP 21 agreement are a far reach. Here we see an expected growth in global CO<sub>2</sub> emissions from 2020 to 2035 for both relevant scenarios, while the 450-scenario dictates a substantial reduction. In other words, the current outlook emphasizes that society would require a shift in trajectory to meet the COP 21 targets.

Without having too much of a pessimistic outlook on the future ahead, the efforts currently being undertaken are relevant and should be further encouraged. Moreover, in the path to becoming a sustainable society, the general focus has been on developing green alternatives, such as wind and solar solutions. Less attention has



Note: NPS = New Policies Scenario; CPS = Current Policies Scenario; 450 = 450 Scenario.

Figure 1.2: Energy scenarios and corresponding CO<sub>2</sub> emissions (Boxem et al., 2016).

been directed towards how we extract and produce hydrocarbons that we rely on now, and also will rely on in the future. If we consider the projected primary energy supply from oil in 2030 given in figure 1.1, the required energy supply from oil will amount to 160 EJ. Assuming a standard energy content in one barrel of oil (bbl), the expected number of barrels of produced oil in 2030 will be 27 billion bbl. The worldwide demand for fossil fuel will continue to grow to meet the expectations of an ever increasing globalization. The future demand for oil is expected to originate from emerging economies, such as China and India (DNV-GL, 2018). The sector wise energy drivers for oil are depicted in figure 1.3; here it is clear that the transportation sector will continue to drive the demand for oil in the next decade, before electrification of the transport sector will reduce the demand gradually. Although the energy requirement, and therefore the energy intensity, will vary depending on how the production occurs, it is reported that the upstream emission intensity is 18.2 kg CO<sub>2</sub>e/bbl on average (Gavenas et al., 2015). Thus, the expected emissions that originate from the worldwide oil production alone amount to 491 Mton of CO<sub>2</sub>e. For comparison, the combined emission from the Netherlands amounted to 195.2 Mton CO<sub>2</sub>e in 2015 (RIVM, 2018). Furthermore, when comparing the emission life cycle of a hydrocarbon, the upstream emission intensity accounts for roughly 10%, whilst the downstream emission makes up the remaining 90% (Gavenas et al., 2015). For clarity, the upstream process concerns the production or uptake of the fossil fuel, whilst the downstream emission relates to when the fossil fuel is combusted, for instance in a car engine. The downstream utilization of fossil has been subjected to technological improvements, where for instance emissions in combustion engines have been reduced. In 1975, the average fuel economy for a conventional vehicle was 18.09 liters per 100 km, while in 2016 the fuel economy per 100 km was 9.41. Consequently the CO<sub>2</sub> emissions have been reduced from 422 gram per kilometer in 1975 to 215 gram per kilometer in 2016 (EPA, 2018). Whats more is the introduction of electric and hybrid vehicles, that allows for an even improved fuel economy. The technological improvements seen downstream is encouraged and

will play an important role in the new low carbon energy society. Nonetheless, little effort towards lowering the climatic footprint has been seen in the upstream process. Furthermore, as oil resources are becoming more inaccessible, the emissions attributable to the upstream process are likely to increase.

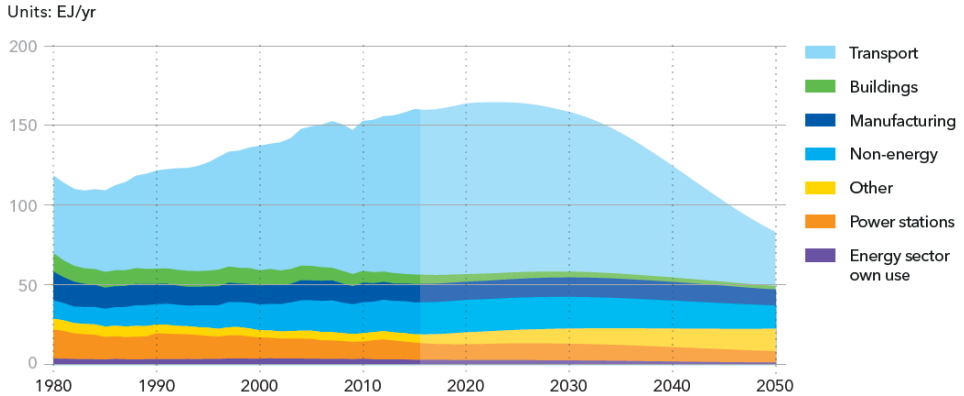


Figure 1.3: Oil demand by sector (DNV-GL, 2018).

As the complete abatement of hydrocarbons still remains a far off ideal, ways of producing and facilitating the upstream oil process must adapt to the emission requirements imposed on our society. A possible solution towards a less emission-intensive production of oil and gas is the integration of renewable technologies in the value chain. With reference to the section above, it is evident that offshore oil and gas platforms utilize and require energy in order to process and extract available resources. Today most platforms are powered through either gas turbines or diesel generators. Offshore wind farms (OFW) can, for example, supply nearby platforms with energy and thereby reduce the emissions created by the platform gas turbines. This requires the participation of both industries, and the benefits from the potential synergy could greatly benefit both. The oil companies will benefit from having a more sustainable produced oil or gas, which in turn will create economic upside in terms of reduced tax on emissions. The wind farm developer could benefit from the experience of working with a partner that has significant experience in offshore operations. Moreover, the wind farm operator would have the possibility to sell excess energy to the platform connected, thus limiting energy curtailment, this however would require a transport cable to the oil platform.

Thus the concept of synergy could be an enabling factor in the coming energy transition. This thesis investigates synergies that can arise in the offshore domain, however the main subject is to conduct a feasibility study of the WINWIN system that is developed by DNV GL and presented in the coming section 1.1.1.

### 1.1.1. DNV GL's WINWIN concept

DNV GL has identified another synergy between the oil industry and the renewable sector. This concept is WINWIN, which stands for wind-powered water injection. The WINWIN unit is based upon a floating offshore wind concept, and is designed to be autonomous. The basic working principle of the WINWIN, relies on a wind turbine that powers a set of water injection pumps, that in turn inject water into an oil reservoir. Briefly explained, the reservoir pressure will be reduced as oil is extracted, so by injecting water in the reservoir, the pressure is maintained, and as such, allows for a prolonged extraction of the oil and an increased recovery factor. Usually, the water injection procedure is facilitated from the host platform, where the gas turbines or diesel generators supply power to the water injection pumps. In certain circumstances, the injection well can be located great distances from the platform, thus requiring additional energy to overcome the friction in the flow-lines. The WINWIN unit is based on a floating substructure, which means that the system can be positioned directly above the injection well, as such minimizing the need for expensive underwater high-pressure flow-lines. Moreover, as the requirement for water injection is not always known before the development of the oil field, it is often found that additional injection might benefit the extraction process at a later stage. As cost and space on an offshore oil rig come at a premium, upgrades to the water injection facility can become expensive. In such cases, the mobility and the stand alone configuration of the WINWIN system might have an advantage over a platform upgrade to facilitate additional water injection.

Compared to conventional solutions, the WINWIN system does not rely on fossil driven generators to produce power. As mentioned, the upstream related emissions are expected to increase due to more inaccessible oil resources, and the need for energy manifests itself as the offshore oil will be located at greater depths, or that the remaining oil in the reservoirs are harder to extract. As such, the WINWIN unit can play an important role to limit the increase of upstream related emissions. Moreover, the WINWIN unit can potentially be an enabling factor for reservoirs previously considered to expensive to further explore.

## 1.2. Objectives

To conclude the introduction, all available literature suggest that oil and gas will remain important energy assets in the coming decades. Amid this, we are witnessing a rapid expansion of renewable energy, and in particular offshore wind in Europe. The question then arises: Can we explore synergies within the two sectors? This thesis will first explore possible synergies in the offshore domain, where we focus on the synergy between wave and wind energy, and also on wind energy and the synergy with oil and gas activities. Furthermore, this thesis investigates the feasibility of the WINWIN concept. To determine its potential it is important to establish the performance of the WINWIN system, and compare it to conventional solutions. As such, we have developed an Excel model that will simulate the yearly performance of the WINWIN system. Finally, a cost analysis of the WINWIN system is

undertaken to compare it to traditional solutions. This thesis also investigates how the major oil companies are incorporating renewable technologies in their value chain. Therefore, the main objectives explored in this thesis can be summarized in the following points:

- Determine the feasibility of the WINWIN system, this shall include a modeling of the injective performance and to perform a cost analysis of the WINWIN concept and benchmark against existing technology.
- What is the potential for successful synergies in the offshore domain for wave and wind energy and the oil industry and wind energy
- How are the major oil companies implementing renewable solutions in their value chain?

The above mentioned points are the main research drivers for this thesis. In order to determine the feasibility, several sub-questions also need to be addressed:

- Develop the main design parameters for the WINWIN system.
- Modelling of the WINWIN performance
- What are the environmental benefits of implementing WINWIN?
- What are suitable locations for WINWIN in Brazil, the Gulf of Mexico, West Africa and the North Sea?
- How has water injection been used in the oil industry up until today.

### 1.2.1. Limitations and assumptions in the thesis

One of the objectives of this thesis is to establish the performance of WINWIN in terms of injection capacity. The WINWIN is an untested idea, where questions regarding the stability of the micro-grid that facilitates the power generated from the wind turbine and the control of the pumps are of particular interest. This is mainly related to the aspect that the injection pumps will be powered by the electricity generated by the wind turbine, and as the output from the wind turbine is fluctuating this will subject the micro-grid for frequency fluctuations and voltage drops that potentially could de-stabilize the system. We assume that the electrical engineering aspect of the WINWIN system is technically feasible, and therefore this aspect is not treated any further in the thesis. Furthermore, the oil and gas industry is notoriously discreet, which means that limited information is found regarding water injection, such as rate or water quality requirements for real reservoirs and platforms. As a result, it is difficult to establish whether the water injection rates are suitable for the chosen reservoirs when analyzing the rates achieved by the WINWIN system. Nonetheless, the research will establish benchmark levels that the WINWIN system is capable of delivering.

### 1.2.2. Methodology

The thesis applies both a qualitative and a quantitative approach. For the objective concerning oil companies and their attitudes towards sustainable energy solutions, a qualitative approach was used. A daily read of relevant news-sources was conducted, primarily in energy-related news outlets, to gather information on the subject. Regarding the WINWIN case study, a more quantitative approach was taken, as we developed a numerical model for the WINWIN performance.

The WINWIN case study was conducted at DNV GL's headquarter in Høvik, Norway, in the period from June to October 2018, in the Renewable Advisory department. The main goal for this thesis is to establish the feasibility of the WINWIN system. It is recognized that the term feasibility may include several aspects, however in this thesis, the feasibility of the WINWIN system refers to two considerations. The first consideration is related to the injection performance of the WINWIN unit i.e. how many barrels will the system be able to inject in to the reservoir, while the second aspect handles the economic performance of the WINWIN system. As such the WINWIN will be compared to conventional technologies for water injection, where the feasibility of WINWIN is determined upon the cost and performance against conventional water injection technologies.

When considering the injection performance, two questions arise: How many barrels will the system be able to inject? How will the injection rates vary from day to day, and from season to season? In order to address these questions, a detailed design of the WINWIN unit must be undertaken before the performance can be modelled. In chapter 4, the key parameters that will have a direct impact on the WINWIN performance are derived. Thus, in the chapter, we establish the offshore wind turbine, the pump systems, and the reservoir specifics, including other parameters that will have an influence on the performance. Furthermore, the modelling of the WINWIN performance was done by using available pump performance diagrams, and modelling corresponding power requirements at given flow rates. This allows a coupling of the power generated from the wind turbine with the output flow of the pumps. A detailed description and outline of the performance modelling is given in chapter 4. In order to add value to the potential business case of the WINWIN system, appropriate locations where oil activity is undertaken were chosen. As such, the wind resources could be assessed to obtain the power output from the wind turbine. The wind data was obtained from the software HOMER, which obtains meteorological data from NASA Surface and Meteorology Database.

As mentioned above, the second feasibility consideration is related to the economic performance of the WINWIN system. This is evaluated by doing a cost analysis of the respective components required by the WINWIN. From the performance assessment, the main components related to the performance were established. However, as the WINWIN system is designed to be a fully autonomous system, situated on a floating structure, a detailed design that includes required components not related to the injection process must also be established. These components

include mooring systems, type of floating structure, maintenance schedules, and installation procedures to name a few. Several other studies have been undertaken to establish the cost of offshore floating wind (see (Myhr et al., 2014)). In the same manner as Myhr et al. (2014), this thesis describes and evaluates the components of the WINWIN system, with the goal of giving a representative cost estimate for each component. Consequently, we are able to predict the overall cost of the WINWIN system. Furthermore, in order to compare the WINWIN system against conventional water injection methods, we establish the cost of two methods that are used for water injection today. The first solution is a so-called topside solution, where the water is injected from the oil platform to the oil reservoir, while the second method is a subsea solution where the pump is located at the seafloor next to the reservoir, and is powered through an umbilical that is connected to the platform. With these methods, we can conclude whether the WINWIN solution is a compatible and competitive option to undertake water injection today.

### 1.2.3. Report Layout

Here follows an overview of the report, and chapters where the different main objectives are discussed. In chapter 2 the synergies between wave and wind are explored. A review of current efforts found in literature with regards to electrification of offshore oil platforms is also found here. Furthermore, the chapter also presents the WINWIN unit. Chapter 3 presents how some major oil firms are adopting renewable energy technologies in their value chain either through integration in value chain or acquiring renewable technology as a stand alone technology. Furthermore, the chapter details the technical aspects concerning water injection and emissions related to oil and gas exploration. Chapter 4 describes the modelling procedure, and the technical aspects associated with the WINWIN unit that is related to the injection procedure. Chapter 5 presents the site assessment work for the WINWIN unit. Chapter 6 presents the WINWIN performance. Chapter 7 presents the cost modelling of the WINWIN unit and the following results. Chapter 8 concludes the thesis, and presents the main findings, reflections, and proposes future work.

# 2

## Synergies in the offshore domain

### 2.1. Synergies in offshore environment

By synergies, we mean the cooperation and/or interaction between stakeholders, a group or on a technology level, across different sectors; as a result, the combined effects are greater than the sum of the two initiatives individually. Although synergies can exist across a wide range of sectors and disciplines, the focus of this thesis is restricted to the offshore energy domain.

The offshore domain has a significant potential for successful synergies. There are several available resources ready for harvesting, such as wind, wave, solar, currents and ocean thermal gradients that are all potential resources for energy harvesting (Esteban and Leary, 2011). However, the widespread utilization of these resources are limited on the global scale predominantly due to a more economic alternative found in the oil and gas resources. These resources could for instance benefit from co-exploitation in the form of a combined wind and wave farm or through integration with existing industries currently operating in the offshore domain. A common denominator for offshore renewable technologies is the necessary cost reduction for large-scale implementation. By combining wave and wind energy, one could see a cost reduction for the combined farm as a result of the synergy, this can be attributed to an enhanced energy yield, a shared operations and administrative scheme that ultimately would result in improved economics and by such lowering the barrier to entry for the widespread implementation of alternative energy sources (Pérez-Collazo et al., 2015, Stoutenberg, 2012). An example of the synergy of renewable sources with other industry sectors in the offshore domain, could be the integrating of offshore wind with the oil industry. Power generation on offshore platforms today are usually undertaken by diesel or gas generators, but with a synergy, nearby wind farms could provide electric power instead. In this scenario, the

wind farm operator has a guaranteed consumer of the energy produced, and the platform has sustainably produced electricity, whilst minimizing fuel costs.

Today the offshore domain serves many different sectors and actors: fisheries, the energy sector, shipping, military, and recreational use. A number of synergies are possible in these different areas. This chapter focuses on the offshore energy sector. Briefly put, the offshore energy sector is comprised of the oil industry and the renewable sector. We consider the synergy of wave and wind, and the integration of offshore wind technology in the oil and gas industry in this thesis.

### 2.1.1. Wave and wind synergy

By 2050, the ocean energy industry - which is comprised of wave and tidal energy - predicts an installed capacity of 188 GW (ICOE, 2010). It is recognized that tidal energy has potential for synergies and further exploitation of the resource, however, the usage of tidal energy devices are restricted to areas where tides are present, often in narrow channels, as such the synergy with offshore wind is limited and is therefore not further treated in this thesis. The offshore wind energy also has ambitious targets towards the future growth in installed capacity: by 2050, an installed capacity of 460 GW is expected (Pérez-Collazo et al., 2015). If these targets are to be realized, a significant cost reduction is required, especially for ocean energy technologies that are yet to experience the implementation as achieved by the offshore wind sector. However, it is believed through an integrated approach, that developers might experience a cost reduction through the synergies that arise on a technological level, but also through legislative synergies (Pérez-Collazo et al., 2015). On a legislative level, Pérez-Collazo et al. (2015) identified the following synergies that follow as a consequence of combining the two technologies.

- A common regulatory framework.
- Maritime spatial planning.
- A simplified licensing procedure.
- Infrastructure planning.

When planning and developing offshore energy projects, there are often uncertainties related to the political ambitions. Thus, a clear and common regulatory framework will facilitate the investment decision; as such, limiting the risks. This is closely linked with the infrastructure planning. Grid connections and facilities are essential for the success of offshore energy technology developments. For instance, the initiative by the Dutch government where the system operator TenneT is responsible for connecting and bringing the energy to shore, will help reduce the barrier to entry. Coordination of maritime spatial planning is required to ensure a sustainable development of the offshore sector. Within the context of combining wave and wind generation, maritime spatial planning could allocate areas where conditions are favorable for the technologies, where the impact on for instance wildlife is identified to be minimal. Lastly, a standardized licensing procedure will greatly benefit

new developers. Regulatory licensing procedures are time-consuming, and in many instances it could be years before the final approval is given. As these technologies are similar (wind and wave), a standardized application procedure could aid further diffusion. Although the mentioned points are also applicable to the development of a specific technology, the realization of an offshore wave-wind farm would require synergy in the administrative processes as outlined above, to incentivise the development of a combined wind-wave farm. Otherwise the administrative tasks would take to long.

On a technological level, the synergy effects of combining a wind and wave farm are perhaps more clear. [Stoutenberg \(2012\)](#) investigated the technological synergies that arise when developing a wave-wind farm. The findings are itemized below:

- Reduced grid integration requirements for variable renewables.
- Reduced offshore transmission infrastructure capacity.
- Increased renewable energy yield per area of ocean space.
- Design and operating synergies.

The combined output of the farm will increase as the wind-wave farm can exploit the wind and wave resources available. The power density of a typical offshore wind farm is assumed to be  $3 \text{ W/m}^2$ , and for a wave energy converter, a capacity of  $6 \text{ kW/m}$  can be expected ([MacKay, 2007](#)). For demonstration purposes, we assume a combined wind-wave single array farm with dimensions  $1000 \text{ m} \times 360 \text{ m}$ . As a rule of thumb, the wind turbine spacing perpendicular to prevailing wind direction should be between 3-5 of the rotor diameter of the wind turbine, hence a width of 360 meters, with a turbine diameter of 90 m ([d'Emil et al., 2001](#)). Furthermore, it is also assumed that 360 m is sufficient spacing for installing the wave energy converter without compromising the turbine accessibility. The total area of the farm is then  $360\,000 \text{ m}^2$ , and assuming the energy density provided by [MacKay \(2007\)](#), we find a combined power density of  $18.6 \text{ W/m}^2$ . The imaginary wind wave farm is depicted in figure 2.1. Although this is a very simplified demonstration of the increase in energy density, and many considerations must be accounted for, such as prevailing wave direction or the resulting wave interaction with the offshore turbines, it is still likely that the combined farm will yield a higher energy output.

A more academic approach where the effects of the of a co-located wind-wave farm was performed by [Astariz et al. \(2015a\)](#). Unlike the case briefly outlined above, where an integrated wave-wind farm was described, [Astariz et al. \(2015a\)](#) explored the benefits of a co-located wind and wave farm. A co-located wind-wave farm is where the two energy generating systems are located adjacent to each other as depicted in figure 2.2. The figure depicts the Alpha Ventus Wind farm with different constellations of the potential wave energy farm. The wind farm located in the North Sea, 45 km north of the German Island Borkum. The wind farm has a nameplate capacity of 60 MW and is comprised of 12 wind turbines. The farm was

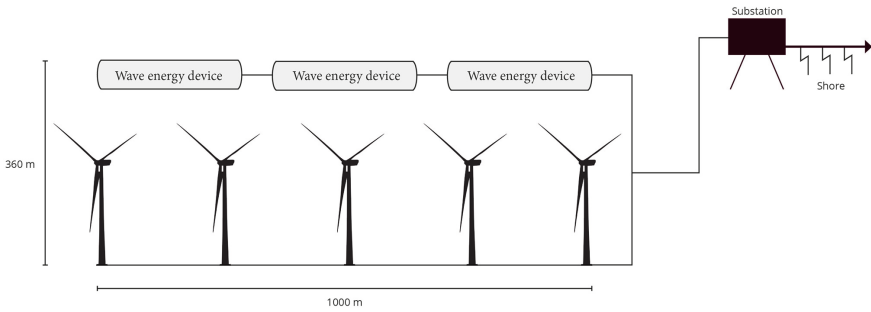


Figure 2.1: Wind-wave farm

first commissioned in 2010. The annual production of the farm was reported to be 224.6 GWh in 2013 (4COffshore, 2015), which results in a capacity factor of 42.6%, a respectable number for an offshore wind farm. Lastly, the wind farm covers an area of  $4 \text{ km}^2$ , which results in a total energy yield per unit area of  $56 \text{ GWh}/\text{m}^2$ . The paper investigated the potential upside of having a co-located wave farm next to the Alpha Ventus wind farm. Four potential layouts of the wave farm were considered as depicted in figure 2.2. The wave energy converter (WECs) utilized was the WaveCat, where each device has a capacity of 1.1 MW. The minimum distance between each WEC was 198, furthermore the number of WECs varied from 28 to 32 depending on the layout. The hydrodynamic parameters, such as local wave conditions, and consequently the energy yield, were numerically modelled through the software SWAN. It was found that the annual yield from the WEC farm resulted in an output of 100-120 GWh, depending on configuration. Alternative B, with reference to figure 2.2, had the highest production. On the other hand, alternative C yielded the poorest performance. This is simply because alternative C had fewer WECs installed. The combined energy yield per unit area, and as such also accounting for the area utilized by the wave farm, led to an increase in output of 4.4-7.3% with respect to the stand alone wind farm. This implies a better utilization of space.

It can also be assumed that the project costs are reduced per installed kW. In a synergy project, the developers might cooperate in the administrative area, such as developing and permitting tasks. Furthermore, necessary infrastructure, such as transmission cables and offshore substations that are major cost components in offshore energy projects, can be shared. The synergy may also benefit from shared operational and maintenance costs. Scheduled maintenance can be undertaken within the same window, and as such share personnel and vessel costs. Even though the maintenance and procedures might require different skill sets, this can be facilitated through common learning. Furthermore, Astariz et al. (2015b) estimated that the levelised cost of offshore wind and wave energy to be 165 and 395 €/MWh respectively. Astariz et al. (2015a) concluded that the levelised cost for the co-located wind-wave farm could be in the range of 199-253 €/MWh. While the levelised cost for the co-located wind farm is still above a stand alone wind farm

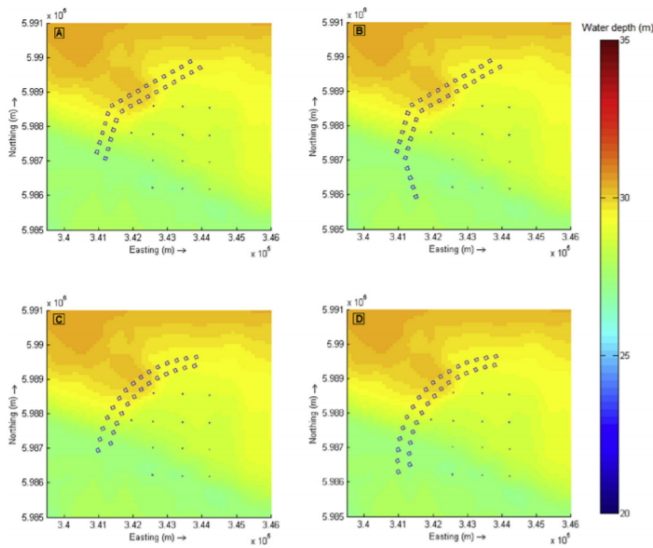


Figure 2.2: Layout of the Alpha Ventus wind farm and the alternative layout (A-D) of the wave farm (Astariz et al., 2015a). Squares represent the layout of the wave farm and the blue dots represent the wind turbines.

that in 2017 was estimated to be 124 €/MWh (IRENA, 2018). As such it is still acknowledged that a stand alone offshore wind farm is per today more cost effective, however with maturing of wave energy technology it is expected that the costs in the future would be competitive to a stand alone offshore wind farm. Furthermore, the levelised cost of a wave-wind farm is below that of a stand alone wave energy farm and as such contributes to the further development of wave energy.

In the above sections the potential upsides of having an integrated wind and wave farm were described. However, the wind farms in the analyses were bottom fixed, which can be considered as a mature and well tested technology. Clark et al. (2019) researched the consequences of having a co-located floating wind and wave farm. Their research shows that the LCOE cost for the integrated floating wind-wave farm was lower than the individual floating wind farm or wave farm. In figure 2.3 the levelised cost of energy (LCOE) of a co-located floating wind-wave farm is compared against the costs of an stand alone floating wind park and wave farm. Here it can be seen that the LCOE of an integrated floating wind-wave farm is expected to be in the range of 660-690 €/MWh compared to 800 €/MWh and 900 €/MWh for a stand alone floating wind or wave farm respectively (an exchange rate of 1€=1.14\$ is assumed). The reason for this is due to better resource utilization per unit area and a shared costing scheme. As such, for two technologies considered at a pre-mature level, there is an economic benefit in considering a synergy farm. Lastly, the levelised cost presented in this sections are not aligned, when comparing the results presented by Clark et al. (2019) and Astariz et al. (2015b), here in particular the costs of

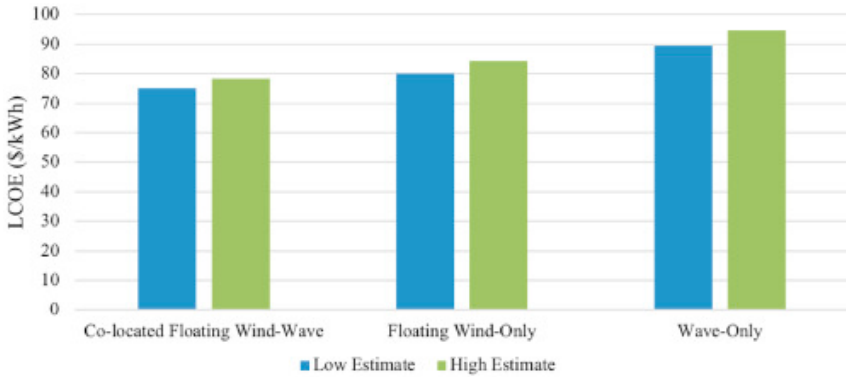


Figure 2.3: Levelised cost of floating wind, wave and co-located wind wave farm (Clark et al., 2019).

a stand alone wave farm is significant. However, the main conclusion from both the research presented implies that the resulting synergy will lead to cost effective solutions. Also, as the wave energy device will limit the impact of waves on the wind turbines, either the floating or the bottom fixed, the system can be further optimized, where possibly a reduction of sea loads can be considered, which in turn will reduce material costs of the monopolies or the floating sub-structures.

The wind resources vary greatly, and as the power output of a wind turbine is related to the cubed of the wind speed, power output can change dramatically over a short period of time. These rapid fluctuations impose stress in the power stability system, which in turn require a costly system balancing infrastructure (Astariz and Iglesias, 2017). By introducing a secondary energy converter device, the stability and predictability therefore increase. Depending on the degree of correlation between wind and wave resources, the variability of the farm is reduced, and the energy output is increased. The degree of correlation will impact this number. A case study that assessed the synergy between the Alpha Ventus wind park with theoretical integrated wave energy, estimated a reduction in downtime of 87 %, and an increase in the capacity factor of 6 % (Astariz and Iglesias, 2017). This, in turn, can reflect the estimation of the park's transmission capabilities. The potential revenue stream from where 100 % of the capacity of the farm could be transported, is evaluated against the associated costs of the electrical cabling required for transporting the energy produced at 100 % capacity. Briefly explained, what is the optimized size of the electrical cable to be installed compared to the marginal revenue streams generated? Stoutenberg (2012) predicted that for a 1000MW wave-wind park with equal installed capacity, transmission requirements could be reduced with 8%, compared to a separate park.

### 2.1.2. Electrification of platforms through wind technology

Electrification of the oil and gas industry, particularly in the North Sea, has been in the interest of regulators (and the industry itself) for a long time. With the realization and expansion of the offshore wind market, several studies have looked into the possible synergy with the aforementioned industries. In fact, the first platform supplied with energy produced from offshore wind turbines was the Beatrice Alpha platform located off the north coast of Scotland. The project also known as the *Beatrice Talisman Demonstrator* consisted of two 5 MW turbines, and was at the time of commissioning, Britain's first deep-water wind project (Bradbury, 2007). The two turbines provided 30 % of the total energy demand of the platform (HIenergy, nd). Most recently, Equinor announced the Hywind-Tampen project. Equinor has decided to explore the possibilities of integrating 88 MW of floating offshore wind capacity to Snorre and Gullfaks as outlined in figure 2.4. It is assumed that the offshore wind farm will account for 35 % of the annual power demand for the combined platforms. Furthermore, Equinor assumes a combined reduction of 200,000 tonnes CO<sub>2</sub> on a yearly basis (Equinor, 2018). In monetary terms, this translates into 4.13 M€ in avoided CO<sub>2</sub> taxations (current CO<sub>2</sub> price: 20.6 €/t (Offshore Energy Today, 2018c)). Besides, savings associated with fuels for gas turbines add to the total economic picture. However, investing in offshore wind requires extensive capital. Publicly available figures assume an installed cost of 4.1 M€/MW (IRENA, 2018). For the Hywind-Tampen project, it is assumed that costs incurred will be higher due to the novel application of floating wind turbines and the subsequent integration with the platforms. Savings can be found as onshore high voltage cables are not required. This typically accounts for 13 % of the total installation costs (IRENA, 2018). Aker BP has also announced interest in the electrification of the offshore installations. The future development of the NOAKA project aims to become the first fully electrified development with zero emissions, which is partly energized by offshore wind (Offshore Energy Today, 2018a).

In the literature researched for this thesis, the main research topics related to the integration of wind power with oil and gas activities are mainly related to two aspects: the potential for a reduction in harmful emissions, and the electrical grid stability. For instance, Korpås et al. (2012) investigated a fictitious platform with a variable load demand ranging from 20 to 35 MW. The power-producing entities included two gas turbines with a total installed capacity of 23 MW, and 20 MW capacity from wind turbines. It was found that the total wind energy penetration accounted for 40 % of the platform's electricity demand. Furthermore, a quasi-steady analysis was initiated in MATLAB to quantify the gas savings compared to the base case where the load is met by the gas turbines alone. Two scenarios were simulated: in the first scenario, both gas turbines were kept online and served the remaining load not covered by the wind turbines. The second analysis allowed for one of the gas turbines to shut down, given specific requirements. The related fuel and emissions savings found are presented in table 2.1. The reason for the different savings found is due to a better operating condition for the gas turbine. It was found that the efficiency increased from 25.64 to 30.13 % when one of the gas turbines was shut down. However, the effects of switching the gas turbines on



Figure 2.4: Hywind-Tampen project overview (Equinor, 2018).

and off could deteriorate the expected lifetime.

Table 2.1: Fuel and emissions savings due to the integration of wind power as reported in Korpås et al. (2012).

Operating Mode	Fuel[M m3]	CO <sub>2</sub> [1,000 tonnes]	NO <sub>x</sub> [tonnes]
1	18.06	39.72	270.83
2	24.45	53.79	366.76

Regarding grid stability, Wei et al. (2013) analyzed the grid stability when a wind farm is integrated as a power source in combination with gas turbines. Three cases were defined where the stability was evaluated against the integration of a 20, 100 and 1,000 MW installed wind turbine capacity. The analysis implemented in SIMPOW evaluated the following cases, under different operating scenarios:

1. Online start of one large induction motor.
2. Loss of one gas turbine.
3. Loss of all wind turbines.
4. Fluctuations in wind speed.

The electrical grid stability was evaluated against the NORSOK standard where the transient frequency response should not exceed 5 %. The largest deviation in frequency and voltage occurred when a sudden loss of wind power was experienced for the 20 MW case. For this case, the frequency variation of -7.3 % and the voltage

variation of -1.7 to 5.3 % under transient conditions was observed, this is above the standard threshold, it therefore implies a maximum integration of wind energy in a stand-alone offshore electrical grid. However, all other simulated cases were within acceptable limits, and [Wei et al. \(2013\)](#) concluded that all cases are theoretically feasible.

## 2.2. Introduction to the WINWIN concept

The WINWIN unit is a concept developed by DNV GL and their industry partners. The WINWIN concept is based on two fundamental needs in order to develop a sustainable future. It is agreed upon that while an energy transition is occurring, where the world is moving towards more renewable energy, the complete abatement of fossil fuels is not yet an option. Fossil fuels will continue to play a vital role in the world energy mix for years to come, as highlighted in section 1.1. However, the production of fossil fuel can still be more environmentally friendly than it is today. The WINWIN concept utilizes the available power in the wind to power water pumps that consequently inject water into the oil reservoir. Water injection is a fundamental process of oil recovery. When the oil is depleted, the internal pressure of the reservoir will decrease. Without means for compensating for pressure loss, the field will have a low oil recovery factor. Water injection methods thus seek to maintain reservoir pressure to ensure acceptable oil recovery rates. Traditionally, water injection is facilitated on the production platform, where gas generators produce electricity that further drives the injection pumps.

### 2.2.1. Description of the WINWIN

The enabling technology of the WINWIN concept is the realization and commercialization of floating offshore turbines. Offshore floating turbines have gained attention due to several reasons. Fixed offshore wind farms now realize their potential, and consequently, developers must seek more great waters to harvest the energy potential found in the wind. Also, approximately 80 % of the available wind resources are found in oceans and seas with depths greater than 60 meters ([Equinor, 2017](#)). Conventional monopiles are only seen economically feasible up to depths of 40-50 meters. This imposes a natural and needed step towards floating offshore turbines. The gained focus on floating offshore wind parks first commercialized in 2017 where Hywind Scotland, a 30 MW floating wind park, was put online. Although Hywind is the first prototype to be commercialized, several other prototypes are currently under development.

Figure 2.5 shows an artistic impression of how the WINWIN concept might look when implemented. The WINWIN concept is designed to be fully autonomous with minimal maintenance requirements. Otherwise, the advantage compared to the traditional solution of gas generators would perish. The system must be able to be remotely operated. Furthermore, the WINWIN concept is comprised by a set "off-the-shelf" components, and as such no new technology inventions are required. The assembling of the system on a floating wind turbine has not yet been executed,

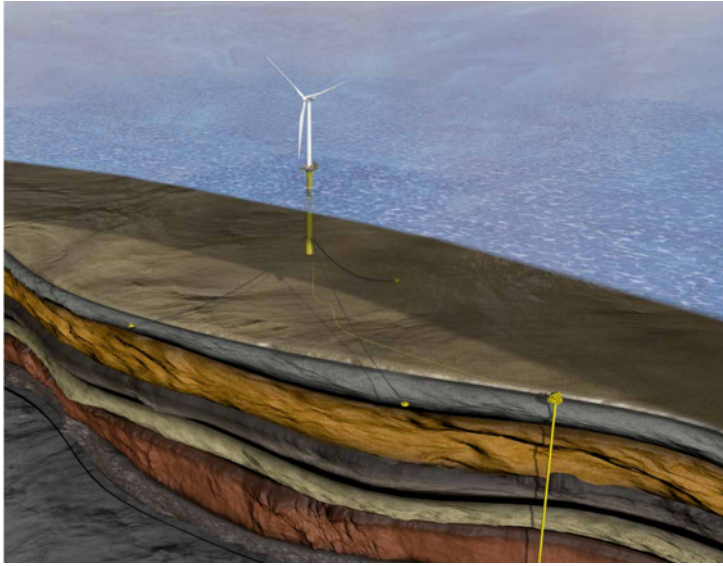


Figure 2.5: Artistic impression of WINWIN concept (DNV GL, 2018).

and the following analysis is therefore, hypothetical. Also demonstrated in the figure is the close proximity to the injection well. This is an important advantage, as it limits the requirement for underwater piping.

The WINWIN concept is made up of the following components, all integrated on a floating wind turbine:

- Wind turbine and tower.
- Water injection pumps.
- Water filtration units.
- Chemical injection pump
- Chemical storage tank
- Lift pumps.
- Battery pack.

**Windturbine and tower:** Several wind-turbine manufacturers have designed turbines specifically for the maritime domain. The sizing of the turbine must be in accordance with the injection targets of the reservoir. During the case study presented in chapter 4, a 6 MW turbine is selected.

**Water injection pumps:** The pump requirements are given by the field operator and reservoir characteristics (i.e., pressure and injection targets). The sizing

of pumps must be put into the case-specific requirement of the field. The pumps should also tolerate marine conditions and the intermittency nature of the power supplied from the turbine. In general, for pumping water, either fixed displacements or variable displacement pumps are used.

**Battery:** The WINWIN unit is designed for autonomy in remote areas and as such requires a designated energy storage system to ensure that all systems are supplied with sufficient energy when the wind is not blowing. Please note that the injection process is only facilitated by the wind turbine, and no injection is powered from the battery, the battery should therefore maintain the readiness of the system. Also, as the WINWIN unit operates in the maritime environment, communication and lights must be enabled to ensure the safety of maritime traffic. Furthermore, the energy storage must be designed to keep systems such as pumps on standby over periods of prolonged time when there is no electricity generated from the wind. In addition, the battery pack must tolerate severe weather conditions and have limited self-discharge. A more elaborate description of the battery is presented in section [7.3.7](#).

**Lift pumps:** Lift pumps are required to transport the seawater from sea-level to the platform deck before the injection pumps take over the water handling procedure. The lifting capacity should, of course, be equivalent to the required capacity of the water injection pumps. Furthermore, the lift pumps should be equipped with a coarse filter to prevent any uptake of debris or organic material. The pumps should be equipped with backwashing capabilities to clean the filters.

**Chemical storage:** Depending on reservoir requirements, the water may be susceptible to different treatment processes, such as sulphate removal or de-oxygenation. Other examples might be the need for biocides, that will prevent bacterial growth and are added in the water before the injection occurs. All the chemicals or treatment equipment are integrated in the WINWIN unit, if the reservoir requires this.

**System redundancy:** Due to the remote operation of the WINWIN unit, any component failure could lead to a substantial downtime of the unit. A level of redundancy should be built in the system. The degree of redundancy should be determined by the case specific design.

**Control system:** An intricate part of the WINWIN concept is the control system. The control system must continuously evaluate and execute depending on several factors and inputs. During start-up, i.e., when the turbine can provide sufficient power, it must implement the correct start-up protocol as well as closing the system down during low wind periods. Furthermore, the control system should ensure safe operation of all situations that the WINWIN unit might encounter.

### 2.2.2. Advantages with WINWIN

It is believed that the WINWIN system provides many advantages compared to current means of water injection. The most prominent factor is the inherent flexibility the floating unit provides. The flexibility allows for allocation of the WINWIN unit in immediate proximity to the injection well. Furthermore, as the oil reservoir is depleted over time, it might be found reasonable to develop and drill for new and alternative injection wells to further increase the oil recovery. Before the development of the WINWIN concept, this decision had several constraints. Firstly, does the platform have sufficient generating capacity in order to provide the required injection targets? Is the distance of the new injection well within an acceptable distance from the host platform? Ultimately the decision of whether to implement an oil recovery scheme further is determined in accordance based on economic factors, i.e., will the net present value of implementing the new recovery scheme be positive? The introduction of WINWIN could add greater confidence regarding the investment decision, and should be considered a potential candidate if additional water injection is required. Furthermore, the WINWIN concept could potentially become a real alternative when the oil platform would require an upgrade to facilitate new water injection, platform upgrades are typically very expensive, this is further treated in section 5.2. Also, as the WINWIN unit does not emit any emissions during operation - as such, it is not susceptible to CO<sub>2</sub> taxation - operational saving could be found. Operators in the Norwegian continental shelf are for instance required to pay 50 €/tonnes CO<sub>2</sub> emitted [Norwegian Petroleum Directorate \(2018\)](#).

### 2.2.3. Other applications of the WINWIN unit

The application of the WINWIN unit within the oil and gas industry is not limited to water injection purposes (as demonstrated in the above case), although this is the designed purpose. In a broader context the WINWIN unit is applicable in all cases where an intermittent power supply can complete the job requirement, however it should be noted that WINWIN refers to the scenario where water injection is undertaken- as such we refer to a floating wind turbine unit. For instance, a floating wind turbine unit can be used to generate power or to produce water for living quarters offshore. The floating wind turbine unit can be fitted with an reverse osmosis plant to turn freshwater out of seawater. This is, of course, not only applicable to offshore living quarters, but describes a case where an intermittent power supply, such as the WINWIN unit, can be an interesting idea.

In recent years, significant attention has been given to H<sub>2</sub> as a future energy carrier. By many, H<sub>2</sub> is regarded as an integral part of the energy transition. H<sub>2</sub> can be stored and later converted to useful energy. The WINWIN concept can be adapted to accommodate for the production of H<sub>2</sub>. A possible future scenario where production of H<sub>2</sub> is undertaken on a floating wind turbine could materialize if hydrogen gains momentum as a fuel for the transportation sector. A thought scenario would for instance be, a WINWIN unit where the pumping system is replaced with an electrolyzer and a storage unit, that will function as a fueling station for the maritime traffic. The floating offshore wind turbine could be placed along shipping lanes

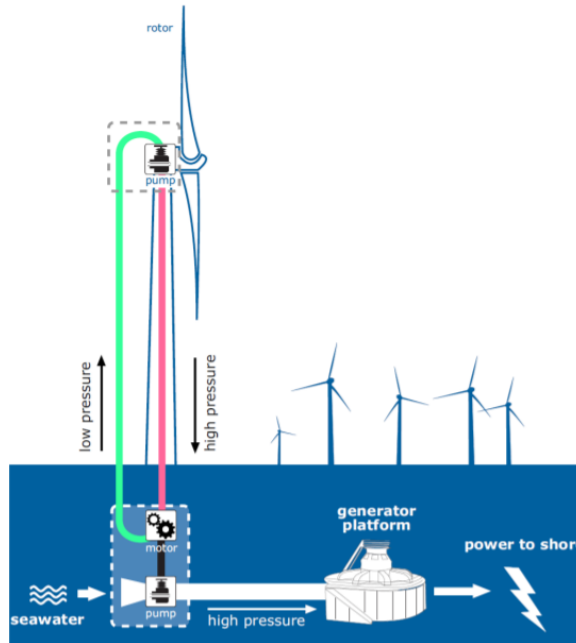


Figure 2.6: Overview and schematic working principles of the DOT (Diepeveen, 2004)

where H2 bunkering could be facilitated.

#### 2.2.4. Comparison with the DOT

The Delft offshore wind turbine (DOT) is a novel method of utilizing the kinetic energy in the wind. The DOT is a result of a research initiative at the University where a thought experiment was conducted. The aim was to redesign the turbine from scratch. How would the turbine look? Also, how could cost in the offshore wind industry be reduced? The DOT is stripped of the conventional generator and gearbox assembly found in wind turbines. Instead, the DOT relies on a closed-loop hydraulic system that is pressurized by the turbine before the hydraulic energy is converted into rotational energy that drives a pump. The pump consequently pressurizes the seawater up to desired pressure, before the water is injected on a Francis turbine that produces electrical power. Although the DOT is still on a conceptual level, researchers have highlighted potential benefits of the concept (S. Kempenaar et al., 2011). First, the nacelle weight is expected to be reduced, due to the abatement of gearbox and generator, and replaced by a hydraulic pump. Reducing the weight of the nacelle simplifies the installation procedures; this then translates into less installation spending. This is mainly due to less heavy lifting requirements and the avoided need for generators and gearboxes. Furthermore, from a structural design perspective, less steel is required; this also translates into less required capital.

Some researchers also believe that the limit regarding size for offshore wind tur-

bines is approaching. Eventually, the current solutions will reach their limits in terms of what is possible on an engineering basis. Therefore the industry must adopt new solutions to satisfy the expected growth in the offshore market. With regards to the use of the DOT as a concept for water injection purposes, the DOT offers some clear benefits. The requirements for water injection pumps, lift pumps, and the microgrid are avoided. It is believed that this will reduce costs. However, as for the proposed WINWIN solution, active control of the platform must be possible; as such, the DOT must be able to generate electricity in conjunction with the water-injection process. This should be technically feasible, where one can imagine a separate water piping system that can run a small kW turbine to charge the battery. According to DOT research, the uncertainty is the hydraulic pump situated in the nacelle. As of now, no commercially available pump is available. However, it is expected that this is no technical showstopper. The feasibility as a stand alone concept or to facilitate water injection in an oil reservoir are two interesting concepts to further evaluate, however DOT is not further treated here as the main focus of the thesis revolves around the WINWIN system.

# 3

## Oil companies and Renewables

This section is intended to give an overview of the development of renewable energy from the perspective of the global oil companies, i.e. how are these companies relating to the energy transition, current outlook and historical lessons to internalise. Furthermore this chapter introduces the mechanics behind water injection and the emissions related to oil exploration

### 3.1. Oil companies and their renewable energy portfolio

In the midst of the current energy transition, the major oil companies must diversify their portfolio to ensure a positive bottom line in the future. Albeit the given statement could be slightly exaggerated, the Paris agreement and the required actions to mitigate global warming will nonetheless affect the economies of global oil firms. Anticipated lower demands for hydrocarbons, taxation on emissions and public acceptance are some of the obstacles that oil companies must navigate through. As a response and a measure to ensure future competitiveness and relevance, major oil companies are now allocating funds and research initiatives to for renewable energy ([Hirtenstein, 2017](#)). Shell and Equinor (formerly Statoil) have for instance, located substantive funds in the wind energy sector. Shell has acquired a 20 % stake in the 700 MW Borselle 3 & 4 wind park (Shell sold down from an initial 45 % stake) ([Reuters, 2017](#)), while Statoil has developed their own first floating 30 MW wind farm outside Scotland ([Equinor, 2017](#)). The above mentioned examples are also a demonstration in the strategy and approach towards renewables. Equinor has taken full ownership and responsibility towards the execution, development and installation of the Hywind Scotland project, compared to Shell that that joined a consortium, and does not have the responsibility of the day to day operations,

the project is instead led by Van Oord. Equinor therefore owns the technology developed and has developed internal competence, however at the risk of carrying the economic downside alone. Shell, being a member of the consortium therefore de-risk the potential downside. As described later, a systematic approach is proposed by [Zhong and Bazilian \(2018\)](#) to classify the oil companies approach towards sustainable energy solutions. In figure 3.1 the annual CAPEX for the major oil firms and the proportion spent on clean energy is depicted. Here one can see that considerable amounts are spent on alternative energy solutions. However, this only comprises a small percentage of total annual spending.

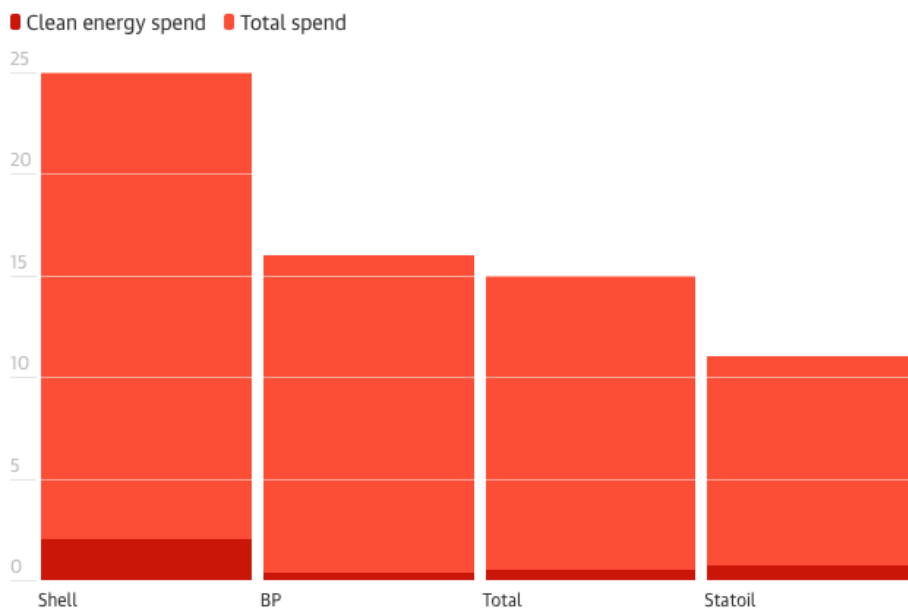


Figure 3.1: Funds allocated to renewable energy by major oil companies (\$ bn) ([Vaughan, 2018](#))

Following the framework put forward by [Chesbrough \(2002\)](#), [Zhong and Bazilian \(2018\)](#) proposed an adapted version of the framework that allows for a systematic and categorized overview of how oil companies are incorporating renewable solutions in their business. Table 3.1 summarizes this adaptation. *Passive* and *Active* are indicators that measure the degree to which the investment diversifies the business operations. Whereas *tight* and *loose* are how well the investments reflect the internal skills and knowledge of the firm. As an example, oil companies that implement alternative sources of energy in their production chain (such as replacing generator capacity with wind energy, solar PV-technology or biofuels to produce oil) are therefore classified as tight incorporations due to their daily interactions with the normal business of the firm, and passive as this does not diversify the business operations. On the other hand, oil companies that use expertise from oil refining processes to produce biofuels (for instance) would be classified as active and tight.

Another example would be Equinor's Hywind Scotland project. Here Equinor has commercialized floating offshore wind and utilized the internal offshore competence of the to realize the project, Hywind and offshore wind is now tightly integrated in the business portfolio of Equinor. Whilst the Shell's involvement in the Borselle windfarm could be classified as tight and passive since Shell is not actively developing the project, however wind energy is closely related to their business portfolio. Lastly, investments and acquisition of stand-alone businesses made through means of venture capitalism are not surprisingly classified as *loose* and *passive*; here, the acquired company have, expertise and technology that might be of interest to the investor, however no incorporation of the technology in core business areas. An example of this would be to acquire a company that develops battery related technology for electric vehicles. An oil company would not typically have any expertise or experience with electric vehicles, but sees this a future area of business. The venture capitalist is therefore able to position themselves in a potentially upcoming market without being exposed to significant risk.

Table 3.1: Classification of how major oil companies include renewable energy in it's portfolio (Zhong and Bazilian, 2018)

Degree of diversifying IOC's commercial business operations	Degree to which renewable solutions are integrated into the business portfolio	
	Tight	Loose
Passive	Integrating in renewables in value chain of oil and gas production	Venture capitalism
Active	Utilize in-house competencies to produce renewable energy	Vertical integration of renewable energy

### 3.1.1. Integration of renewables in the value chain

Renewable integration has recently gained attention by fossil producers. The integration of smart, sustainable solutions may give rise to better economics as well as improving environmental footprint. Moreover, by integrating renewables, the oil companies can develop at their own pace, and make use of internal competence to develop company know-how in an emerging field of energy, and as such, be better positioned for the energy future of tomorrow. Moreover, having a sustainable outlook and forward-thinking company profile is well cherished by media outlets and shareholders. For instance, when Aker BP released their quarterly results for 2018, the company gained media attention for wanting to incorporate wind energy and make the NOAKA field development the first carbon emission-free field on the NCS (AkerBP, 2018). Aker BP also received significant media attention in international news (Offshore Energy Today, 2018b). Additionally, company stocks increased with 8 % in the following days (Bloomberg, 2018). The increased value cannot be solely awarded to the awareness generated by the news when it reported that the integration of an offshore wind farm would supply energy to the platform. However, it demonstrates that market and media outlets respond positively to sustainable solutions, both in terms of increased share prices and positive media attention.

Through the research conducted by [Zhong and Bazilian \(2018\)](#), they identified the use of solar thermal technology as the most commonly adopted integration of renewables in the production line; although, only two such synergies were identified. Solar thermal technology is used to replace natural gas that is used to heat up the steam before it is injected into the reservoir. The steam generated reduces the viscosity of the oil, and as such makes it more accessible ([Kovscek, 2012](#)). This is an alternative to water injection and is also categorized as an enhanced oil recovery technique (EOR). Unlike the study of this thesis case scenario, solar thermal has been developed and field tested. Solar thermal recovery was first applied to the oil field Coalinga. Due to the accumulation of heavy crude oil, extraction required enhanced recovery techniques([Chevron, 2011](#)). Chevron partnered with BrightSource, a solar thermal plant developer, to deliver the thermal solar plant. The project consisted of over 7600 mirrors spread over an area of  $0.4 \text{ km}^2$ , with a thermal capacity of 29 MW ([BrightSource, 2011](#)). The success of the project is also unknown. However, [Zhong and Bazilian \(2018\)](#) indicated that BrightSource took a loss of 40.2 M\$. Chevron has not continued the application of solar thermal recovery. Despite the unknown success of the Coalinga project, EOR has gained attention once more from an oil company through thermal solar - this time, Aera Energy. Aera Energy aims to build an 850 MW thermal solar plant to provide steam and power for the Belridge oilfield. When commissioned in 2020, the integration of renewables in the production chain will offset the field's carbon emissions with 376000 tons  $\text{CO}_2$  ([Mooney, 2011](#)).



Figure 3.2: Coalinga oil field and solar thermal tower ([BrightSource, 2011](#))

The intermittent nature of renewables are giving rise to uncertainties associated with the intended application purpose. This is also the case when solar thermal is applied in oil recovery. Due to the daily and seasonal patterns of the sun, the quality and amount of steam produced will vary. Conventional methods today uti-

lize natural gas for combustion to produce the steam required; the injection rate and stability is therefore, controllable. [Sandler et al. \(2014\)](#) conducted an extensive analysis of the possible integration of the solar thermal oil recovery method with an oil field located in San Joaquin Valley, California. Here they simulated the variable injection rates of steam in the commercial simulator package CMG STARS. The conclusions to be drawn were that the solar thermal enhanced recovery method performs comparably well to the constant rate injection. The cyclic nature of the thermal solar-produced steam does not compromise the overall oil recovery potential, as long as the net yearly injection rates are met. It should be noted that the production of oil is slightly reduced during the winter months. The simulation results are depicted in figure 3.3. The observable lag in oil produced through the solar thermal method can be attributed to the heat loss experienced during low injection of steam, that again results in low oil mobility. Furthermore, the economic evaluation of a 100 % integrated solar thermal plant, suggested a favorable or equal net present value compared to the conventional solutions. The natural gas alternative is subjected to uncertain gas prices, while the solar thermal plant is characterized by high upfront capital investments; as such, the choice of discount factor plays an important role. [Sandler et al. \(2014\)](#) used a discount rate of 10 %, that must be considered conservative in the energy industry. The inverse relationship between discount rate and high CAPEX therefore results in a more favorable net present value for natural gas combustion, when higher discounts rates are applied. The opposite is therefore also true when low discount rates would be applied. To conclude the overall results presented by [Sandler et al. \(2014\)](#), they indicate that there is potential for the further utilization of solar thermal as an enhanced recovery technique; but the likely success of the synergy requires more field studies and conclusions drawn from real-life experiences. Despite the lack of public knowledge of the implantation from the Chevron Coaling project, the industry is pushing forward with the aforementioned 850 MW solar thermal plant in Belridge, and 1 GW plant currently under construction in Oman, that combined, will save the operators and the environment with 676,000 tonnes CO<sub>2</sub> and 291 M m<sup>3</sup> of natural gas ([Helman, 2015](#), [PowerTechnology, 2018](#)).

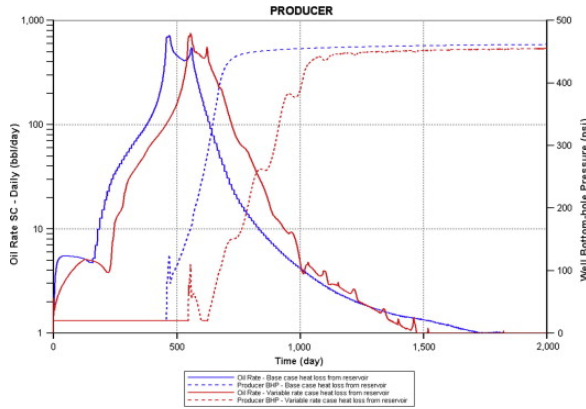


Figure 3.3: Comparison of recovered oil with steady rate injection (blue) and intermittent (red) (Sandler et al., 2014)

### 3.2. Introduction to water injection

As the core function and purpose of the WINWIN concept is enhanced oil recovery (EOR), a brief introduction will be given over oil recovery techniques with emphasis on waterflooding.

When oil is depleted from a reservoir, the internal pressure will drop. In the early stages of production, the internal energy and pressure are sufficient for a satisfactory production rate. General oil terminology distinguishes the three phases of oil production as follows; primary, secondary and tertiary production phases. As mentioned, during the primary phase, the internal reservoir energy allows for oil extraction, normally 5–15% of the oil in place can be extracted. During the second phase water or gas can be injected to compensate for the pressure drop; this will target the remaining oil and an additional 30% approximate increase in the recovery is expected (Petro Industry News, 2018). The tertiary production phase can be undertaken in various ways, i.e. through gas injection, polymer flooding, or steam flooding, with the intention to further improve the oil molecule mobility (Udy et al., 2017). In literature however, the secondary and tertiary phases are commonly interchanged, as water injection in particular is commonly used with polymer flooding. (Alvarado and Manrique, 2010). The final recovery factor (that is: the amount of oil recovered, divided by the available resources) finally depends on several factors; including oil recovery techniques, reservoir geology and the chemical composition of the oil. Some reservoirs are achieving a recovery factor of 70% through water injection Alvarado and Manrique (2010). However, it is estimated that the global recovery factor ranges from 20–40% (Muggeridge et al., 2014). Figure 3.4 simply demonstrates the oil and water interaction.

The factors that determine the oil recovery factor are given through the following relationship (Muggeridge et al., 2014).

$$E_R = E_D * E_V * E_A \quad (3.1)$$

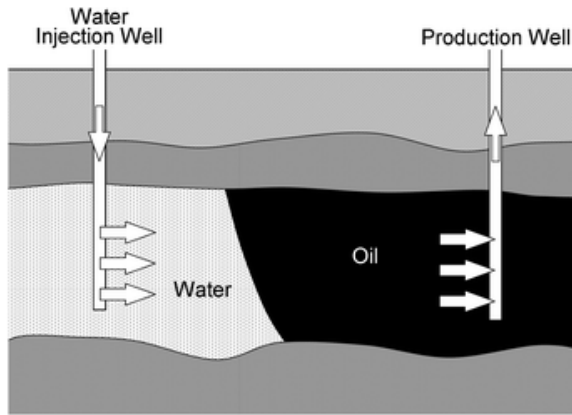


Figure 3.4: Schematic overview of waterflooding process (Shah et al., 2010)

Where  $E_R$  is the total oil recovery factor,  $E_D$  is the fractional amount of oil that is displaced by the water on a microscopic level.  $E_V$  and  $E_A$  are the vertical and area displacement factors respectively. Hence, one can understand that even though respectable factor components are achieved, the overall efficiency  $E_R$  remains low. One of the main factors that characterize the efficiencies above is how well the water displaces the oil; the interaction is heavily dependent on capillary effects as can be seen in figure 3.5. Here, one can observe that the oil is trapped in the rock pores after the onset of waterflooding.

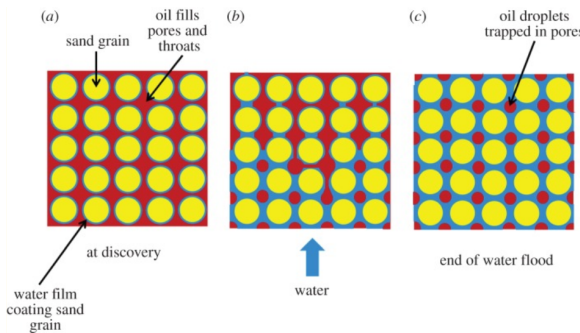


Figure 3.5: Capillary effects (Muggeridge et al., 2014)

Another important parameter is the mobility ratio. The mobility of a fluid is given in equation 3.2.

$$M = \frac{k_r}{\mu} \tag{3.2}$$

Where  $k_r$  is the relative permeability of the fluid in the reservoir and  $\mu$  is the viscosity of the fluid, the mobility ratio  $M$  of the displacing fluid over the displaced fluid can

indicate the flow characteristics. If  $M$  is greater than 1 then the displacing fluid (i.e. water) moves faster than the displaced fluid, and oil is likely to be left behind, as illustrated in figure 3.5. If  $M$  is less than one, the displaced fluid moves faster than the displacement fluid and therefore gives a good efficiency. As the permeability of the reservoir is hard to influence, measures to ensure appropriate mobility are to change the viscosity of the oil through, for instance, thermal heating or increasing the viscosity of the water through i.e polymers.

Table 3.2: Enhanced oil recovery methods and oil requirements (Taber et al., 1997)

EOR Method	Gravity ( $^{\circ}$ API)	Viscosity (mPa-s)	Composition
<b>Gas Injection methods</b>			
Nitrogen and flue gas	35-48	0,2-0,4	High C1-to C7
Hydrocarbon	23-41	0,5-3	High C2-to C7
CO2	22-36	1,5-10	High C2-to C12
Immiscible gases	12	<600	NC
<b>Waterflooding</b>			
Micellar/Polymer, ASP and Alkaline flooding	20-35	13-35	Light intermediate
Polymer Flooding	>12	10-150	NC
<b>Thermal/Mechanical</b>			
Combustion	20-35	1200-5000	NC
Steam	>15	4700-200000	NC

Table 3.2 displays suggested EOR methods for different oil properties. The  $^{\circ}$ API is a measure of the density of oil compared to water, where an  $^{\circ}$ API<10 the oil is heavier than water, and when the  $^{\circ}$ API>10 the oil floats on water. As such, one can understand why the properties of oil dictate the EOR methods; for instance, where the  $^{\circ}$ API is lower than 10, waterflooding becomes unsuitable as the water will float above the oil. Furthermore, the viscosity also influences the procedure, for high viscosity oils, heating is required to increase the mobility of the oil molecule. Of course, several factors should be accounted for when selecting an EOR method, such as reservoir characteristics and economics. However, this is outside the scope of this work.

### 3.3. Water injection today.

In the offshore industry, water injection is predominantly undertaken from the platform. Dedicated generators provide power for the water lift, filtration processes and the delivery of pressurized water to the injection well. The location of the injection pump can either be located on the platform itself or configured as a subsea pump. The injection pressure and injection requirements are reservoir dependent, but typically one would expect pressure >100 bar and injection rates > 2400  $m^3/day$  (Aabø, 2015) (Haugstad, 2018).

After a period of water injection, a breakthrough will occur; that is when the injected water reaches the production well, and the produced oil is, therefore, a mixture of oil and water. This will, in turn, increase the power requirements of the the platform as the water-oil mixture has a higher density compared to oil. Crude oil has a density of 710  $kg/m^3$  at 10°C (EngineeringToolbox, 2017). Another consequence

that might arise is the production of sand. The injected water dissociates the sand within the reservoir and sand oil is produced. In the North Sea, for instance, there is now more production of water than oil from some of the fields and the field operator for the reservoir Gullfaks has decreased their production rates with over 50 % due to sand accumulation (Aabø, 2015). Nonetheless, a rule of thumb for the North Sea dictates that around 7-18 % of the oil be available to recover without any enhanced recovery techniques, with water injection, however, doubling of the production rate is estimated. The field Ekofisk, for instance, had an expected oil recovery factor of 17 % prior to water injection; after water injection, 50 % recovery was achieved (NDP, 2018)

Due to the nature of waterflooding where the sole purpose is to displace the oil towards the production well, the injection must be placed at a sufficient distance from the production well. This implies that the water must in certain circumstances be pumped several kilometers away from the platform at sufficient pressures. This again adds generating capacity to the platform which implies a significant cost to the field developer, and makes the process more environmentally intensive. In addition to the added generating capacity, pressure losses in the pipeline sometimes require additional booster pumps in order to maintain the required water pressure.

### 3.3.1. Waterinjection on Ekofisk

Ekofisk was discovered in 1969 by Phillips Petroleum. The discovery was the starting point for the Norwegian oil adventure, and at the time considered to be the largest reservoir found offshore. Ekofisk covers an area 10x5 km, and initially, the reservoir capacity was estimated to  $546.79 M m^3$  and  $158.95 \times 10^{12} m^3$  in oil and gas respectively. Production was initiated in 1972. Due to the relative low oil recovery achieved, research towards water injection was initiated in 1982, and concluded that water injection would be well suited for the field. Consequently, in 1987 full-scale water injection commenced with an injection capacity of 375,000 barrels of water per day, split over 30 injection wells. From figure 3.6 the effects of waterflooding can be seen. In 1987 the field produced around 70,000 barrels of oil per day, ten years later, 800,000 barrels of water were injected per day and 290,000 barrels of oil were produced (Hermansen et al., 1999). It should also be noted that oil price collapse in 1986 could also - to some extent - manifest the lower quantity produced in the years 1886/87. Moreover, figure 3.7 displays the mentioned occurrence of water breakthrough, implicating that the injected water has now reached the production well and the peak period for oil production is over.

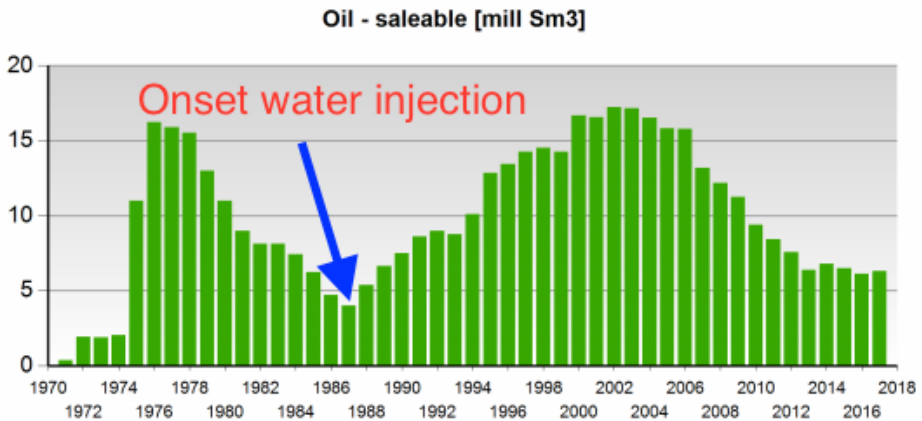


Figure 3.6: Oil production before and after onset of water injection. (NDP, 2018)

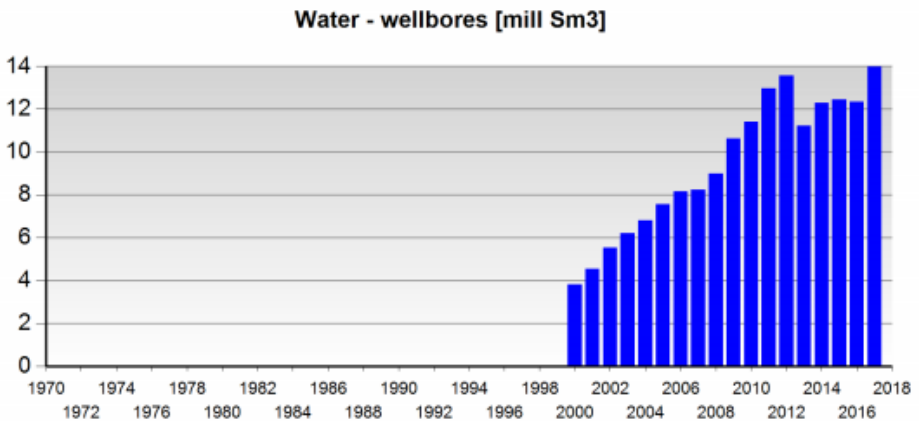


Figure 3.7: Produced water as result of water breakthrough, note that measurements started in 2001. (NDP, 2018)

### 3.3.2. Emission from oil and gas production.

The majority of the greenhouse gas (GHG) emissions associated with fossil fuel occur downstream during combustion. However, roughly 10% of the emissions occur upstream when considering the life cycle of hydrocarbons (Gavenas et al., 2015). Naturally, the means of production influences the relative percentage. Nonetheless, it is clear that emissions related to the production of fossil fuel contribute to a significant amount of global GHG emissions. For oil-producing countries, production can be a dominant source of the nation's GHG emissions; for instance, 20% of the total domestic emissions of Canada originate from oil activities, and for Norway it is even 27 % of the total emissions generated (Gavenas et al., 2015).

Globally, emissions related to the production of oil or gas vary. From figure 3.8 CO<sub>2</sub> emissions related to oil and gas production on a regional basis are highlighted. The global average is 129 kg CO<sub>2</sub>/kg oil. Africa, North America and the Middle East are the outliers at both ends, with emissions ranging from 48-206 kg CO<sub>2</sub> per tonnes oil produced. Although figure 3.8 does not differentiate between offshore and onshore production, it is estimated that 30% of the global oil production occurs offshore (EIA, 2015).

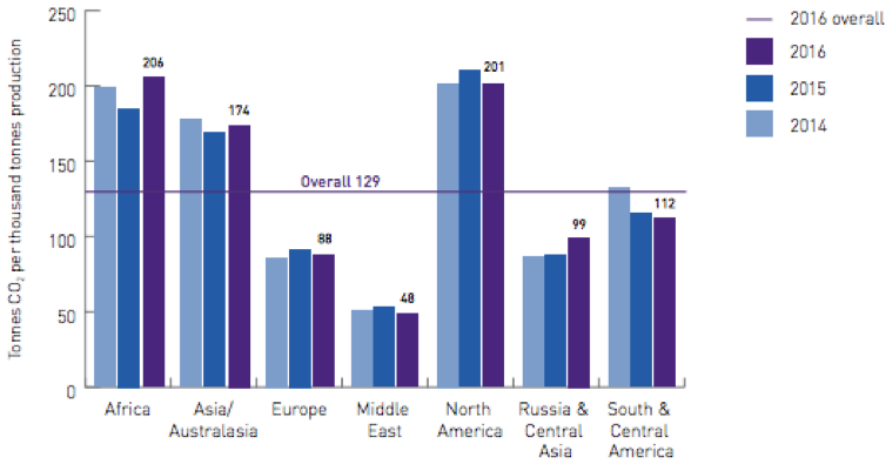


Figure 3.8: Global CO<sub>2</sub> emissions from Oil and Gas production (IOGP, 2017)

Figure 3.9 depicts the global variation in energy intensity associated with the production of oil. The energy intensity of the production of shale oil is well reflected in the statistics for North America. Shale oil production is commonly associated with high energy requirements, due to the relatively higher density of the oil (Gordon, 2012). On the other hand, the Middle East has low energy requirements, this is due to the relative accessibility of the oil (typically light oils). When comparing figure 3.8 and figure 3.9, the energy intensity corresponds well with the related CO<sub>2</sub> emissions as illustrated in figure 3.8. Africa, however, does not follow this trend; this could be due to lenient environmental policy rules with regards to oil production and outdated technology. Europe has ambitious CO<sub>2</sub> targets with the emission trading system that demands energy efficiency, and consequently, one can see a reduction in CO<sub>2</sub> emissions. Also, countries might impose additional CO<sub>2</sub> taxing schemes such as the Norwegian CO<sub>2</sub> tax which dictates an additional surcharge of 50 €/ton CO<sub>2</sub> emitted (Gavenas et al., 2015).

In the paragraphs above we have explained the relationship that relates energy intensity to corresponding emissions. In table 3.3, a breakdown by source of the CO<sub>2</sub> emissions on the Norwegian continental shelf is shown. Here we can see that gas turbines account for 84.6% of the total CO<sub>2</sub> emissions. As gas turbines power conventional water injection, platform operators can reduce their GHG emis-

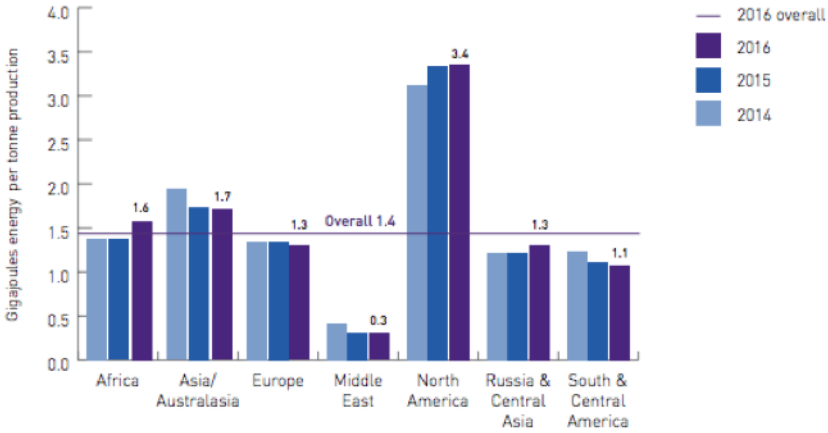


Figure 3.9: Energy usage per tonne production (IOGP, 2017)

sions by implementing the WINWIN solution. However, it must be realized that the power the turbine usage cannot solely be attributed to power the water injection pumps, nonetheless the water injection process requires a significant proportion of the electric power on offshore platforms.

Source	CO2 (in mill. tonnes)	Share (in %)
Boilers	0.2	1.5
Engines	0.75	5.7
Flaring	0.99	7.5
Other sources	0.01	0.1
Turbines	11.16	84.6
Well testing	0.07	0.6

Table 3.3: Emissions by source for the Norwegian Shelf (Norwegian Petroleum Directorate, 2018)

Lastly, the energy requirements (and thus, the related emissions throughout the reservoir's lifetime) are not static. Generally, the energy required to produce oil will increase over its lifetime. In figure 3.10 this relationship is demonstrated. Furthermore, Gavenas et al. (2015) concluded in their research article that a field producing 20 % of peak production has about three times higher the emissions factors.

Having thus established the relationship between the depletion of reservoirs and the corresponding increase in emissions, it is important to realize that the extraction of oil or gas is not a linear process. External factors such as low carbon taxing or high oil prices give the operators incentives to ramp up production through enhanced oil recovery techniques. On the contrary, strong emission taxation will perhaps lower the production incentive, while increasing the focus on more sustainably produced oil. Nonetheless, by implementing the WINWIN unit, the operator can continue oil

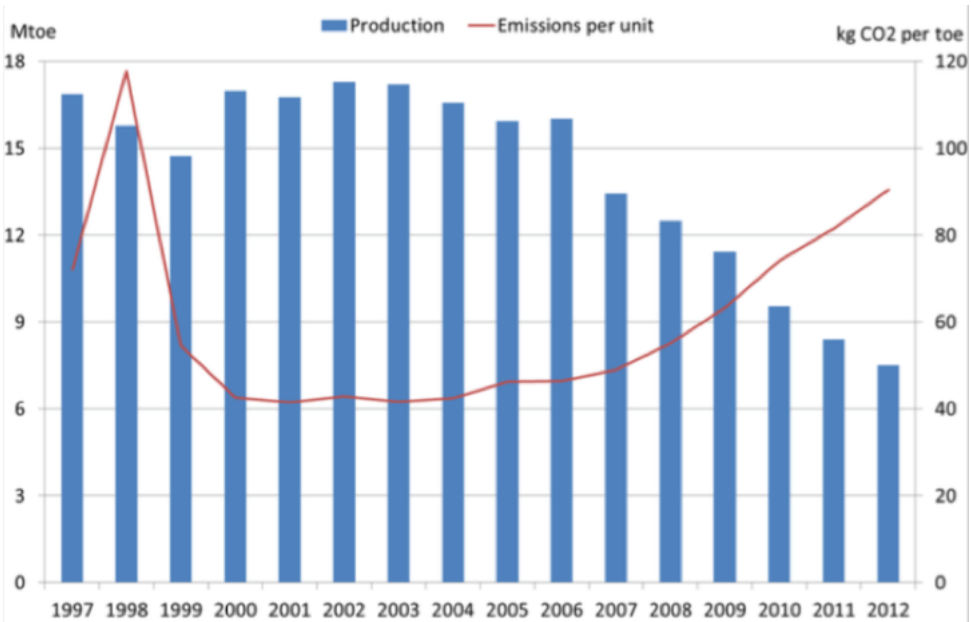


Figure 3.10: Ekofisk oil production data and related emissions per unit (Gavenas et al., 2015)

extraction without increasing emissions.

### 3.3.3. Concluding remarks

This section was intended to give the reader a brief overview of how the hydrocarbon industry is adapting to the energy transition. It was found that the major oil companies do to some extent, incorporate renewable technologies in the production of oil, most notably highlighted in this section, through solar thermal power. As such having tight and passive integration of renewable technology. However, Equinors endeavours into the offshore wind world is a combination of both, where renewables are are thought to be incorporated into the production chain like in the Hywind Tampen case, but also acquiring new business areas through Hywind Scotland wind farm. Shell's approach is different where the step in to the world of renewables is hedged through a consortium. Lastly, the cases presented here are not definitive, oil companies are profit seeking like most business, as such when real business cases are identified, the industry are likely to adapt for the future energy market.

In section 3.3 a high level overview of the current usage of water injection was shown. Furthermore, it was also established the relationship where the depletion of oil reservoirs and the energy requirements that has a increasing relationship, i.e. when the oil reservoir is drying up more energy is required to extract the remanding oil. Thus, in the coming decades where the world will rely on existing and new

discoveries of oil reservoirs will sustain, it is likely to imagine a industry where the emissions will continue to increase, unless smart solutions are adapted to facilitate the oil extraction. The WINWIN unit can be such a technology.

In the next chapter the technical aspects of the WINWIN unit is presented, with the accompanying modeling methodology.

# 4

## WINWIN system modeling and technical aspects

*This chapter concerns the simulation methodology and technical aspects of the WINWIN system. By the technical aspects it is meant the components and parameters relevant to the injective performance of the WINWIN unit, such as injection pumps, wind turbine and wind resources. In chapter 7 we undertake a cost appraisal of the whole WINWIN system that also concerns other components not relevant to the injective performance.*

### 4.1. Establishing the base case design

To perform an analysis of the WINWIN concept in terms of production rate, that is how many barrels of water will the WINWIN unit be able to produce over a year, an understanding of wind turbine performance, reservoir considerations, auxiliary loads and pump design is required. In this thesis and as specified in the objectives of the thesis, the goal is to establish the performance, in this context the performance of the WINWIN system will be measured in terms of barrels of water produced and consequently injected into the reservoir. One barrel of oil is approximately 159 liters. Moreover while it is understood that the performance of the WINWIN unit can include several things such as the electrical grid stability, the performance of the wind turbine on a floating substructure and so forth, it is emphasized that this is not within the scope of the thesis and will not be considered further.

Many parameters will influence the performance outcome, such as water depth, choice of wind turbine, hub height and the type of pump system used. For instance the water depth will influence the required underwater piping which in turn will influence the frictional resistance the pump must overcome which again will influence the size of the pump. As the WINWIN unit is designed to be autonomous the only source of energy will be generated from the wind turbine and will therefore

be responsible to serve the loads required by the system. The wind turbine must be of sufficient size to be able to power the system, and must be dimensioned accordingly. The amount of barrels of water produced is also of relevance, to ensure that the WINWIN system are able to perform on similar terms as the conventional applied technology. Thus, in the coming sections we will establish the base components and parameters that will form the basis of the performance analysis. Lastly it is emphasized that the components and parameters described in this chapter do not make up the whole design of the WINWIN unit, however they will influence the injective performance of the system. In chapter 7 the full WINWIN design is specified. The components and case-specific considerations to be established in order to determine the injective performance of the WINWIN are highlighted in the points below.

## 4

- Required water injection levels.
- Water and reservoir depth.
- Wind resources.
- Lift pumps.
- Water treatment consideration.
- Water injection pumps.

#### 4.1.1. Modelling considerations

Through the nature of modelling real scenarios, several considerations and assumptions have been performed in order to obtain and conduct this analysis. We have also refrained from certain modelling procedures that would further establish the feasibility of the WINWIN system as this was considered to be outside the scope of the thesis. First, as mentioned in the introduction to the thesis, we have assumed that the control system and associated electrical microgrid is capable of controlling and operating the WINWIN in a reliable way. We therefore assume that the electrical engineering is able to safely convert the power generated by the wind turbine, and that the electrical systems are capable of handling and converting the volts and currents, so that the pumps can inject water when power is available from the wind turbine. Furthermore, during the modelling of the WINWIN system, we will not consider how the reservoir is responding to the injection process, and the subsequent rise of pressure within the reservoir. Thus, we assume a constant reservoir pressure. The oil yield as a result from the water injection is also not modelled, as this is highly dependent on the reservoir characteristics, and not within the scope of the thesis. Such modelling procedures would require detailed engineering software packages. The results modelled can however be considered as inputs to a potential oil yield modelling as a consequence of water injection. Lastly, it is emphasized that the components considered in this chapter, are only related to the injection process of the WINWIN system. Other components that make up the overall WINWIN system, such as the floating substructure, mooring lines, maintenance and operations

costs, are worked out in chapter 7 in order to determine the economic cost of the WINWIN system.

#### 4.1.2. Water injection levels

Determining the water injection rate for optimal production is a highly complex procedure due to the dynamic interaction between the reservoir, injection wells, producing wells and capacity at surface (Liu et al., 2012). The injection rates are therefore highly dependent on the reservoir characteristics and must be assessed on an individual basis. Furthermore, required injection rates also vary over reservoir lifetime, where typically injection rates are expected to increase over field maturity. For instance, the Ekofisk's capacity was initially 35000 *bbl/day* before upgrading the capacity to 120000 *bbl/day* in 1992 (OGJ, 1990).

It is desirable to establish typical industry injection rates to compare them against the performance of the WINWIN unit. Available information regarding actual injection rates is difficult to obtain. Nonetheless, the Norwegian petroleum directorate (NDP) monitor the amount of produced water from reservoirs in the North Sea. See table 4.1 for an overview over the five most significant discoveries in the North Sea, and the produced water from the respective fields. The table also indicates the minimum and maximum daily amount of water produced. NDP commenced the yearly monitoring in 2000, and data obtained show how the general trend is increasing year to year with regards to produced water. Although produced water often occurs naturally in oil reservoirs - and therefore can be considered a natural byproduct of oil extraction - produced water is also a result of water injection. That is when the water has displaced the oil towards the producing well and a so-called "water breakthrough" has occurred. As such, table 4.1 can serve as an indication of the possible injection rates undertaken in the North Sea. Thus, under the assumption that produced water can serve as an indication of typical water injection rates found in the industry, table 4.1 demonstrates the different water injection requirements. For instance, the field Ekofisk (the most significant discovery in the North Sea) produces on average 163188 *bbl/day*. Compared to Eldfisk that produces on average 18294 *bbl/day* it is clear that no relationship can be drawn from original reservoir estimate. However, from the five fields listed, a daily average produced water rate can be found to be 78238 *bbl/day*. It is presumed that this amount of water is injected on average, but also facilitated by several injection wells. We can conclude that the WINWIN unit should at least be able to produce more than 20000 *bbl/day* on average to be considered an option compared to alternative solutions. Lastly, no information regarding required pump capacity can be derived from the table as

#### 4.1.3. Reservoir depth and water depth

The reservoir depth and water location will influence the required piping to facilitate the water injection process. The flow-line required will influence the system curve that is elaborated later on in section 4.1.9. From a systematic analysis of 76 oilfields in the North Sea, it was found that the typical reservoir depth varies from 1300m-

Table 4.1: Overview of the largest oilfields discovered in the North Sea, and corresponding water production rates.

Field	Orig. recoverable oil [ $M m^3$ ]	Min [bbl/day]	Max [bbl/day]	Average [bbl/day]
Ekofisk	546,79	67200	241233	163188
Snorre	306,66	105108	182648	137757
Valhall	151,93	3446	11889	8200
Heidrun	196,55	17230	75816	63755
Eldfisk	135,96	3446	36185	18294

4850m. For the base case to be analyzed, that the reservoir is located 2000 meters below sea level, thus total piping required will be 2000 meters

#### 4.1.4. Wind resources

Outlined in section 5.1, the performance of the WINWIN concept will be analyzed in four different locations, all of which have a strong history of oil exploration. The local wind resources are obtained from the software HOMER. HOMER is developed by NREL and allows for an analysis of microgrids. The software sizes accordingly the system based upon the local resources and load requirements. Initially, it was assumed that HOMER would be suitable for the simulation of the WINWIN case, however, due to the inherent system dependency of the WINWIN and only one source of energy, HOMER was not suitable for this scenario. HOMER is designed to evaluate a multi-source energy generating platforms where the level of the renewable penetration suited for the scenario designed can be evaluated. Thus for the purpose of evaluating the WINWIN case where only one source of energy is available HOMER is of little use. Nonetheless, HOMER provides high-quality wind resource data with an hourly time step, based upon the geographical input. Wind data is generated from NASA Surface Meteorology and Solar Energy database, that averages the wind speed over a ten year period (July 1983 - June 1994) (NREL, 2018). The wind data is scaled accordingly to match the specified hub height of the turbine. The HOMER software also provides the turbine power output based upon the power curve.

#### 4.1.5. Lift pumps

The pump system is comprised of two systems, namely the low-pressure system and high-pressure system. The low-pressure system is the seawater lift pumps, and the high-pressure system is the water injection pumps that are responsible for injecting the treated water into the reservoir. The low-pressure system's main requirements are to deliver sufficient capacity to the high-pressure system. Furthermore, the lift pumps must be submerged at sufficient depth in order to avoid intake of unwanted particles and materials that might block the filters. For system redundancy, the system should have two water lift pumps that individually deliver sufficient flow and pressure. It should be noted that the lift pumps will not be treated or modeled any further within the *performance* case study. The assumptions stated are believed to be technically feasible to implement. After inquiring two pump manufacturers, the power requirements at full capacity correspond to approximately 150 kW each, as later described in section 4.2.1 and 4.2.2 the maximum injection capacity of the

injection pumps are 410 and 460  $m^3/hr$ . It is also assumed that the lift pumps can satisfy the suction head requirements imposed by the injection pumps.

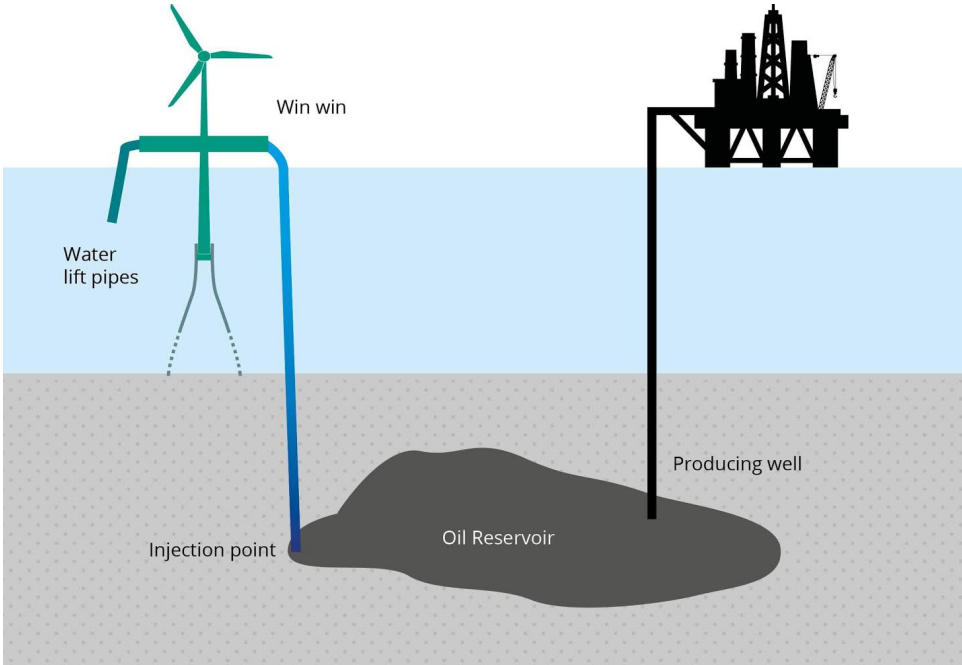


Figure 4.1: Representation of the WINWIN concept. The floating turbine is located above the water injection well. The wind generates power to drive the systems on board, and the pumps are responsible for injecting water into the reservoir.

#### 4.1.6. Water treatment options

Depending on reservoir requirements, the water might be treated, or certain chemicals might be added. For the base case, we assume that only filtration of the water is required. The lift pumps could facilitate the filtration before the water is fed to the injection pumps. Concerning the method of modeling (described in section 4.5) the choice of water treatment options added to the system, would imply less available power that could be directed to operate the pumping system. For the base case we only consider water filtration that is already implemented by the lift pumps.

#### 4.1.7. Wind Turbine

The WINWIN concept philosophy is largely based on "off-the-shelf mentality"; therefore the chosen wind turbine is a 6 MW generic offshore wind turbine. The hub height is assumed to be 100 m above sea-level. This number also includes the free-board provided by the floating substructure. The power output of a turbine

can be estimated through the following equation (NREL, 2014).

$$P = \frac{1}{2} A \rho U^3 C_p \quad (4.1)$$

Where  $A$  is the swept area by the rotor,  $\rho$  is the density,  $U$  is the wind speed, and  $C_p$  is the power coefficient. The power curve is estimated using the available public information from the 6 MW Siemens offshore turbine, such as rotor diameter, and cut in and cut out wind speed. Moreover, the  $C_p$  value was assumed to be 0,45 in the power region (Ragheb, 2014). In the power region, the power curve is estimated through the relationship that  $P$  is proportional to  $U^3$ . In figure 4.2 the power curve is depicted. The cut in wind speed is 3.5 m/s and the cut in wind speed is 25 m/s. The power curve is fed into HOMER, which estimates the resulting power on the hourly basis calculated from the wind conditions. For reference, the wind resources are scaled according to the logarithmic law. Turbine losses are also accounted for, where it is assumed that internal electrical losses and other losses within the system are 3%.

4

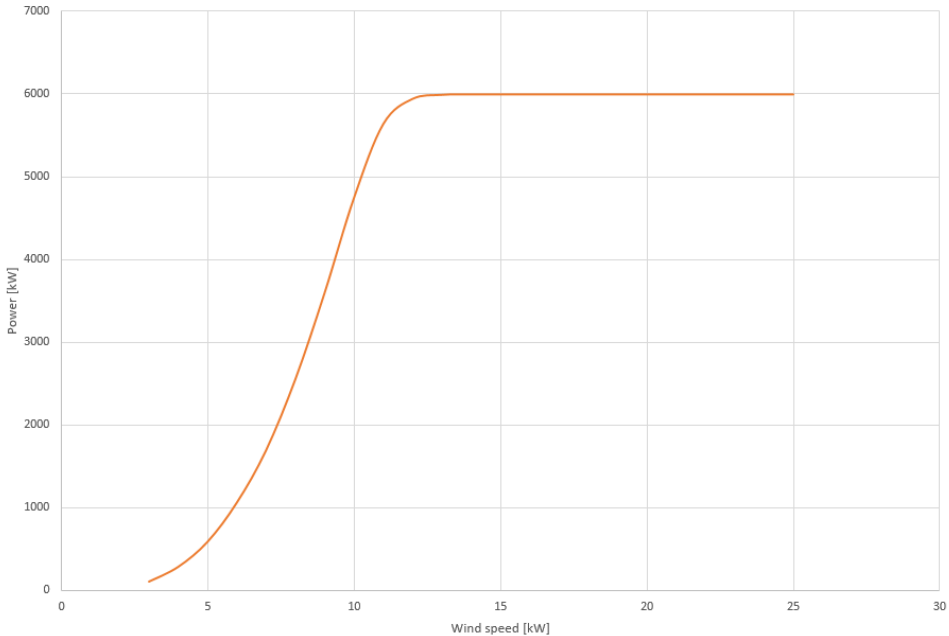


Figure 4.2: Power curve for the 6 MW wind turbine.

#### 4.1.8. Pumping system

In terms of the pumping system two options can be considered, namely centrifugal pumps and positive displacement pumps. Centrifugal pumps impose kinetic energy on the working fluid, as such pressure is generated and the result is flow. Positive

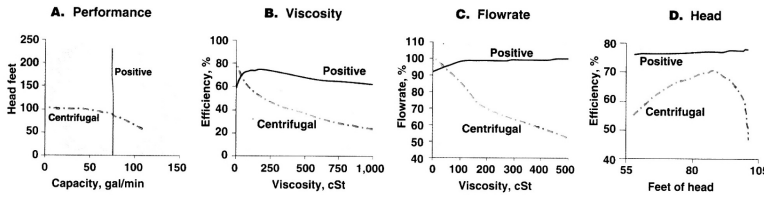


Figure 4.3: A comparative overview of centrifugal pumps against positive displacement pumps (Petersen and Jacoby, 2007).

displacement works by entrapping a confined amount of the fluid and pushes it forward, where flow is imposed and pressure results (Petersen and Jacoby, 2007). Furthermore, Petersen and Jacoby (2007) stated that 70% of the the commercial US pump market were comprised of kinetic types of pumps and the remaining pumps sold were positive displacement pumps. One can therefore assume that the cost of centrifugal pumps are more acceptable, and that the more widespread use of centrifugal pumps dictates confidence in terms of reliability resulting in less downtime. Referring to figure 4.3 differences between main operational differences of centrifugal pumps and positive displacement pumps are depicted. As illustrated centrifugal pumps operates with a varying flow dependent on the head, whilst a positive displacement pump provides a constant flow indifferent of head imposed. Thus careful engineering must be undertaken when positive displacement pumps are installed, as the pump will not self regulate if the pressure becomes to large, and may therefore may lead to damage on equipment unless appropriate safety measures are implemented. Moreover one can see that the positive displacement proves more efficient and more capable of handling liquids containing high viscosity. As the intended medium for working fluid for the WINWIN concept is filtered seawater ( $cP/cSt \approx 1$ ), centrifugal pumps provides a marginal advantage as the efficiency's are higher. However under varying head conditions positive displacement curves exhibits almost constant efficiency, centrifugal pumps however clearly has an best operating point. From an energy efficiency perspective this clearly favors the positive. According to DNV GL experts both pump types can be used. In industry centrifugal types are commonly used for water injection purposes, while positive displacement pumps are well suited for handling varying power inputs such as provided by the wind turbine. Furthermore it is believed that due to the aforementioned reasons above, and referring to the WINWIN design philosophy where simplicity and costs are of concern, the as of now best solution will be to select centrifugal pumps.

Two pump configurations are included in this performance analysis. The first option is to have two identically sized pumps that either can operate in parallel or individually. The second solution consists of two pumps that are differently sized. One small pump that can operate during low power availability, and a larger pump to operate during high wind speeds. In the next section, the system curve is outlined; this will permit an appropriate matching of pumps with system requirements. DNV GL contacted two pump manufacturers that all have a reputable experience in the

oil and gas industry, to provide pump solutions based upon the given criteria. The pump manufacturers are kept anonymous throughout the report; however, size, capacity, and pump performance diagrams are shown.

#### 4.1.9. System curve

The analysis of the pump system is crucial when appropriate pumps are to be selected. The pump must be designed to overcome the system requirement in order to achieve satisfactory performance in terms of target flow rate and pressure. In order to model flow in piping systems, the adopted Bernoulli equation (in conjunction with the equation of continuity) is used.

$$\Delta H_{system} = \Delta Z + \frac{\Delta P}{\rho g} + \Delta H_{major losses} + \Delta H_{minor losses} \quad (4.2)$$

Here  $\Delta H_{system}$  stands for the required *head* that must be accounted for by the pump system.  $\Delta Z$  is the elevation difference,  $\Delta P$  is the pressure difference. The major and minor losses are associated with the head losses experienced in the system due to friction losses, and the physical layout of the system - such as pipe bends, risers and valves - can be found through the following equations

$$\Delta H_{major losses} = f \frac{L}{D} \frac{V^2}{2g} \quad (4.3)$$

Where  $L$  and  $D$  represent the length and the diameter of the piping system, and  $f$  is the Darcy-Weisbach friction factor. Although the friction factor  $f$  is a function of Reynolds number and the duct surface roughness  $\epsilon$ , Churchill developed an empirical equation to deduce the friction factor under varying flow conditions. Note that the equation only applies to turbulent flow conditions (Johnson, 1998). For laminar flow conditions ( $Re < 4000$ ) the friction factor is given as  $f = \frac{64}{Re}$ . The Churchill equation is given as

$$f = 8 \left[ \left( \frac{8}{Re} \right)^{12} + \frac{1}{(B + C)^{1.5}} \right]^{\frac{1}{12}} \quad (4.4)$$

Where B and C is given as

$$B = \left( 2.457 \ln \frac{1}{\left( \frac{7}{Re} \right)^{0.9} + \left( \frac{0.27\epsilon}{D} \right)} \right)^{16} \quad (4.5)$$

$$C = \left( \frac{37530}{Re} \right)^{16} \quad (4.6)$$

Where  $\epsilon$  is the surface roughness of the pipe material. Typical roughness for various materials is easily available from manufacturers' data sheets. Lastly, minor losses

Fitting	Loss Coefficient K
Well roundend inlet	0,05
Sudden expansion ( $D_1/D_2=0,5$ )	0,5
90 degree bend	1,4
Outlet	1
45 degree elbow	0,35
Foot valve	0,8

Table 4.2: Relevant K values for WINWIN case study. Adapted from (Johnson, 1998).

can be found through the following relationship

$$\Delta H_{\text{minor losses}} = \sum K \frac{V^2}{2g} \quad (4.7)$$

4

Where  $K$  is the loss coefficient that depends on the system configuration.  $K$  values are typically tabulated and are based on losses associated with pipe bends, valves and pipe couplings to name but a few. Estimating the loss coefficient for the purpose of this case study is therefore an uncertain task, as a correct layout of the piping configuration (including number and types of valves) is unknown. For the purpose of this exercise, the loss coefficient  $K$  is estimated to be 5. In table 4.2, relevant K values for the case study are shown. The dominant friction losses are associated with the major friction losses due to the high L/D ratio. Furthermore, the pressure difference  $\Delta P$  is assumed to be 200 bar, which is equivalent of 2038 m head. It is assumed that the water lift pumps deliver the fluid at the suction side at conditions similar to atmospheric pressure. The hydrodynamic pressure caused by the elevation difference between the pump and point of injection, works in favour of the pump system. The  $\Delta Z$  is 2000 m. The system curve is visualized in figure 4.4. Having established the pump head requirements at given flow rates, appropriate pumps can be found.

## 4.2. Technical description of the pump systems

This section presents the technical performance of the two pump systems considered for the WINWIN unit. As previously mentioned, the two pump solutions presented in the following sections were proposed to DNV GL by two reputable pump manufacturers based upon the generic reservoir pressure of 200 bar and depth below sea level of 2000 meters and a target injection level between 20000 to 80000 bbl/day.

### 4.2.1. Pump solution 1 (P1)

The first pump solution is comprised of two identical sized variable speed centrifugal pumps, that either can operate singly or in parallel. When the wind turbine is operating close to its rated capacity, the two pumps can operate in parallel to increase the injection rate. In figure 4.5, the operational envelope of the pump system is depicted together with the system curve, the operational envelope is

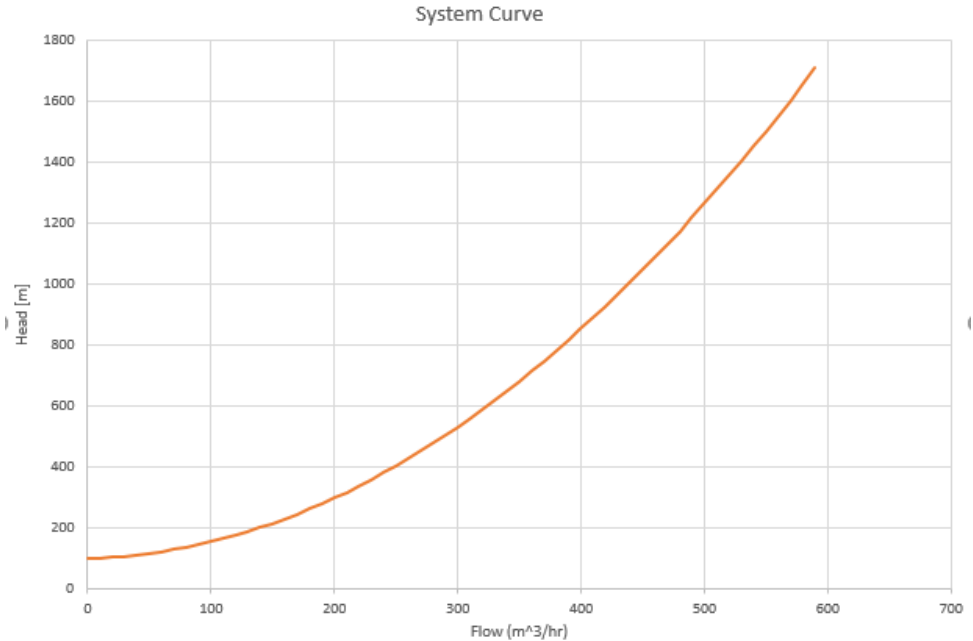


Figure 4.4: Required pump head plotted against flow rate for the WINWIN system, from equation 4.2.

provided by the manufacturer. The lower operating limit for the individual pump is approximately 500-460 m head with capacity  $100 \text{ m}^3/\text{hr}$  to  $250 \text{ m}^3/\text{hr}$ . At full rotational speed, the pump delivers a head of 1350-1180 m with a corresponding flow of 200 to  $400 \text{ m}^3/\text{hr}$ . When the pumps operate in parallel, the lower boundary yields a head range from 480-390 m with a flow rate of 200 to  $460 \text{ m}^3/\text{hr}$ . The upper operational range of the combined pumps can deliver flow at a head range of 1350-1180 m with a flow rate of 390 to  $460 \text{ m}^3/\text{hr}$ . These boundaries make up the design envelope of the pumps. However, the system curve and where it intersects the pump head curve dictates the operating point of the system. Here it can be seen that the maximum output we can obtain from the pump is approximately  $475 \text{ m}^3/\text{hr}$  at a corresponding head of 1700 m. It can also be observed that the system curve does not intersect the operational envelope of pumps before a flow rate of  $240 \text{ m}^3/\text{hr}$ . This does not necessarily imply that the pumps will not operate below this. For instance, by alternating the system curve, also known as throttling, the system curve will be shifted up. This can be achieved by closing the discharge valve. However, in the modeling of the pumps we assume the flow rates considered above, so the pump will start injecting with a flow rate of  $240 \text{ m}^3/\text{hr}$  and with an upper limit of  $480 \text{ m}^3/\text{hr}$ . The resulting output will, therefore, be a conservative estimate.

The benefits of having two identical pumps manifest themselves with regards to maintenance. For two identical pumps, spare parts can be shared. In addition, ex-

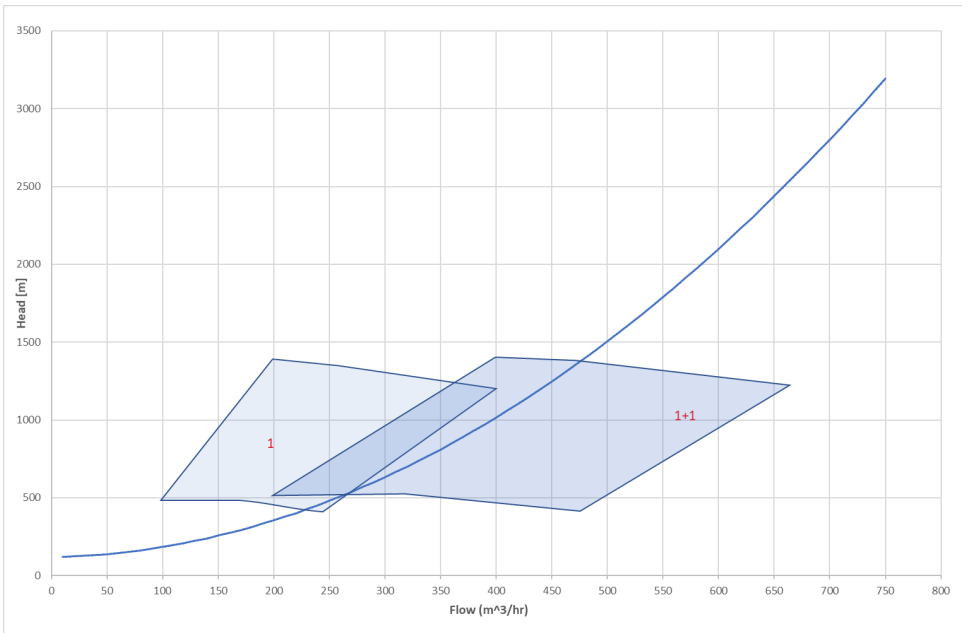


Figure 4.5: Operational envelope of pump solution 1 and the system head curve. Operational envelope is provided by pump manufacturer.

pected scheduled maintenance is identical, which is an advantage compared to two differently sized pumps that might have different maintenance schedules. However, the pumps might suffer in low wind conditions, and as a consequence, they might have a smaller operating window compared to a differently sized pump system.

#### 4.2.2. Pump solution 2 (P2)

The second pump solution consists of two differently sized pumps. Their design envelope is depicted in figure 4.6 provided by the pump manufacturer. The larger pump covers the upper operating region while the smaller pump operates when limited power is available. The pumps are not configured to operate in parallel. A control algorithm that matches the available power with the best fitted pump decides which pump to operate. From figure 4.6 one can see that the two pumps have overlapping regions, where both can cover the target injection rate. The control algorithm should be able to establish the most energy-efficient pump at the available power, provided by the turbine at any time. It can be seen in the figure that the smaller pump has a lower operating head of 480-270 m at a flow rate of 80-280  $m^3/hr$ . The upper boundary yields a head of 1020-850 m. With a flow rate range of 130-410  $m^3/hr$ . The operational conditions for the larger pump yields a head of 500-400 m, and a flow rate of 140-390  $m^3/hr$  for the lower boundary. While for the upper region the pump can handle a head 1490 to 1180 m with a corresponding flow of 245-625  $m^3/hr$ . As mentioned above, the system curve will

dictate the operational points of the pumps. From figure 4.6 the system curve intersects the design envelope of the pump at a flow rate of  $210 \text{ m}^3/\text{hr}$ , and in the intersect the design envelope of pump two at a flow rate of  $460 \text{ m}^3/\text{hr}$ .

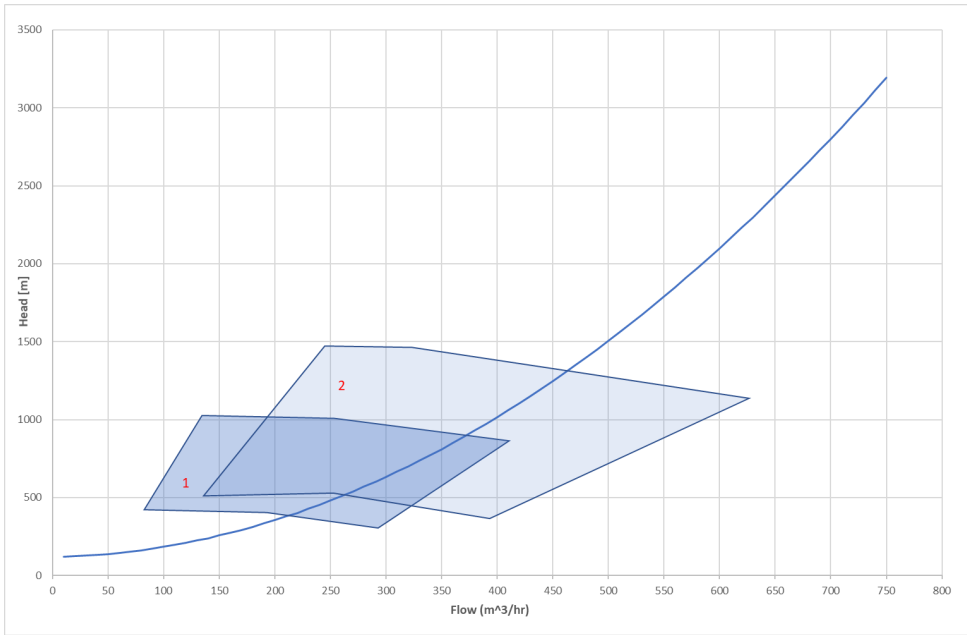


Figure 4.6: Operational envelopes for the pumps described and system curve for the WINWIN system. Operational envelope is provided by pump manufacturer.

The solution proposed covers a sizeable operational area, especially when limited power is available. Furthermore, having overlapping boundaries might result in unwanted "flickering" mode of operation, where the two pumps are shut down or started up within a short period, causing unstable operations of the pump and unnecessary wear and tear. To avoid this, a robust control algorithm is required.

#### 4.2.3. Power requirements of P1 and P2

In the above section we presented the pump solutions P1 and P2 with their respective design envelope. Other relevant information would be the power consumption of the pumps proposed. This information was provided by the pump manufacturer. In figure 4.7 we see the pump power requirements for P1 and P2 at full capacity, which corresponds to the upper operating range of the pumps.

### 4.3. Reservoir and safe injection levels

Up until now the the chapter has been concerned with the parameters and components of the WINWIN system, limited attention has been given to the implications caused by the reservoir. After all, WINWIN does not inject into a vacuum. For

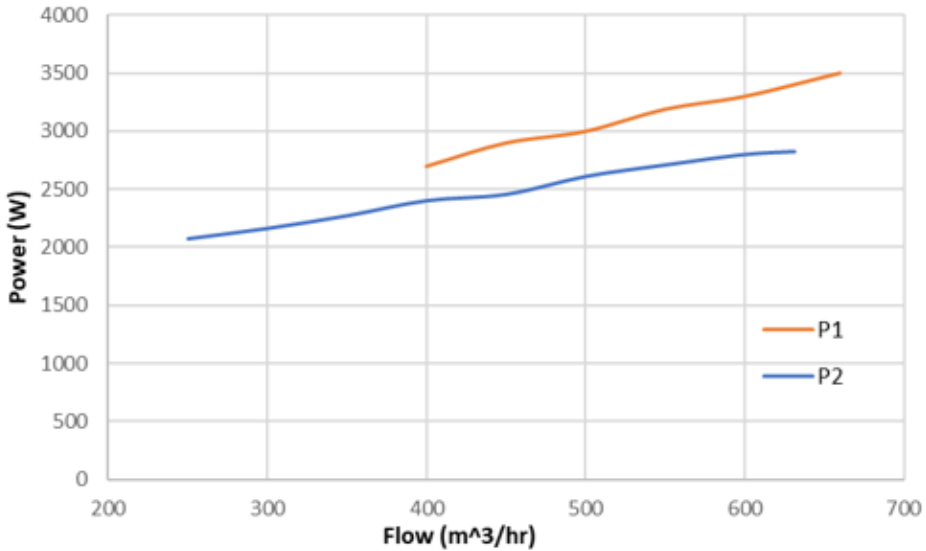


Figure 4.7: Power requirements for P1 and P2 at full capacity obtained from pumps data sheet.

the modeling procedure we assume a reservoir pressure of 200 bar. Referring to table 4.3, it can be seen that reservoir pressures are also case specific. Unfortunately, field data for the remaining fields listed in table 4.1 were not attainable. Nonetheless, it is assumed that a reservoir pressure of 200 bar represents a realistic scenario. However, it is recognized that the pressure within the reservoir does not remain constant, due to depletion of oil and injection of water. As we assume a constant reservoir pressure when we analyze the performance of the WINWIN, the coming paragraphs will identify the upper injection limit tolerated by the reservoir.

Table 4.3: Original reservoir pressure for Snorre and Ekofisk

Field	Original Reservoir pressure [Bar]	Source
Ekofisk	450	<a href="#">PetroWiki (2015)</a>
Snorre	120	<a href="#">Cubitt et al. (2004)</a>

As described, the water injection well is located at a sufficient distance from the producer well, and the fundamental idea of water injection is to effectively sweep the oil towards the producer well, and to maintain pressure. However, due to the permeability of reservoir geology, build-up of pressure around the injection point might occur. Therefore, it is of interest to determine the max allowable injection rate of the WINWIN system to avoid fracture in the reservoir. The permeability is a measure of how well liquids are allowed to pass through rock pores. Typically, permeability is measured from 1 to 1000 md where a permeability rating of 1000

md allows for more fluid or gas to pass through, compared to a permeability rating of 1 md.

For monitoring water injection processes, Hall plots can be used. In figure 4.8 a typical Hall plot is presented. One of the main assumptions when deducing Hall plots, is that of a steady state flow over prolonged periods. With reference to figure 4.8, if the injection process occurs as desired, a straight line is expected. Deviations from the straight curve would imply an error in the process. For instance, the deviations could indicate a fractured zone where the injected water could divert from the intended target of the water, which means that the water flows out of the reservoir. On the other hand, due to sudden heterogeneous characteristics of the reservoir, that result in unexpected levels of permeability, plugging might occur. This results in a sharp increase in the Hall plot as seen in figure 4.8. A basic analysis of the mechanics of the hall plot will follow next as outline by IHS Inc. (2014). First, the Hall plot equation is given in equation 4.8.

$$Q_w = \frac{0,00707kh(p_{wi} - p_{avg})}{\mu(\ln \frac{r_e}{r_w} + s)} \quad (4.8)$$

Here  $Q_w$  is the steady state injection rate where the subscript w is added to emphasize steady flow conditions,  $k$  is the reservoir permeability,  $h$  is reservoir thickness,  $p_{wi}$  is the measured pressure at injection well outlet,  $p_{avg}$  is the average reservoir pressure,  $\mu$  is fluid viscosity, and the ratio  $r_e/r_w$  is the wellhead radius over reservoir radius. Finally,  $s$  is the so-called skin factor, which is a dimensionless factor that accounts for sudden pressure drops in the reservoir. The equation can further be simplified, by assuming that  $k$ ,  $h$ ,  $r_e/r_w$  and  $s$  are constant and represented by  $C$ , the equation 4.8 reduces down to:

$$Q_w = C(p_{wi} - p_{avg}) \quad (4.9)$$

The integral with respect to time  $t$ , yields the total volume injected.

$$\int_0^t (p_{wi} - p_{avg}) dt = \frac{1}{C} \int_0^t i_w dt \quad (4.10)$$

$$\int_0^t (p_{wi} - p_{avg}) dt = \frac{W_i}{C} \quad (4.11)$$

Equation 4.11 can be plotted as seen in figure 4.8, where  $\frac{1}{C}$  is the slope, which will remain constant, under the assumption that none of the parameters, represented by  $C$  will change, which will result in a deviation from the straight line in the graph. For more information regarding Hall plots, the reader is referred to IHS Inc. (2014). In order to obtain the higher injection limit for the WINWIN system, it is assumed that the reservoir has a fracture pressure that should not exceed 266 bar. The fracture pressure is the pressure where the rock formation in the reservoir cracks. Therefore, a conservative estimate is given, and 266 bar is used as the limiting

factor. Through the Hall plot equation, the corresponding water injection level that results in a bottom hole pressure of 266 bar can be found. By rearranging equation 4.8 and solving for  $p_{wi}$ , we obtain the reservoir pressure as a function of injected water. It can be seen that the injection level should be constrained to 81000 *bbl/day*. This corresponds to an hourly injection rate of  $533\text{m}^3/\text{hr}$ . As outlined in the description of the pump systems to be evaluated namely, P1 and P2, the maximum obtainable injection rate was found to be 475 and  $460\text{m}^3/\text{hr}$ , and therefore we can allow the pumps to operate without any restriction from the reservoir. The reader is advised that only one of the pump systems will be utilized for the WINWIN system. However, if larger pumping units were considered, the reservoir restriction should be considered. It should be noted that the equation assumes steady state conditions, thus under the varying operating conditions, the actual bottom hole pressure might be different. Furthermore, as emphasized by IHS Inc. (2014), the parameters used to deduce the Hall plot is based upon monthly injection pressures, monthly injection volumes and average reservoir pressures, as such it is believed that the result found through this analysis where the limiting injection rate that was constrained to 81000 *bbl/day*, only will yield the reservoir fracture pressure if this is the monthly average injection rate. Nevertheless, it serves as a reasonable estimate in this high-level analysis. Finally, values used for calculating the bottom hole pressure can be found in Appendix A.2

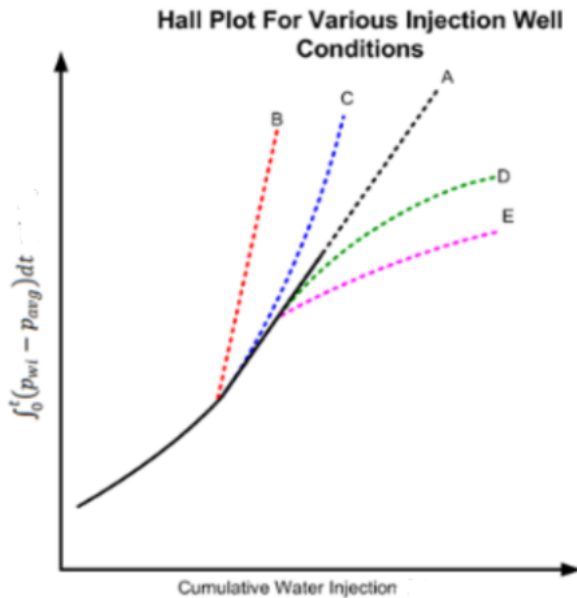


Figure 4.8: Hall Plot representation and fault detection modes (IHS Inc., 2014)

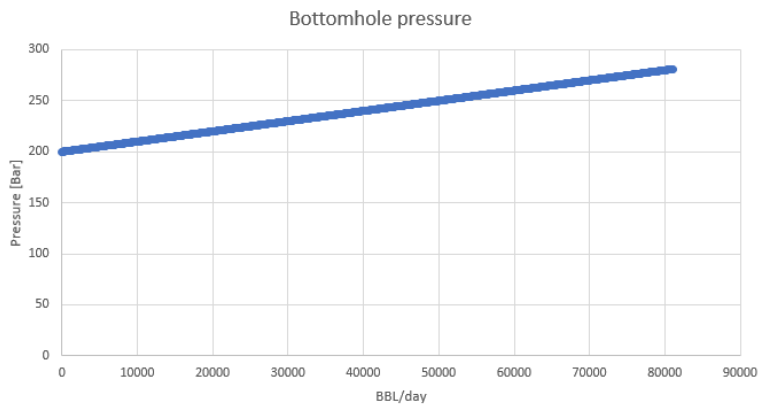


Figure 4.9: Predicted bottom-hole pressure plotted against barrels injected according to equation 4.8.

## 4.4. Methodology for modeling the pump system

The following subsection describes the methodology to deduce a power-flow relationship for system P1 and P2. As mentioned above, HOMER outputs the available power generated by the wind turbines, thus it is necessary to develop a relationship for the corresponding power the pumps will deliver. The methodology is as proposed by Carlson (2000), Chantasiriwan (2013), Zhang et al. (2012)

The affinity equations can be used to determine the relationship between the pump variables, such as head, power and flow. Considering that the pump used in the WINWIN project is a variable speed drive centrifugal pump, where the diameter of the impeller remains constant, the affinity equations can be presented as in equation 4.12.

$$\frac{Q_1}{Q_2} = \frac{N_1}{N_2}, \quad \frac{H_1}{H_2} = \left(\frac{N_1}{N_2}\right)^2, \quad \frac{P_1}{P_2} = \left(\frac{N_1}{N_2}\right)^3 \quad (4.12)$$

Here Q is the flow rate, N is speed of pump, P is power and H is head. The subscripts 1 and 2 refer to the operating points of the pump. For instance, one can see that if the pump speed is halved, the flow is reduced by 50%. If the head is reduced by 75%, 87,5% less power is required. However, the application of the affinity laws is often wrongly applied. This is true when a static head is present in the system such as in this in this case. For a more in depth explanation the reader is referred to appendix A.1 for clarification.

As we do not know the actual operating point of the pump at a certain time, a mathematical representation of flow, pressure and power requirements of the system is required. Carlson (2000), Chantasiriwan (2013), Zhang et al. (2012) suggested to model the pump curves through a polynomial representation, in order to determine the power-flow relationship of the pump system. The methodology is outlined in the following section.

Now we consider the arbitrary variable speed pump curve and the system curve presented in figure 4.10. Here the relationship between flow  $Q$ , head  $H$  and pump speed  $N$  is illustrated. The total head is analogous to the friction the pump must overcome at a specified flow rate. Moreover, by reducing the impeller speed  $N$ , the capacity and the discharge rate are reduced. The system curve is also plotted in the same figure, and as outlined in section 4.1.9, friction in the system is proportional to velocity squared. In all practical senses, the area where the system curve intersects the pump curve, dictates the operating point of the pump.

As proposed by Carlson (2000), Chantasiriwan (2013), Zhang et al. (2012) each pump curve can be expressed as a quadratic polynomial function with flow rate ( $q$ ) as a variable, and can be represented by the following equation.

$$h_{max} = aq_{max}^2 + bq_{max} + c \quad (4.13)$$

Where  $a$ ,  $b$  and  $c$  constants and the subscript  $max$  correspond to the operation mode when the the pump operates at maximum speed. The constants can be determined

trough graph fitting tools such as Matlab or Excel. Similarly, the system head curve can be represented in the same manner.

$$h_{system} = dq^2 + eq + f \tag{4.14}$$

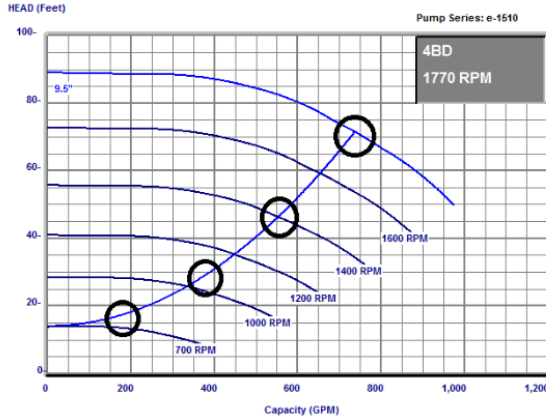


Figure 4.10: Example of a variable speed pump curve system and system curve, please note that GPM stands for Gallons per minute (1 GPM= 0,23 m<sup>3</sup>/h) (C. Edmondson et al., 2016).

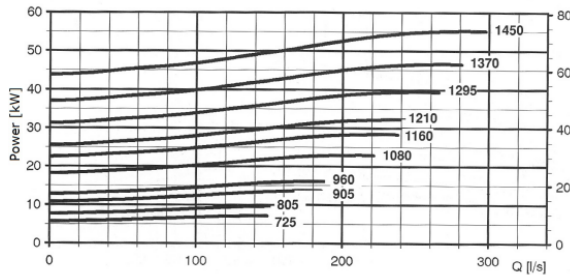


Figure 4.11: Typical representation of the required pump power, rotational speed, and flow (Zhang et al., 2012).

In figure 4.11 a typical power-flow graph for a variable speed pump is depicted. Here the number given at each line corresponds to a rotational speed of the pump. It can be seen that the pump capacity and discharge rate reduces when rotational speed is reduced. Furthermore, the impeller speed can usually operate down to 0.5 of speed  $N_{max}$ .

Differently from the system head and pump head curve where a quadratic equation was applied to represent the system, Zhang et al. (2012) suggested that a cube fitting line would represent the power function more accurately. The power at max

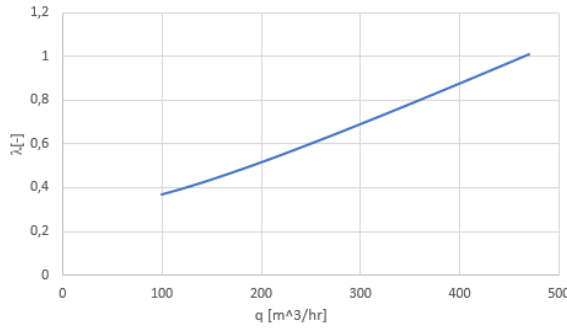


Figure 4.12: Relationship between the dimensionless pump speed  $\lambda$  and flow of pump (Equation 4.19).

rotational speed of the pump can be represented as follows.

$$P_{max} = gq_{max}^3 + hq_{max}^2 + iq_{max} + j \quad (4.15)$$

Now a relationship between the rotational speed of the pump and the flow can be evaluated. From the affinity laws presented in equation 4.12, and by introducing the variable  $\lambda = \frac{N}{N_{max}}$ , where  $N$  represents an arbitrary pump speed and  $N_{max}$  corresponds to max rotation speed of the pump, equation 4.15 and 4.13 can be written as:

$$h = aq^2 + bq\lambda + c\lambda^2 \quad (4.16)$$

$$P = gq^3 + hq^2\lambda + iq\lambda^2 + j\lambda^3 \quad (4.17)$$

Now the pump curve and the power estimate are a function of the ratio  $\frac{N}{N_{max}}$  and the flow  $q$ . By equating the system curve and the pump curve, the relationship between flow and rotational speed can be found, as outlined in equation 4.18.

$$aq^2 + bq\lambda + c\lambda^2 = dq^2 + eq + f \quad (4.18)$$

Yields

$$\lambda = \frac{-(bq) \pm \sqrt{(bq)^2 - 4(c)(aq^2 - dq^2 - eq - f)}}{2c} \quad (4.19)$$

From equation 4.19 the relationship between pump speed and flow can be obtained by setting flow as a variable. This is illustrated in figure 4.12 where the pump speed ratio is plotted against flow. Here, when  $\lambda$  is one, this would correspond to a max speed of the pump, and consequently the rated flow rate of the pump. From the example in figure 4.12, the flow rate is around  $450 \text{ m}^3/\text{hr}$ . This relationship also allows for a linear representation:

$$\lambda = kq + l \quad (4.20)$$

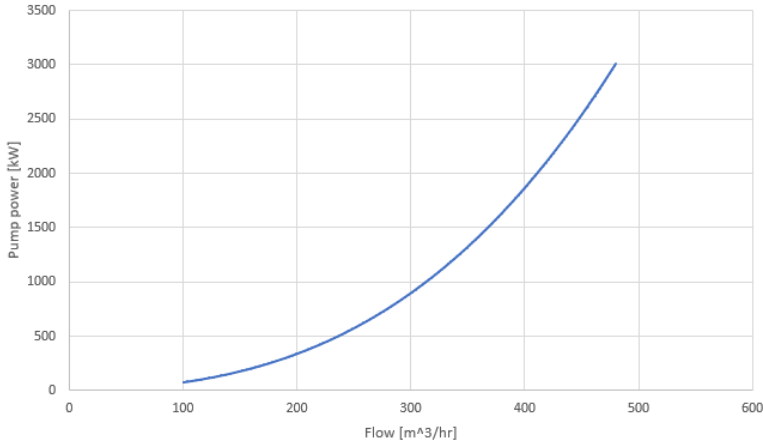


Figure 4.13: Flow power relationship for a variable speed drive pump, curve derived from equation 4.21.

Where  $k$  and  $l$  are system-dependent constants. The linear representation of  $\lambda$  can therefore be substituted in equation 4.17. We now obtain the following equation 4.21, is presented below.

$$P = gq^3 + hq^2(kq + l) + iq(kq + l)^2 + j(kq + l)^3 \quad (4.21)$$

Equation 4.21 is plotted in figure 4.13. Lastly we present equation 4.22 and adapt a quadratic representation of the graph plotted in figure 4.13.

$$P = mq^2 + nq + o \quad (4.22)$$

Again, here  $m$ ,  $n$ , and  $o$  are constants given by curve fitting tools. It should be noted that the procedure outlined only applies to a particular system and the resulting constants are dependent on the respective manufacturer's pump curves and system curve. In addition, as compared to the power-flow relationship for the respective pumps where a cubic fit was proposed, the resulting pump power given in equation 4.22 is reduced to a second order polynomial through curve fitting of a second order polynomial to equation 4.21. This is done to reduce the modeling complexity. Equation 4.22 is dependent on flow, head, pump speed and the performance of the individual pumps and system. The equation therefore provides a more accurate result compared to a straightforward application of equation 4.12 (Chantasiriwan, 2013).

#### 4.4.1. Application of the pump modeling methodology.

The approach outlined in the section above, allows for a flow estimate of the pump when power is available. In this section we present the application of the modeling method proposed in 4.4 to the WINWIN system particulars.

The system curve shown in figure 4.4 is approximated with curve fitting tools, and corresponding values are shown in table 4.4. These coefficients  $d$ ,  $e$  and  $f$  are the same as shown in equation 4.14.

<b>d</b>	<b>e</b>	<b>f</b>	<b>R<sup>2</sup></b>
0,0053	0,1221	119,02	1

Table 4.4: System curve in figure 4.4 represented by  $d$ ,  $e$  and  $f$  coefficients found from data fitting tools.

	<b>a</b>	<b>b</b>	<b>c</b>	<b>R<sup>2</sup></b>
<b>P1</b>	-0,0003	0,0533	1353,8	0,9845
<b>P2</b>	-0,0021	1,0748	1310,7	0,9936

Table 4.5: Coefficient values for the head-flow relationship, as stated in equation 4.13.

In table 4.5, the coefficients obtained from curve fitting of the head-flow relationship in figure 4.5 and 4.6 for system P1 and P2 are shown.

	<b>g</b>	<b>h</b>	<b>i</b>	<b>j</b>	<b>R<sup>2</sup></b>
<b>P1</b>	2E-05	-0,0323	20,163	-1472,1	0,9955
<b>P2</b>	-8E-06	0,0095	-1,7002	2020	0,9965

Table 4.6: Pump power coefficients as referred to in equation 4.15.

Lastly, the coefficients related to the power-flow relationship at  $N_{max}$  from figure 4.7 are shown in table 4.6 that refers to equation 4.15. Now the steps outlined in equation 4.16 through 4.22 can be performed. The resulting coefficients can be found in table 4.7 and the final flow-power relationship for the system is depicted in figure 4.14.

	<b>m</b>	<b>n</b>	<b>o</b>
<b>P1</b>	0,0237	-6,8196	801,34
<b>P2</b>	0,0187	-4,8328	531,74

Table 4.7: Coefficients that yield the final power at flow rate  $q$ .

From figure 4.14 we see that P2 is less energy intensive compared to P1. The systems also have different operating regimes, where we can see that P2 can operate when limited power is available in the system. However, P1 has a higher discharge rate, which is favorable when the wind turbine is operating at a high capacity. It should be noted that when the wind turbine is operating at rated power (6MW) the discharge rate of the respective pump systems, P1 and P2 will be  $480 \text{ m}^3/\text{hr}$  and  $460 \text{ m}^3/\text{hr}$ . We now have a relationship for flow-power of the respective pumps,

and by matching the power produced by the wind turbine, the performance of the WINWIN system can now be evaluated.

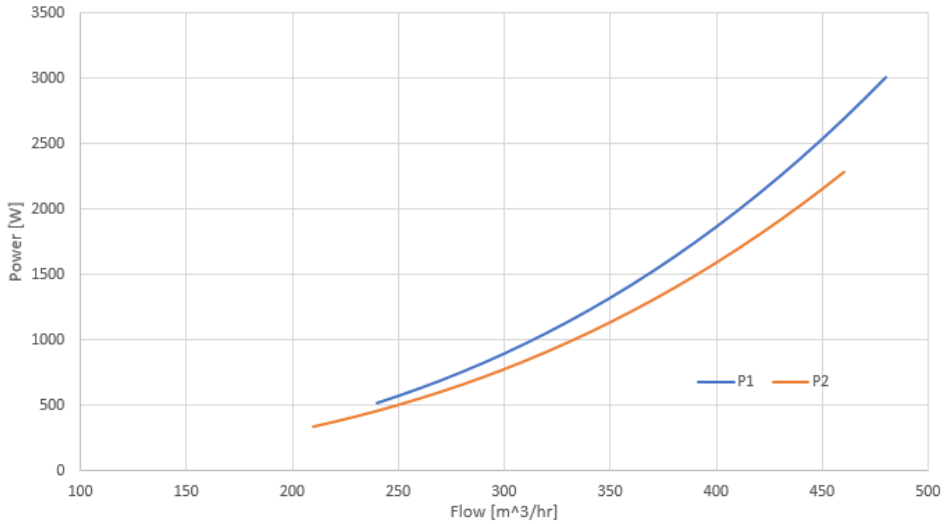


Figure 4.14: Power requirements and operation range of the two pump systems, P1 and P2 based upon variables presented in table 4.7 applied in equation 4.22.

### 4.4.2. Limitations and assumptions

In the procedure outlined above, we assumed an immobile system curve. Thus, when a dynamic system curve is considered, the modeling approach must be reiterated. The coefficients will vary if the system head increases or decreases. Whether or not the assumption applied through this modeling holds true or not, is debatable. For instance, the pressure in the reservoir is will increase as result of injection in turn this will reduce the amount of flow delivered to the reservoir as the pump must overcome more frictional work, on the other hand, the reservoir pressure will decrease when the pumps are not injecting, i.e when the wind is not blowing so less work must be overcome by the pumps and a higher flow rate can be provided, of-course within the design envelope of the pump. As such, the net sum would equal out. For further analysis of the performance, it is therefore recommended to include the effects of a varying reservoir pressure as a result of the injection. It is believed that the Hall plot equation, can be incorporated in the system head curve, however as the Hall plot relationship is based upon monthly average parameters, it is recommended to further analyze the appropriateness of incorporating the Hall plot equation in the modelling procedure. While it is believed that the Hall plot equation can be used to determine the pressure after water injection, establishing the reservoir pressure after a periods of no injection, is also important to establish. This is however also dependent on the level of the extraction of oil, and should be determined in conjunction with full model of the reservoir including the extraction of oil and injection of the water. Furthermore, the underlying assumption for the modeling of the power-flow relationship assumes that parabolic curves can represent the system curve, head curve, and power curve. This is demonstrated in the following in the tables presented above namely table 4.15, 4.5 and 4.4, as appropriate  $R^2$  values are obtained. Finally, Chantasiriwan (2013) investigated several pump curves provided by different manufacturers, and concluded that the affinity laws apply to commercially available pumps. The outlined procedure is also given for one pump, and not when the system is operating in parallel. However, as the pump manufactures provided the design envelope for the whole system and the power required at max capacity, it is suggested that the method provides a good representation of the flow and power relationship of P1 and P2. Finally, in the modeling we only consider the injection pumps, which means that the lift pumps are not evaluated here. In the modeling, we assume a constant power requirement of 300 kW from the lift pumps during operation.

## 4.5. Summary

This chapter has described the the technical aspects of the WINWIN system and considerations undertaken in order to obtain an accurate estimate of the injection capacity. Here we summarize the main parameters that are used in the modeling of the WINWIN system.

Table 4.8: Parameters for base case 1.

Parameter	Base Case
Geographic location	North Sea, GoM, Brazil, and West Africa
Water depth [m]	200
Reservoir depth [m]	1940
Reservoir pressure [bar]	200
Pump systems considered	P1 and P2
Injection capacity [m <sup>3</sup> /hr]	210-480
Turbine rating [MW]	6 MW
Wind data	NASA Surface Meteorology and Solar Energy Database

## 4

#### 4.5.1. Flowchart of the modeling process

In figure 4.15 a flowchart of the performance modeling is outlined. The model is developed in Excel but also relies on output from HOMER. First the power curve is obtained from a representative 6MW offshore wind turbine. The power curve is then imported into HOMER. Furthermore, based upon chosen locations, as specified in chapter 5.1, HOMER extracts wind resources from NASA Surface Meteorology Database. HOMER then gives the hourly energy yield of the turbine. The output power is imported into Excel, where the available power is matched with the pump requirements. If proven sufficiently, the model then evaluates whether wind has been stable for the last N hours. This restriction has been added to avoid unnecessary start and stop cycles that might give rise to unwanted tears to the pump systems and other components. The wind confidence interval is evaluated from one to eight hours. Furthermore, the maximum injection rate is dependent on the pump configuration chosen.

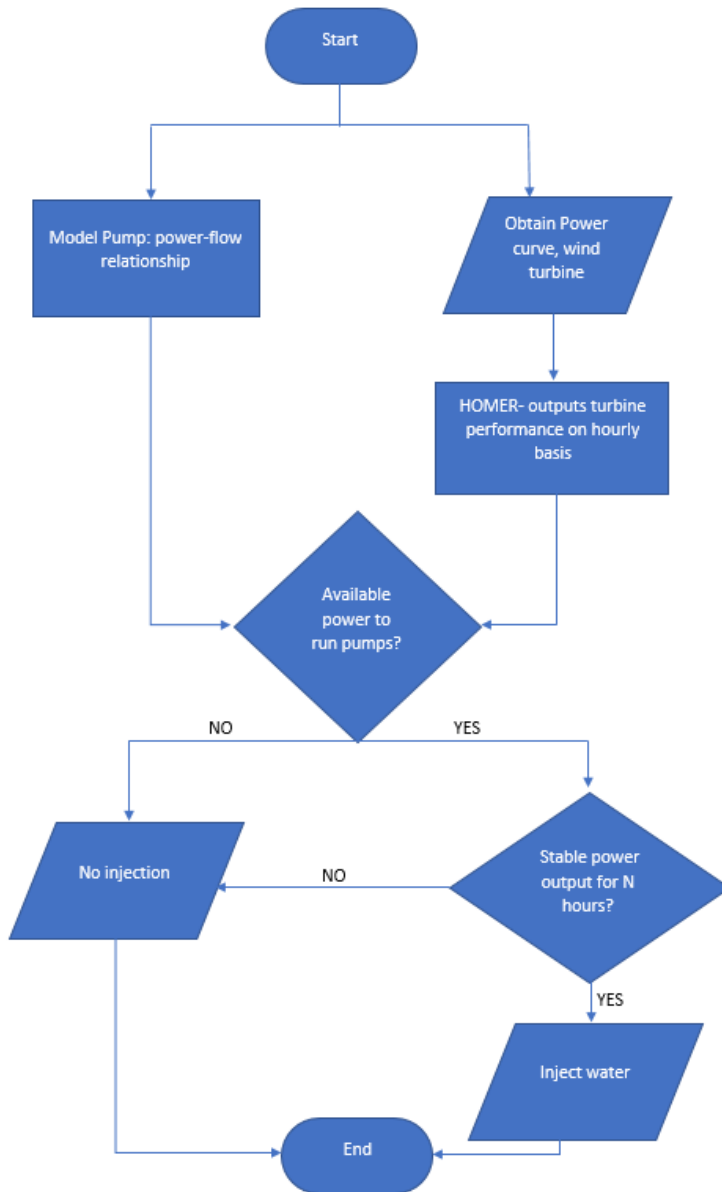


Figure 4.15: Flowchart for WINWIN performance modeling.



# 5

## Site assessment and considerations

*This section is intended to inform the reader of the rationale behind the selected areas: in Brazil, the North Sea, the Gulf of Mexico and Africa, where the performance of the WINWIN unit are to be analyzed. Furthermore this chapter also presents two general observations where the WINWIN unit will have an advantage over conventional water injection solutions, namely brownfields and situations where there is a considerable distance from the injection platform to the injection well.*

### 5.1. Introduction

In order to assess the potential application of the WINWIN system, it is preferable to select four realistic locations where WINWIN could be used. Naturally, the performance of WINWIN depends on several factors, where the most influential parameter is the local wind conditions. However, selecting locations based upon the local wind resources would not reflect a real business scenario. Therefore, to further gain insight into the possible application of WINWIN, the case study must be located in a typical offshore environment, where oil activity is undertaken, and wind resources are assessed afterward. Furthermore, as this is a high-level screening of the potential markets of the WINWIN unit, we consider the offshore oil hubs where the majority of the offshore oil production occurs. These hubs are the gulf of Mexico, the North Sea, West Africa, and Brazil. The selection criteria are presented and explained in greater detail in section 5.3. However, first in this chapter, we identify two situations where the WINWIN system will have an advantage over conventional water injection systems. The conventional water injection system where gas or diesel generators runs the injection pumps at the oil platform.

## 5.2. Possible scenario's where WINWIN should be considered

A good candidate for the WINWIN unit is brownfields. Brownfield is oil lingo for a field that has reached its production plateau or where a decline in production has occurred (Schlumberger, 2018). For instance, the field Ekofisk can be considered a brownfield. From figure 3.6 one can see that the field reached its peak production between 2002-2006 and has since experienced a decline in production. Furthermore, a common denominator typically associated with brownfield platforms is the limited available space on the platform itself. The lack of available space and generating capacity can be due to several reasons:

- It is a highly complex task to foresee and predict the development and exploration of the field, thus during design and construction the platform and components, the platform is designed for the expected lifetime.
- Adaptation and development of technology has allowed for further extraction of oil that previously was evaluated not feasible.
- Production and investments in oil recovery is highly dependent on oil prices, as such investment decisions towards upgrading platform capacity and methods are influenced by the volatility in hydrocarbon prices.

In many cases involving brownfield projects, improvements in drilling technology and developments in enhanced oil recovery have allowed for a prolonged extraction of hydrocarbons. However, as stated in section 3.3.2, because the oilfields' energy requirements increase towards the end of their lifetime, combined with a finite amount of available space and generating capacity on the host platform itself, this gives rise to questions regarding the future extraction. The platform might require a substantial upgrade in order to facilitate additional power requirements and equipment. These platform upgrades require (of course) substantial amounts of capital. Such was the case for platform Njord A. The platform Njord A is connected to the Njord field that was discovered in 1986 with an original production capacity of 66  $Mm^3$  oil equivalents. In 2017 the field had produced 41  $Mm^3$  oil equivalents (NPD, 2018). Originally the field was planned to end production in 2013, however when it was realized that more oil equivalents could be extracted, it was decided that a platform upgrade was necessary to continue production. A substantial upgrade of Njord A was undertaken, allowing it to be in production for at least two more decades (Hovland, 2017). The total cost for the upgrade is estimated to 527 M€ (Stangeland, 2017). The platform upgrade of Njord A serves as a demonstration of how capital-intensive such projects can be, but are by no means representative for all platform upgrades undertaken. In addition, additional costs, such as well abandonment and loss of revenue from production, must be accounted for. It is not clear how much more recoverable oil equivalents the operators estimated. However it is reasonable to assume a substantial upgrade from the original estimate to justify the investment decision. One can therefore imagine a scenario where a brownfield development can be a potential candidate for the WINWIN unit.

Instead of upgrading and retrofitting the existing platform to accommodate the new generating capacity, the WINWIN unit can be used.



Figure 5.1: Njord A being assisted to shore by towing vessel KL Sandefjord (Equinor, 2016)

The scenario above highlights some of the challenges and costs when platform upgrades are required to extend the field's lifetime. Other scenarios might arise when available platform capacity is present, both in terms of space and/or generating capabilities. Here the WINWIN concept is competing on different economic terms with reference to the case mentioned above. Namely, the distance from the host platform to the desired point of injection of water. High-pressure offshore pipelines are capital intensive. Kaiser (2017) investigated the costs associated with laying pipelines in the Gulf of Mexico in the period 1985 to 2014. Adjusted for inflation, pipelines and installation costs amounted to 1.83 M€/km. Hence the distance from the source of power to injection point is a significant cost factor. In figure 5.2 a schematic illustration of the infrastructure of the field Maria is displayed. It can be seen that the water injection process is undertaken at platform Heidrun before it is transported 43 km to subsea station Maria H for injection. Based upon the assumptions proposed by Kaiser (2017), pipe laying costs equal 78.7M€. Another case where there is a significant distance between the source of power and the injection site is the Tyrihans development. Unlike the case with Heidrun, where the water is processed at the platform, a subsea power cable is extended 31 km from the platform Kristin. The power umbilical drives two centrifugal pumps located on the seafloor with a total capacity of 5.4 MW. At full capacity the system can deliver 128,000 BBL/day (Grynning et al., 2009). The cost for subsea power cables is estimated around 614 €/km (Slätte et al., 2014). According to Equinor, the raw seawater injection project at Tyrihans would result in an additional 10% in recov-

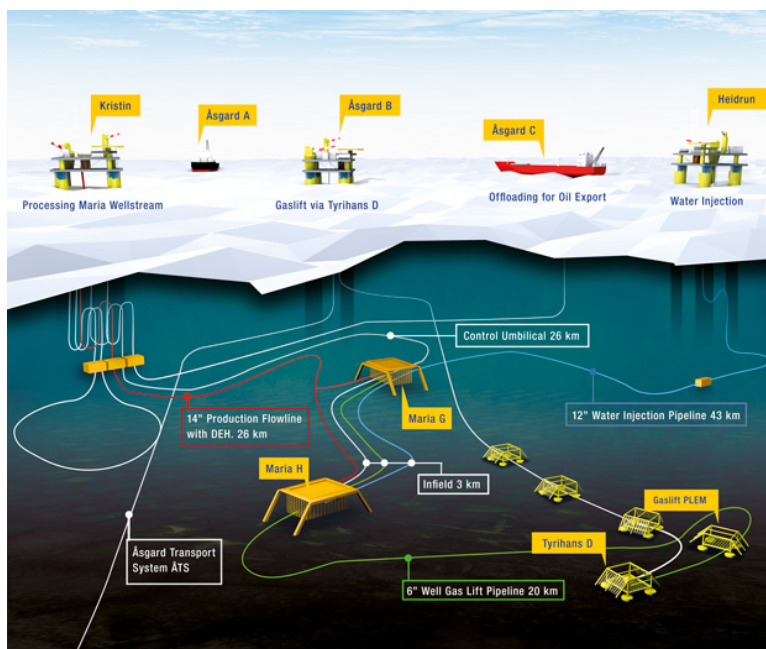


Figure 5.2: Schematic overview of oil field Maria (Molde, 2015)

erable oil. Given the initial estimate of recoverable oil, this would yield an addition of 18.1 MMBL of oil (Petro, 2009). With the current price of oil, this results in 1.3 B€ in income.

In the aforementioned cases we have seen two examples on how water injection is facilitated when the field is well developed i.e. brownfields, and how water injection is facilitated when there are large distances between the platform and the injection well. For both cases, extensive capital is required and the solutions are inefficient. Through the use of the WINWIN system, which can be towed and directly positioned over the injection well, the required length of high pressure-underwater pipelines or power cables and/or costly subsea pumps can be minimized. Concerning brownfields situations, retrofitting can potentially be mitigated through a selection of the WINWIN technology. The scenarios outlined are evaluated to pose as realistic scenarios and alternatives to conventional water injection. With the above mentioned scenarios in mind, the following section identifies site specific parameters that will further strengthen the viability of application for the WINWIN unit.

### 5.3. Definition of the selection criteria

The above sections have emphasized and outlined in greater detail, the currently accepted best business case scenarios for WINWIN, and should preferably be reflected in site selection criteria. However, the scenarios outlined above are difficult to identify without direct insights in the operational portfolio of the oil companies, and this information is to a large extent withheld from the public eye. Nonetheless, it is desired to identify the performance of the WINWIN system in the mentioned offshore oil hubs identified as Gulf of Mexico, the North Sea, West Africa and Brazil. Therefore, the site selection will utilize information that is available to the public. Such information is for instance the water depth. As the WINWIN unit is based upon a floating substructure, water depths are of concern. Industry experts from DNV GL recommend water depth in the range 100-1000 meters for floating offshore wind structures. Moreover, port facilities should be located within a reasonable distance to allow for an efficient maintenance program. Lastly, the selection process does not consider the reservoir particulars. It is assumed that fields and corresponding reservoirs are suited for water injection. Thus the following considerations are of concern when selecting the location of application:

- In a location where oil exploration is undertaken.
- Considerable distance from host platform to the injection well.
- Water depth requirements in the range of 100-1000m.
- Relative proximity to shore.

It should be noted, the above mentioned criteria will serve as the leading guidelines for the site selection. Other parameters, where for instance information regarding platform lifetime and production numbers as well as distances to injection wells are available (such as is the case for the North Sea), this information will also be considered when selecting a site. Lastly, the wind conditions will also be regarded if the above criteria has not been identified or partly identified.

The methodology applied in the site selection process is largely based upon available information found on the internet and governmental databases such as the Norwegian Petroleum Directorate database. Of course, this is only applicable to the site selection in the North Sea. For the other oil hubs, information is obtained from the respective oil companies that operate in the region, as well as research papers and weather data.

#### 5.3.1. Site selection for North Sea

The region considered when selecting the location North Sea location is based upon the the two business scenarios considered in section 5.2. Through the database provided by NDP the oil reservoirs Maria, Heidrun, Tyrihans, Åsgård, Kristin, Trestakk and Morvin, was identified as is illustrated in figure 5.4. The oil fields Maria, Tyrihans and Heidrun rely on water injection for recovery. The solution chosen is inefficient,

as explained in section 5.2, with long distances from the source of power to the point of injection as the main cause of inefficiency.

The platform Heidrun delivers water to the subsea station Maria H 43 km away. This requires significant power and energy. Subsea booster pumps along the flowline are also required to compensate for pressure losses. Furthermore, according to a press release from Wintershall, the field's operator, the total pipe laying costs amounted to 261 M€. This included the construction of 22 km gas lift pipe, 43 km water injection pipeline, and 26 km pipeline for a conventional well stream (Wintershall, 2015). This resulted in construction costs of 2.78 M€/km. Water depths in the area are 298 meters and therefore a suitable depth for floating structures with regards to mooring options. Heidrun has been producing since 1995.

The average age of the platforms that support the water injection processes (Kristin, Åsgård and Heidrun) is 18 years, as such maybe retrofitting could be an option in the next decades (NDP, 2018). Although this field is now developed, it might be found in the coming years that more water injection is required, where the WINWIN unit could facilitate this. Figure 5.3 depicts the location chosen for WINWIN assessment in the North Sea (65° 19'N, 7° 19'E). The chosen location is located 175 km north of Kristiansund, which is a city with good port facilities.



Figure 5.3: Chosen location for WINWIN case study

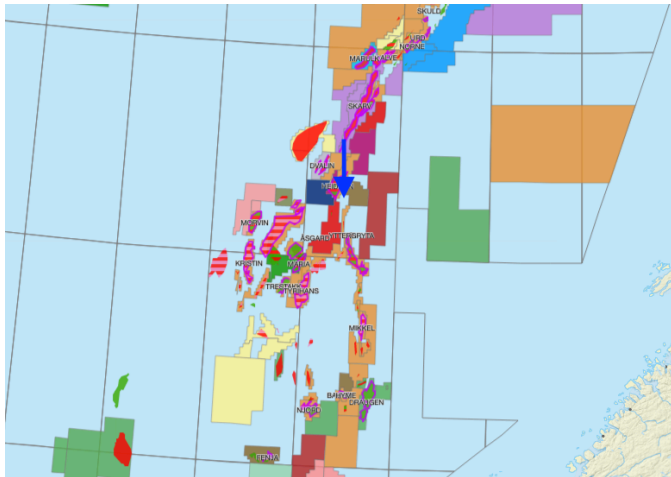


Figure 5.4: Significant oil and gas activity in immediate location (Norsk Petroleum, 2018)

### 5.3.2. Site selection for the Gulf of Mexico

The Gulf of Mexico (GoM) accounts for 16% of the US crude oil production, and produced in 2016 over 1.6 *MBBL/day* of crude oil (EIA, 2018). Methods of oil extraction in GoM seldom rely on water injection. In over 450 reservoirs, water injection has only been undertaken in 18 deepwater reservoirs. The recovery factor in the GoM is 32%, which implies good primary recovery, considering the limited use of enhanced oil recovery techniques (Li et al., 2013). However, by adapting water injection, some fields could further increase their recovery factor. Furthermore, considering the water depths of the operational platforms in the GoM presented in table 5.1, only 12% is within the desired range for floating offshore turbines. Nonetheless, this still makes up 244 platforms.

Table 5.1: Overview of number of platforms and corresponding depths (Bureau of Safety and Environmental Enforcement, 2018)

Water depth [m]	Platforms	Percentage distribution [%]
0-100	1710	86
101-1000	244	12
>1000	32	2

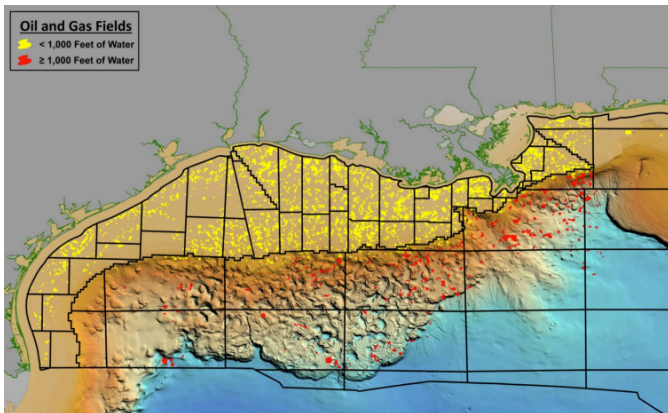


Figure 5.5: Overview over oil and gas fields in GoM. Yellow markers indicate fields in water depths below 1000 feet, and red markers indicate fields in waters more than 1000 feet (Nixon et al., 2016).

Unfortunately, detailed in-depth field statistics over operational fields that utilize water injection, such as those for the North Sea sector, were not found. It is still desirable to include GoM within the scope of this study. Thus, wind data in conjunction with areas of high oil activity will serve as the decision criteria. In figure 5.5 and 5.6 an overview of oil fields and available wind resources is depicted. The available wind resources in GoM are scarce relative to wind speeds found on the east coast of the US. The location with higher wind resources is found along the coast of Texas, with an expected annual wind speed of approximately 8 m/s. From figure 5.5, the area with the most prominent wind resources also coin-

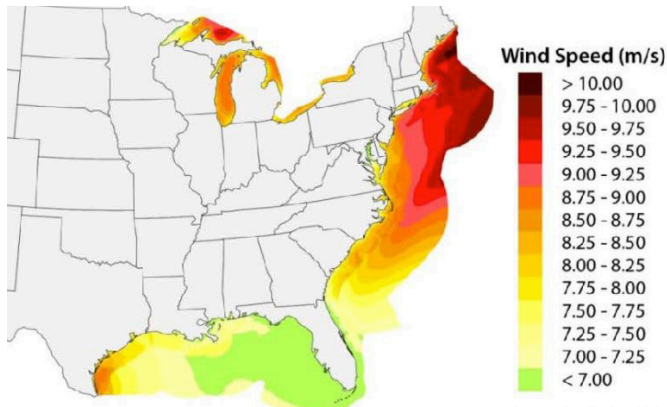


Figure 5.6: Wind resource data over the US offshore domain at 100 meters (NREL, 2018).

cides with areas where oil activity is undertaken. Furthermore, the bathymetry of the area is suited for the application of floating offshore structures with expected water depths around 200 meters. The location chosen for the case study is situated approximately 70 km east of Corpus Christi ( $27^{\circ}40'52.09\text{N}$ ,  $95^{\circ}53'24.49\text{W}$ ).

### 5.3.3. Site Selection for West Africa

West Africa is a significant contributor to the world's oil production. West Africa is chosen as a point of interest as one of the partners in the WINWIN project has ongoing projects and developments in the region. In figure 5.8, daily offshore hydrocarbon production is illustrated. Angola and Nigeria are in the lead with 1705 and 1398 *BBL/day* respectively, placing them in the top ten in offshore oil producing countries. Historically, hydrocarbon exploration dates back to 1960, where vast reserves were found next to the Niger Delta. Recent discoveries are now mainly found in deep waters (Knight and Westwood, 1999).

In 2016, Exxonmobile announced its discoveries in the Owowo field, where it was estimated up to 1 *B.BBL* recoverable. The field is located in approximately 140 meters of water depth, and made up of sandstone, making it well suited for water injection purposes (ExxonMobil, 2016). In the absence of more relevant information, the Owowo reservoir will serve the location for further analysis of the WINWIN system. The precise location can be found in figure 5.9 with coordinates  $3^{\circ}46'35.58\text{N}$  and  $7^{\circ}59'52.94\text{E}$ .

### 5.3.4. Site selection for Brazil

Brazil, only surpassed by Saudi Arabia, is the second largest contributor to global offshore oil production. In 2016, Brazil produced on average 2.6 *MBBL/day* (Rys-



Figure 5.7: Chosen location for WINWIN case study

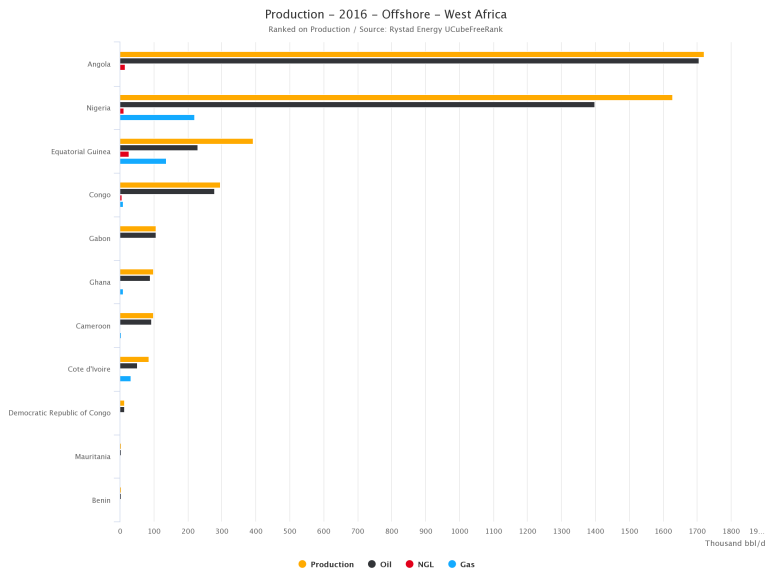


Figure 5.8: Hydrocarbon production overview

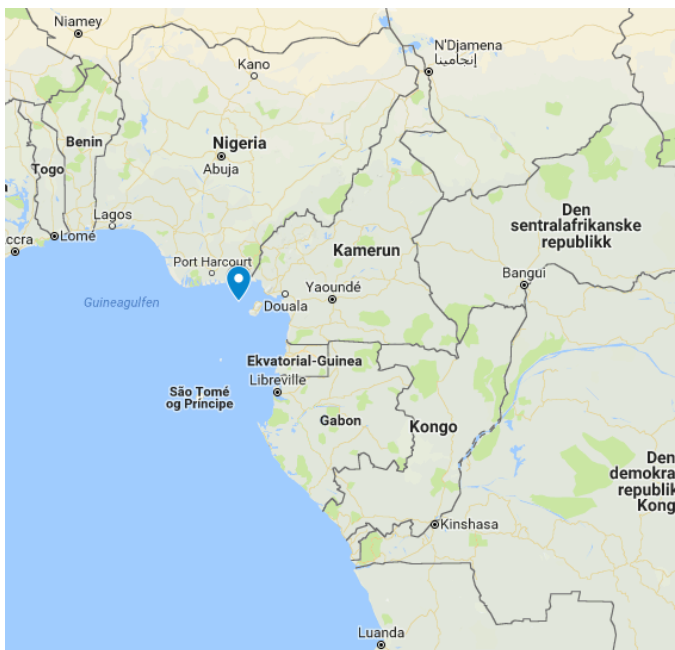


Figure 5.9: Site selection for West Africa.

Energy, 2018). Despite being a top oil producer, with extensive proven reserves, the recovery factor is only estimated to 21%. Recovery factor on the Norwegian continental shelf is assumed to be over 50% (ANP, 2018). Although it is not fully explained why the recovery factor for Brazil is low, compared to the global average, it is reported that around 35% of the majority of the fields in Brazil are now considered mature (ANP, 2018). Mature reservoirs require extensive recovery techniques as highlighted in section 3.3. One reason could be the relatively low internal focus on recovery techniques where only 24 EOR projects have been initiated. This is a relatively low number considering that Brazil has over 440 oil fields (Rodriguez, 2018).

The offshore activity in Brazil is mainly found in the following three basins: Campos, Bahia and the Sergipe-Alagoas basin (Becker, 1999). The Campos basin accounts for 80% of the total oil output, produced from 41 fields (Equinor, 2018). Furthermore, the Campos basin covers an area of 100,000 km<sup>2</sup>, and is located off the coast of Rio de Janeiro. The bathymetry (water-depth) of the field varies from shallow water to ultra-deep waters (de Castro and Picolini, 2016). In figure 5.10 an overview of developed fields in the Campos basin are presented. From the bathymetry lines, the majority of the fields are within acceptable depths for application of floating structures. A screening of the shallow water fields was conducted, where the Enchova (22°56'9.42"S, 38° 56'42.39"W) field was evaluated to be the most promising field for application of WINWIN. The Enchova field is situated in water depths between 100-500m, and is surrounded by similar well-developed fields. The hydrocarbon output has steadily declined in all surrounding fields including Enchova (Petrobras, 2017), and Petrobras suggest several enhanced recovery techniques, including water injection, to prolong the field lifetime.

## 5.4. Summary of Site Selection

Extensive research concerning the appropriate site selection for the WINWIN concept was undertaken. Acquiring public information regarding fields, wells and water injection status, proved to be challenging as this information often is considered business sensitive. As such, the decisive criteria for West Africa, Brazil and the Gulf of Mexico were shifted due to the limited public knowledge available. Nevertheless, the chosen locations do represent areas where significant oil activity is carried out, and it is believed that the sites chosen will add value to the WINWIN project. Finally, a summary is given in table 5.2.

Table 5.2: Overview of selected areas for further analysis of the WINWIN system.

Area	Coordinates	Water depth [m]	Distance to Port[km]
North Sea	65° 19'N, 7° 19'E	298	175
Gulf of Mexico	27° 40'N, 95°53'W	200	70
West Africa	3° 46'N, 7°59'E	140	175
Brazil	22°56'S, 38° 56'W	500	60



Figure 5.10: Overview of the Campos basin with location and associated field names (Offshore Technology, 2018)



# 6

## WINWIN Performance results

This chapter gives an overview of the performance of the WINWIN system. Here we present the injection rates over a year for the WINWIN unit at the locations specified in chapter 5. The specific locations are summarized in table 5.2, and as mentioned the selected areas are located in the oil hubs of the North Sea, the Gulf of Mexico, Brazil and West Africa. The results presented are based upon the methodology outlined in chapter 4, and a summary of the methodology is presented in figure 4.15.

### 6.1. A guide to the results presented.

The following chapter will present the results. The results presented are the injection rates for the locations chosen with pump configuration P1 and P2. The P2 pump configuration is outlined in section 4.2.2, and is comprised of two pumps, one smaller pump and one large pump. The P1 pump configuration is outlined in section 4.2.1 and is comprised of two identically sized pumps. The operational envelope for the pump system P1 and P2 are found in figure 4.5 and 4.6 respectively. Moreover, the injection rates are presented on a quarterly and a two-weekly average for clarity. In the accompanying tables, some parameters are listed that relates to the operational strategy. The operational strategy is the number of hours required of wind before the WINWIN system will start to inject. That is the WINWIN will not start to inject before the wind has been above cut-in wind speed for the system for at least 1 hour. This is implemented to assure steady wind conditions and unwanted start-ups and shut-downs of the system. The operational strategy evaluated in this chapter is based upon a 1-hour wind confidence interval. In appendix B the results of an operational strategy of 3 and 8 hours are presented. The parameters listed in the tables to be presented are the following:

- *Total barrels injected* - That is the total amount of barrels injected in the reservoir.

- *Avg. daily bbl injected* -Average barrels of water injected per day.
- *Non injecting hours* -The amount of hours per year that the WIN-WIN is not operating, due to the operational strategy chosen and insufficient wind.
- *Longest continuous downtime* -The longest period identified in a year when WIN-WIN is not injecting. This is of importance for the battery capacity required.
- *Number of stops in a year* -Number of start/shutdown sequences in a year.

## 6.2. North Sea

This section presents the WINWIN performance results for the North Sea location.

### 6.2.1. Wind conditions

Before the results are presented, we consider the wind conditions in the North Sea, where the monthly average wind speed is shown in figure 6.1. The average wind speed is found to be 8.78 m/s.

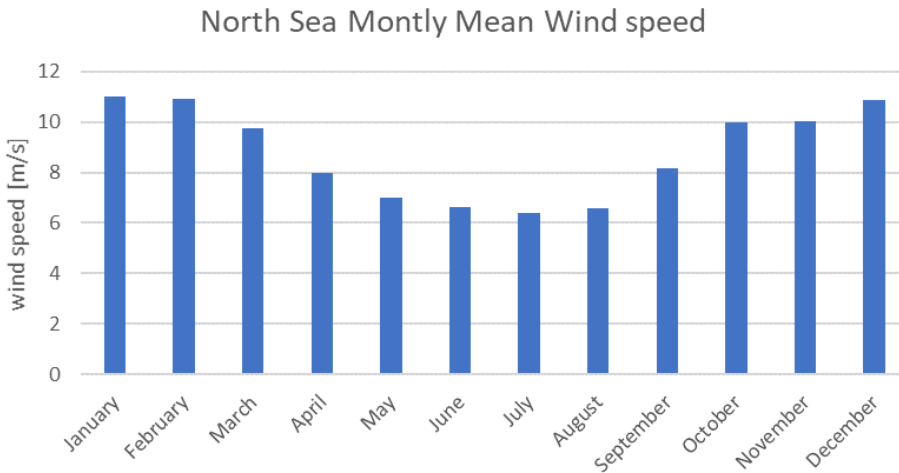


Figure 6.1: Monthly average wind speed

### 6.2.2. Injection performance for North sea location

In this subsection the performance of the WIN-WIN unit with the pump configurations P1 and P2 is shown. In table 6.1 key performance parameters are indicated. In figure 6.2 and 6.3 the injection performance of P1 and P2 are shown respectively.

Table 6.1: Comparison of P1 and P2 in North Sea location

<b>Parameters</b>	<b>P1</b>	<b>P2</b>
Total barrels injected [Mbbbl]	17.9	18
Av. daily bbl injected	49205	49505
Non Injecting hours	2218	2023
Longest continuous downtime [hr]	35	34
# of stops	419	405
Ops strategy [hr]	1	1

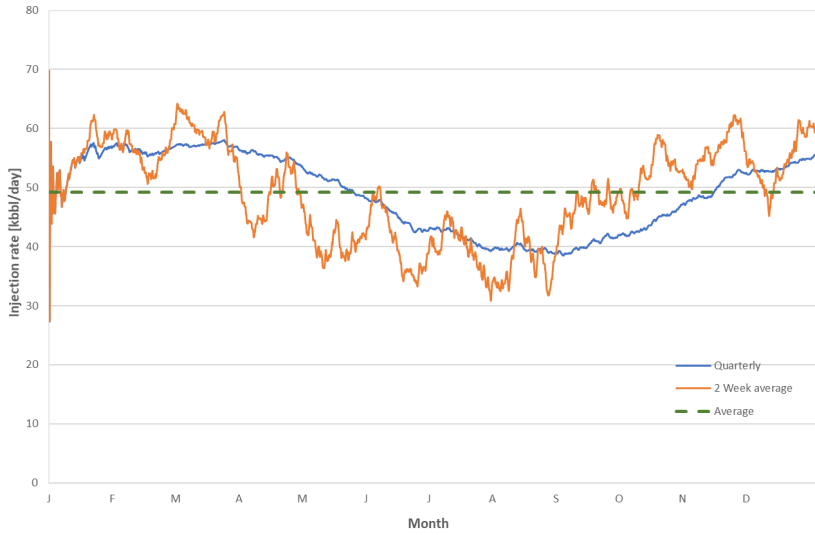


Figure 6.2: WIN-WIN performance with P1 configuration for North Sea site.

6



Figure 6.3: WIN-WIN performance with P2 configuration for North Sea site.

## 6.3. Brazil

In this section the WINWIN performance in Brazil is presented.

### 6.3.1. Wind conditions in Brazil

In figure 6.4 monthly mean wind speed for the Brazil location is shown. The annual mean wind speed is 6.1 m/s.

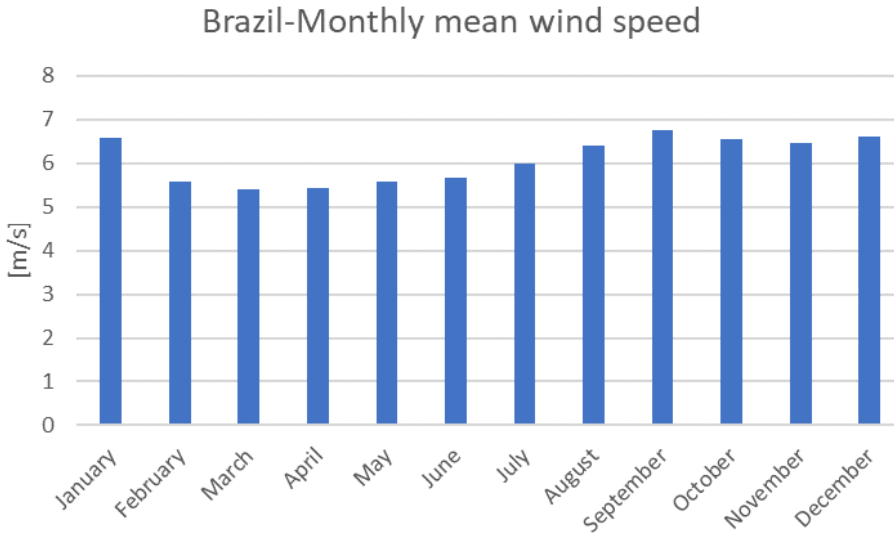


Figure 6.4: Brazil wind speed

### 6.3.2. Injection performance for Brazil location

In table 6.2 key performance parameters are indicated, and in figure 6.5 and 6.6 the performance of P1 and P2 is shown.

Table 6.2: Comparison of P1 and P2 in Brazil location

Parameters	P1	P2
Total barrels injected [Mbbbl]	12	12.6
Av. daily bbl injected	32860	34527
Non Injecting hours	3966	3721
Longest continuous downtime [hr]	71	67
# of stops	473	475
Ops strategy [hr]	1	1

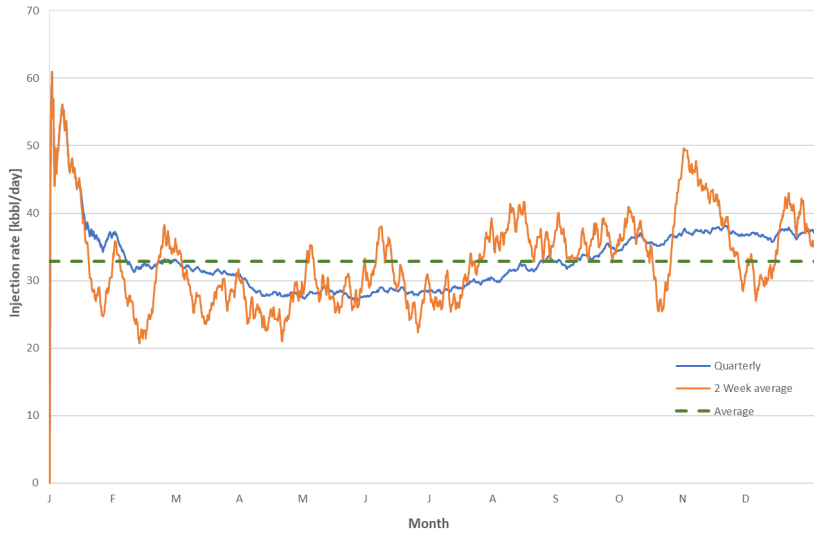


Figure 6.5: WIN-WIN performance with P1 configuration for Brazil site.

6

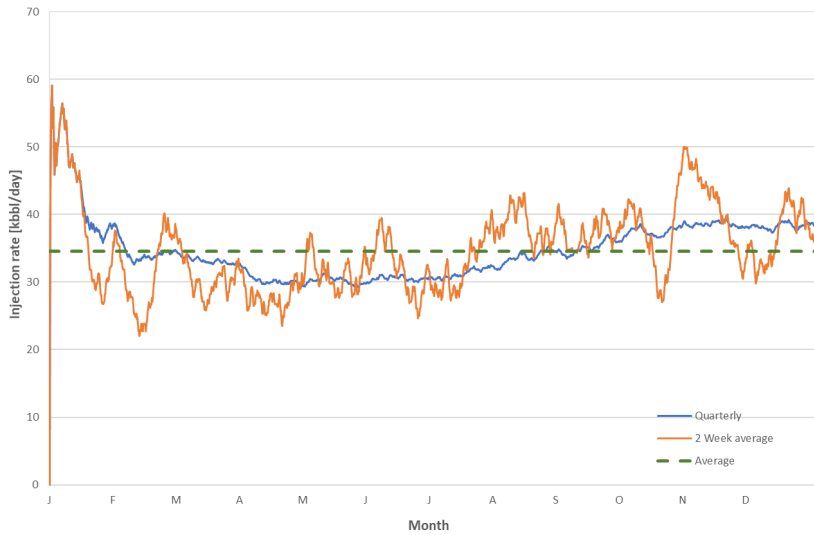


Figure 6.6: WIN-WIN performance with P2 configuration for Brazil site.

## 6.4. GoM

Here we present the results for the WINWIN unit situated in GoM

### 6.4.1. Wind conditions in GoM

In figure 6.7 the mean monthly wind speed for GoM is presented. The mean annual wind speed is 6.1 m/s.

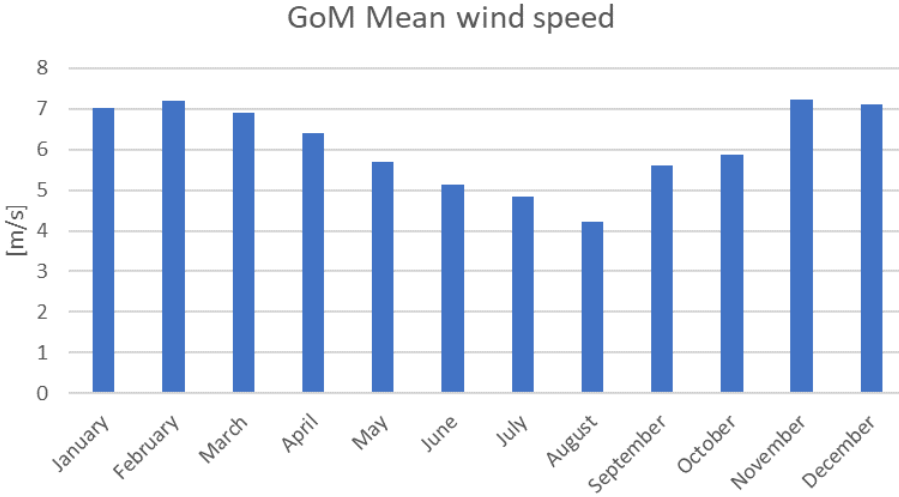


Figure 6.7: Mean wind speed GoM

### 6.4.2. Injection performance for GoM location

In table 6.3 the key performance parameters are shown, and in figure 6.8 and 6.9 the WINWIN injection performance for pump configuration P1 and P2 are shown respectively.

Table 6.3: Comparison of P1 and P2 in GoM location

Parameters	P1	P2
Total barrels injected [Mbbbl]	11.9	12.6
Av. daily bbl injected	32800	34485
Non Injecting hours	4250	3878
Longest continuous downtime [hr]	57	57
# of stops	494	492
Ops strategy [hr]	1	1



Figure 6.8: WIN-WIN performance with P1 configuration for GoM site.

6



Figure 6.9: WIN-WIN performance with P2 configuration for GoM site.

## 6.5. West Africa

In this section the WINWIN performance in West Africa is presented.

### 6.5.1. Wind conditions in West Africa

In figure 6.10 the mean wind speed distribute per month for West-Africa is shown. The annual mean wind speed is 3.6 m/s.

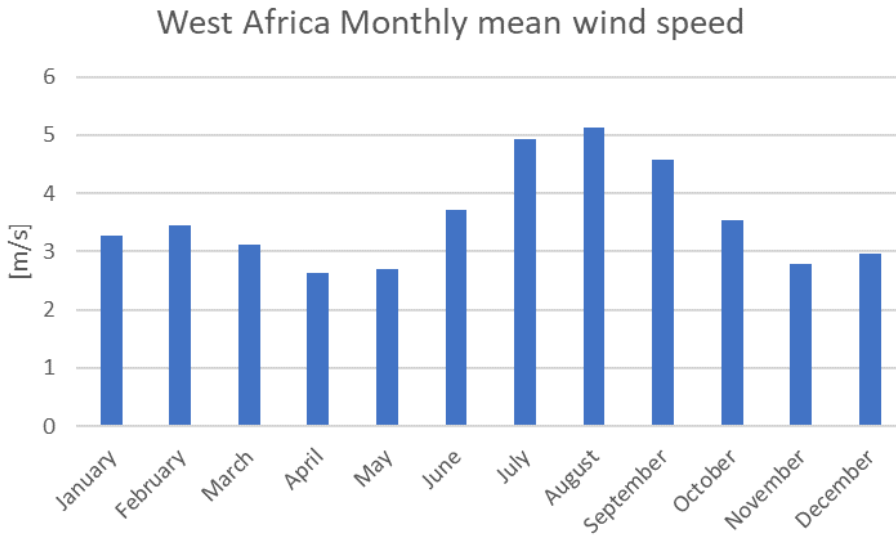


Figure 6.10: Mean wind speed in West Africa on a monthly basis

### 6.5.2. WIN-WIN performance in West-Africa

In table 6.4 a summary of the performance parameters are presented. In figure 6.11 and 6.12 the WINWIN injection performance for P1 and P2 configuration are shown.

Table 6.4: Comparison of P1 and P2 in West-Africa location

Parameters	P1	P2
Total barrels injected [Mbbbl]	3.1	3.7
Av. daily bbl injected	8528	10183
Non Injecting hours	7403	7089
Longest continuous downtime [hr]	383	232
# of stops	257	301
Ops strategy [hr]	1	1

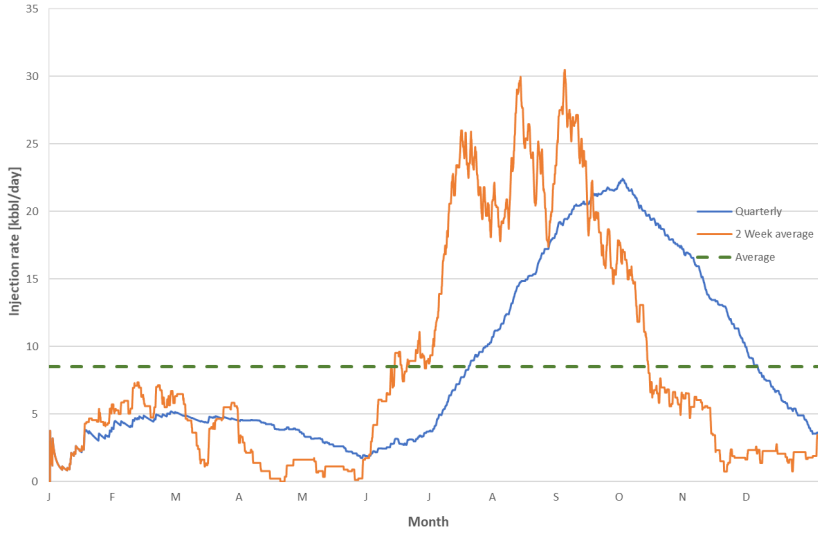


Figure 6.11: WIN-WIN performance with P1 configuration for West-Africa site.

6



Figure 6.12: WIN-WIN performance with P2 configuration for West-Africa site.

## 6.6. Analysis of the WINWIN performance results

In section 6.2 to 6.5, the performance of the WINWIN unit was analyzed for the pump configuration P1 and P2. Based upon the location and the site-specific wind conditions the performance of the WINWIN unit varies. The marginal wind conditions found in West Africa yielded 3.1-3.7 mbbl produced depending on the choice of pump configuration. While for the North Sea location a total of 18 mbbl was injected. Moreover, the seasonal wind conditions and consequently the variation in injection rates could be observed. Brazil has the most stable quarterly injection rates, with a difference in quarterly injection rates of only 10000 bbl. On the contrary, the Gulf of Mexico experienced a difference of over 21000 bbl on the quarterly average. Whether or not the reservoir tolerates the observed variations in injection rates is outside the scope of this thesis. However, it is recommended that this observation is included in future studies.

Table 6.5: Summary of performance results and capacity factor of wind turbine.

Site	Capacity factor Wind Turbine	P1 [mbbl]	P2 [mbbl]	Annual Mean Wind Speed [m/s]
North Sea	0.55	17.9	18	8.78
West Africa	0.09	3.1	3.7	3.6
Brazil	0.32	12	12.6	6.1
Gulf of Mexico	0.32	11.9	12.6	6.1

A summary of injection rates are listed in table 6.5. The relationship between mean annual wind conditions and total injection is important, where an increase in annual mean wind speed of 2 m/s could increase the total injection volume of approximately 6 Mbbl as demonstrated in table 6.5. From figure 7.3 it could be seen that P1 required more power compared to the P2 configuration. As the P2 configuration is comprised of one large and one smaller pump, this configuration is more optimized to handle the power output from the turbine, however the configuration is more vulnerable to pump failures as the P1 configuration has more redundancy due to two identical pumps. Furthermore, the operational range for the two systems was from 210-460 m<sup>3</sup>/hr and 240-480 m<sup>3</sup>/hr for P2 and P1 respectively. It was found for all cases and operational strategies that the P2 system had higher total injection volumes despite the lower injection rate capacity. This can particularly be observed for the locations with comparatively low wind resources. Moreover, as expected the P2 system had more operational hours compared to the P1 system, due to the lower power requirements. Thus a compromise arises where a trade-off against barrels injected and the operational wear and tear of the system must be considered. For instance for the Brazil case: Can the operator tolerate an offset of 600 kbbl injected in order to save 245 hours in pump operation? The P1 pump configuration operates for 245 hours less per year compared to the P2 configuration, however the P2 configuration are able to deliver 600 kbbl more per year. Also of consideration is the longest continuous downtime-numbers reported. This is related to the amount of battery capacity installed on the WINWIN unit. When no power is generated

from the wind turbine the battery must ensure standby mode on the pumps as well as supplying other load consumers such as communication and light, thus for cases where long down-times are experienced, such as the West Africa case, the WINWIN system will require appropriate sizing of the battery system. Lastly, the number of pump stops is also reported. This number indicates how many stops the pumps experience over a year. Shutdown and start also causes stress and tear on the pumps and should be minimized. Due to active hours of operation the P2 configuration experiences more pump stops, as for instance in the Brazil case where the P1 configuration experienced 257 stops, 301 stops for the P2 configuration. This should also be evaluated when selecting the appropriate pump configuration. Furthermore in appendix B the performance of the WINWIN unit when applying a 3 and 8 hr wind confidence interval is presented. This strategy is imposed to see the consequences of having such an operational scheme as it is desired to limit the start-up and shutdown of the systems. For instance the result for the North Sea yields a total injected volume of 12.1 mbbl for the P1 system and 12.4 for the P2 system when a wind confidence strategy of 8 hours are used. The number of stops are reduced to 246 and 243 times per year as compared to 419 and 405 times per year when the 1 hour wind confidence strategy is applied for pump configuration P1 and P2 respectively. The main conclusion from prolonging the wind confidence strategy yields fewer stops for the for the Pumps, however at a compromise of injection capacity.

## 6

Lastly, through the results presented in this chapter the injection performance of the WINWIN unit is demonstrated. It is believed that injection capabilities demonstrated in the North Sea, Gulf of Mexico and Brazil are of industry interest. In chapter 7 the economic performance of the WINWIN is analyzed, that will explore how the WINWIN compares to conventional methods of water injection.

## 6.7. Sensitivity analysis on performance-major repair

Until now the results presented do not account for scheduled or unforeseen maintenance incidents. WINWIN is designed to operate autonomously, yearly maintenance and unforeseen events are expected to occur. In the following section, we analyze how an incident will affect the performance. Although it is difficult to predict when such an event will occur, it is decided to run two scenarios. We simulate a major major failure will occur once during summer and once during winter. It is evaluated that Brazil and Norway pose as the most relevant areas for full-scale implementation based upon the injection rates above, furthermore the Norwegian government has strong focus on developing fields that has a low carbon footprint, which is exemplified by Hywind Tampen project discussed in section 2.1.2. In Brazil, it seems that an internal awareness of the relatively low recovery factor has increased attention towards implementing enhanced recovery techniques, this coupled with promising wind resources, Brazil serves as an exciting market for WIN-

	Summer		Winter	
	Normal	Failure	Normal	Failure
<b>Brazil [kbbl/month]</b>	962	945	789	743
<b>The North Sea [kbbl/month]</b>	1110	1032	1723	1395

Table 6.6: Modelled sensitivity analysis

WIN. The baseline scenario will compromise the following events;

- Major component failure, where WINWIN does not inject.
- Service personnel will be required through a chartered vessel sailing from nearest port.
- Maintenance will require 12 hr repair.
- An initial response time of 36 hr.
- For the event occurring due the winter season, a 3 day delayed response time is accounted for due to unfavourable weather.
- Winter incident is set to occur 1st of February, summer incident is set to occur 1st of July.
- Wind confidence strategy is set to 3 hrs.

The nearest port facility for the North sea case is Kristiansund, located 175 km away. Assuming vessel speed of 12 knots will lead to a transfer time of 7.8 hr. For the Brazil case that is located 100 km east of Rio De Janeiro results in a transfer time of 4.5 hr. Hence the total downtime for an incident occurring during summer results in 52.5 and 55.8 hrs for Brazil and North sea respectively. For a incident during winter yields a downtime of 127.5 and 124.5 hrs for North Sea and Brazil respectively. In table 6.6 the incident analysis and the effect of production is shown. It is shown that WINWIN performance is most affected if a major failure occurs during the winter season for the North Sea location. Here the output is reduced with 18.4 %. If the failure occurs during the summer months injection levels are reduced with 7%. For Brazil, the most severe reduction occurred during winter and yielded a reduction in output of 5.9%. For a failure during summer, yielded a reduction of 1.7 %. The seasonal variation concerning wind conditions is a natural explanation of these numbers. Moreover, the seemingly minor differences in weather conditions in Brazil allows for a more flexible maintenance approach, compared to the North Sea where there is a large seasonal difference, scheduled maintenance should preferably occur during the summer months. Through this simple analyses, the possible consequences of a major failure was demonstrated, where it could be observed that a failure occurring during the winter months for the North Sea location would influence the performance of the WINWIN unit the most. Furthermore, this high-level analysis serves as a first approach assessment to the WINWIN performance due to a failure. The complexity of a failure or expected downtime could be different from analyzed here. However for the purpose of this analysis it found sufficient.



# 7

## Economic analysis and preliminary design.

This chapter presents the economic analysis of WINWIN. First, the economic modeling approach is presented before a structured review and rationale of the individual cost components are outlined. It should be underlined that the assessment represents the authors view alone, and has no affiliation with DNV-GL.

### 7.1. Background

In chapter 4, the performance of WINWIN was evaluated under different wind conditions. In this chapter, the concept is assessed in terms of the economic viability. As previously mentioned, the WINWIN system allows for different water treatment processes, depending on the reservoir requirements, which can include de-oxygenation, sulfate removal, chemical injection or desalination. Here we will assume the base case, where filtered seawater is injected. Parameters that form the foundation for this analysis are presented in table 4.8.

The sections first explain the financial modeling procedure, then a breakdown of CAPEX and OPEX estimates follows, before a sensitivity analysis is conducted. It should also be noted that a short rationale is presented for the selection of appropriate technology - such as the choice of floating technology or type of anchor required.

### 7.2. LC-Method

In order to evaluate the economic performance of the WINWIN concept, this thesis implements the levelized product cost (LC) method proposed by [Reichelstein and Rohlfing-Bastian \(2015\)](#). The LC method is similar to the typically applied levelized cost of energy (LCOE) method, that is useful when assessing different energy gen-

erating technologies. However, in this context, the result will return cost per unit of a produced barrel. The LC method returns the break-even cost per unit of water produced and is referred to as the required revenue approach (Brown, 1994). This implies that the methodology returns the value that corresponds to a net present value equal to zero. However, it should be noted that the cost found only dictates the levelized cost of injecting water with the WINWIN unit; it does not account for the cost associated with the extraction platform or the injection well. As such, the LC cost described in this thesis can be regarded as a contribution to the overall break-even cost per oil barrel produced. The formula is given in the equation below, where the discount factor is represented by  $\gamma = \frac{1}{1+r}$

$$LC = \frac{\sum_{t=1}^T (c_t + w_t) \gamma^{-t}}{\sum_{t=1}^T k \gamma^t} \quad (7.1)$$

Where  $c_t$  is investments and costs in year  $t$ ,  $w_t$  represents operation and maintenance cost in year  $t$  including decommissioning, and  $k$  is the yearly amount of barrels produced.  $T$  represents the useful lifetime of the asset. The LC method presented above does not include tax attributions. The tax avoidance is justified as the WINWIN does not sell the produced units. Thus income tax would not be applicable. Moreover, LC methods often account for a capacity decline factor over asset lifetime. The capacity factor is assumed to remain constant over the project lifetime, and is not treated further.

### 7.2.1. Discount Rate

The discount rate represents the cost of capital. In essence, the present value of a cost occurring today is higher than if the cost would occur in a year's time, meaning that money has time value. The discount rate expresses the expected return on investment. Thus, for low-risk projects, one can assume a lower discount rate, while for high-risk projects, companies typically demand a higher discount rate.

The LC method yields a break-even price which implies that the business debt over total assets ratio remains constant. In this context, finance theory suggests that the appropriate discount rate is the Weighted Average Cost of Capital (WACC) method (Comello et al., 2017). In figure 7.1, Hundleby (2016) demonstrated the influence of the discount rate (WACC) on the LCOE results for a typical offshore wind-project, with typical CAPEX and OPEX values. Here one can see that a discount rate of 10% can contribute to approximately 50% of the LCOE, thus deciding the appropriate discount factor is of high importance when evaluating any project. The WACC must be calculated based upon the firm's financial status. For the context of this thesis, the suitable discount rates were found in the literature. GrantThorton (2017) conducted a market survey obtaining discount rates for four segments of renewable energy projects. The segments were solar, onshore wind, offshore wind and hydro. The four projects were carried out in 12 countries considered to be developed countries. Here the discount rates applied to hydro projects were lower compared to onshore and offshore wind, as the risks associated are lower. The discount rates

for offshore wind are in the range 6.25%-8.25%. Considering that the WINWIN is a floating installation we can assume a discount rate of 9%. The influence of different discount rates will also be evaluated.

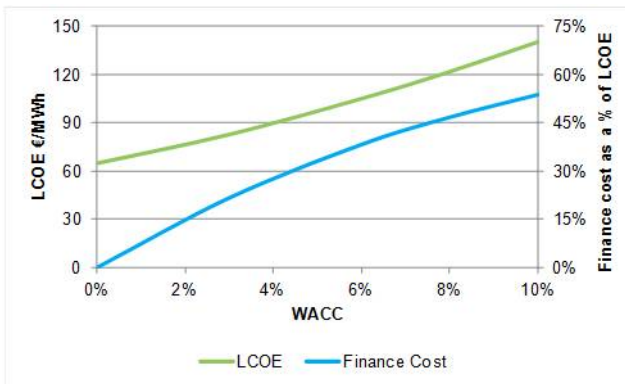


Figure 7.1: Cost of capital as a percentage share of LCOE (Hundleby, 2016)

### 7.2.2. Assumptions and specifications

In this analysis, WINWIN is assumed to be directly positioned over the injection well. The injection capacity is as identified in the Tyrihans case where WINWIN injected 49000 BBL/day on average. Yearly injection rates are assumed to remain constant over project lifetime. Furthermore, the analysis assumes that the floating substructure is compatible with the modifications required to accommodate the WINWIN components, and that the concept is technically feasible. Thus the hydrodynamic stability is not compromised. Lastly, it is suggested to use a discount rate of 9%. Specifications and assumptions regarding the alternative solution are stated in section 7.6.

## 7.3. Capex Breakdown and choice of technology

In the following subsections the CAPEX breakdown is presented. The CAPEX represents the aggregate total costs of the project.

### 7.3.1. Choice of Substructure

Several types of floating technologies are applicable; first, there will be an evaluation of the appropriate substructure to use in the WINWIN concept, and then the cost will be assigned.

Today, floating offshore wind concepts have predominantly utilized either a spar-buoy or a semi-submersible concept for the substructure. Other concepts are available, such as the tension leg platform or a barge concept. However, we will only consider the spar-buoy and the semi-submersible technology, as these have reached commercial deployment. WindFloat is a company that makes use of a

semi-submersible floating technology, and has successfully completed a five year testing phase of a 2 MW turbine with satisfactory results (Principle Power, 2016). The spar-buoy concept was applied in the Hywind-Scotland project, which is also known as the first commercial floating wind farm. Semi-submersibles use buoyancy for stabilization, which in turn requires a complex steel-intensive substructure. The total mass of the semi-submersible used in the WindFloat concept was estimated to be 2500 tons (Myhr et al., 2014). Being buoyancy based, a semi-submersible has a low draft compared to the spar-bouy for instance; this in turn implies that the semi-submersible is easy to tow. IRENA (2016) summarized the advantages and disadvantages of the two technologies. A compiled version is presented in table 7.1.

Table 7.1: Evaluation of floating technology concepts, adapted from IRENA (2016).

Technology	Pros	Cons
<b>Spar-buoy</b>	<ul style="list-style-type: none"> <li>-Good hydrodynamic behaviour.</li> <li>-Simple design.</li> <li>-Low installation costs.</li> </ul>	<ul style="list-style-type: none"> <li>-Requires heavy offshore lifting during installation, only possible in sheltered deep water.</li> <li>-Requires deep waters (&gt;100 meters).</li> </ul>
<b>Semi-submersible</b>	<ul style="list-style-type: none"> <li>-Constructed in dry dock.</li> <li>-Low draft.</li> <li>-Suitable in shallow waters (&gt;40 meters).</li> <li>-Low installation costs.</li> </ul>	<ul style="list-style-type: none"> <li>-Motion response from waves.</li> <li>-Steel intensive.</li> <li>-Complex fabrication.</li> </ul>

The Hywind concept has been commercially deployed in Scotland, where five turbines with a capacity of 6 MW each provide energy to Scottish households. Since Hywind has reached a more developed technological stage compared to the WindFloat concept, it is decided that WINWIN will use a spar-buoy as the floating substructure. The spar-buoy concept is the only substructure that has successfully demonstrated its commercial potential at MW scale required for the WINWIN project. Moreover, as highlighted in table 7.1 the spar-buoy concept exhibits a more favourable hydrodynamic behavior and a simple design compared to the semi-submersible.

In table 7.2 a few parameters used in assessing the substructure and tower assembly costs, are shown. The numbers indicated are obtained from Equinor, the project owner of the Hywind-Scotland project, and are therefore believed to give an accurate estimate of the particulars listed. Lastly, the WINWIN model requires an additional modification to accommodate the water injection system. It is concluded that the system would require a total deck-space of 24 square meters. The deck-structure should be constructed just above the transitional piece.

### 7.3.2. Cost of substructure

The main drivers related to estimating costs for the substructure are the cost of steel and the required manufacturing and assembly process. Myhr et al. (2014) proclaimed that the labor cost equivalent to the material costs under the assumption of non-complex structures. The steel costs were estimated to 1000 €/ton. However, a manufacturing complexity factor of 1.2 is proposed. The factor reflects the manufacturing complexity of the spar-buoy design, including the required platform deck. In comparison Myhr et al. (2014) suggested a complexity factor of 2 for

Rotor diameter	75 m
Tower	83 m
Max tower diameter	7,5 m
Tower Mass	670 tons
Substructure length	91 m
Substructure diameter	14 m
Substructure mass	2300 tons
Mooring chains	2400 m
Mooring mass	1200 tons
Suction anchors	900 tons

Table 7.2: Hywind-Scotland 6 MW turbine parameters, water depth 90-120 meters. Please note that mass given represents total mass required. (Equinor, 2015)

a semi-submersible substructure. Thus manufacturing cost is 1200€/ton. These valuations include all aspects of the construction and assembly process, and the sub-structure is assumed complete and ready for float out.

Concerning the accuracy of the steel cost, manufacturing expenses and the complexity factor, Myhr et al. (2014) indicated no sources; however as stated in the article, no negative feedback was given by the stakeholders involved.

Finally, the deck assembly required for the WINWIN system is estimated to increase the total weight by 4% of the substructure with reference to the Hywind spar-buoy found in table 7.2. Thus the total material consumption is 2392 tons for the substructure. The manufacturing and steel costs are found in table 7.3.

Table 7.3: Substructure cost estimates

Substructure Mass [tons]	2392
Steel cost [k€]	2392
Manufacturing cost [k€]	2870.4
Complexity	1.2
Total Cost [M€]	5.3

### 7.3.3. Mooring lines

The mooring system is required to maintain the translational and rotational movements of the floater within acceptable limits. Several types of mooring configurations are available. Catenary, taut leg and tension leg mooring systems are the most widely used concepts. The catenary mooring system consists of free hanging lines, where gravity imposes a restoring force on the floating unit. The mooring lines in the taut leg system are pre-tensioned and are anchored at an angle between 30-40° to the seabed. The tension in the chain provides the restoring force. Lastly, in the tension leg mooring system, the wires are tensioned through buoyancy of the floating unit. The tension restricts the horizontal movement to a minimum and

heave, pitch and roll motions are considered almost negligible (ABC-Mooring, 2015).

The suitable mooring configuration depends on the type of floating concept. For the spar-buoy technology, a catenary mooring solution is typically considered (Campanile et al., 2018). For the Hywind-Scotland case, Equinor used a catenary mooring system. As indicated in table 7.2 we see that each mooring line was 900 meters with a weight of 400 tons per chain. It is therefore decided that the cost estimate should be based using a catenary mooring system.

Campanile et al. (2018) researched the catenary mooring requirements for a 5MW offshore semi-submersible turbine, in water depths varying from 50-80 meters and 200-350 meters. The mooring line requirements at 80 meters resulted in a line of 322 meters and a total chain mass of 771 tons. In comparison, the Hywind-Scotland catenary moorings mass were 1200 tons, which is a 55% difference in mass. One would assume that the ballast-stabilized spar-buoy would require less mooring than the buoyancy based semi-submersible where movement due to hydrodynamic responses are expected to be higher. It could be reasoned that the Hywind-Scotland utilized higher factors of safety. Moreover, there is a difference in the turbines used and water depths (120 vs 80 meters). Detailed engineering of mooring lines are considered outside the scope of this thesis.

Interestingly, it was found that the required mooring weight and consequently the cost, was reduced from 50 meters to 80 meters of water depth. The wave forces can briefly explain this phenomena; when the floating system is subjected to wave loads, the system will move. In shallow waters, the proportion of the mooring lines lifted from the seabed will be higher than in deep waters. The mooring lines are therefore more exposed to the wave loads which will require appropriate dimensioning of the mooring lines. For the water depths 200-350 meters the requirements concerning chain mass increased. As such, indicating a "sweet spot" where a cost reduction in mooring expenses can be achieved as illustrated in figure 7.2. It should be noted that the costs illustrated represent the total mooring costs and are not given per line basis.

In order to estimate the required mass for the WINWIN unit, we apply a semi-empirical approach. The Hywind-Scotland project required a mooring line length of 900 meters, with a total mass of 1200 tonnes at a water depth of approximately 100 meters. Contrary to this, Campanile et al. (2018) estimated a line length of 602 meters, and a total mass of 950 tons at a water depth of 200 meters for a semi-submersible. From these numbers, it can be reasoned that a spar-buoy would require more mooring mass compared to a semi submersible. It is also recognized that the catenary mooring system applied in the Hywind-Scotland case could be optimized further. It is therefore proposed to use a mooring line system with a total mass of 1200 tons. We apply the same cost assumed by Campanile et al. (2018), namely 2000 €/t. The resulting mooring line cost is then 2.4M€. This does not account for installation.

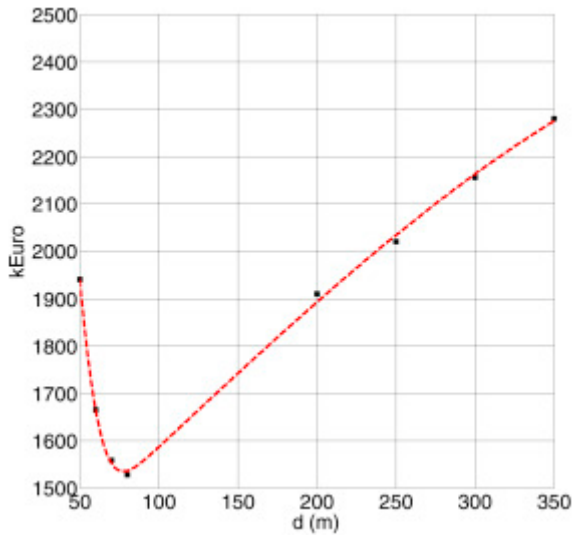


Figure 7.2: Mooring costs predictions as a function of water depth, where the price per ton is 2000 € (Campanile et al., 2018).

#### 7.3.4. Anchors

The anchor is attached to the mooring lines and must provide resistance to the pulling loads. Several types of anchors are available and compatible with floating offshore wind. Here, two types of anchors are considered, albeit at a high level. Usually, three anchors are required per floating unit. The first anchor to be considered is the drag embedment anchor, which is partly or wholly submerged in the seabed. The resistance of the soil in front of the anchor provides the holding capacity in the horizontal direction. The embedment anchor has limited resistance against vertical loads. The second anchor type considered is the suction anchor, and as the name implies, it relies on suction forces. The suction anchor is a cylinder with one open end that is placed on the seabed. The water is sucked out, and the difference in pressure drives the anchor down, which results in good horizontal and vertical load carrying capacity (Vryhof, 2015).

As the drag embedment anchor provides limited vertical resistance, it is considered unsuitable for the WINWIN concept. This is reasoned by the level of redundancy required in the anchor and mooring system. If for instance, a situation occurs where an anchor is lost, the suction anchors will provide more system redundancy compared to the drag embedment anchors. Moreover, the WINWIN unit is likely to operate in the vicinity of a production platform where any encounters could lead to severe consequences, hence strict requirements are placed on the load carrying capabilities of the anchors, where suction anchors are the for now, best option.

In literature, the price of suction anchors varies. Kjelstad (2018) stated that the

cost was five times higher than a drag anchor, which translates to 13,5€/kg. While Myhr et al. (2014) assumes a price of 10,25€/kg. This thesis assumes a price of 12€/kg. Uncertainty regarding the dimensions - and consequently, the total mass - is subjected to different ideas; Equinor (2015) stated a total mass of 300 tons per anchor, thus 900 tons in total. Arany and Bhattacharya (2018) estimated the dimensions required for the Hywind-Scotland suction anchors, and taking the same case specific properties, Arany and Bhattacharya (2018) concluded a total mass per anchor of 100 tons. Assuming a constant steel density of  $8050\text{kg}/\text{m}^3$  gives a total weight for the three anchors of 300 tonnes. Lastly, (Myhr et al., 2014) assumed the total mass of the suction anchor to be 140 tons for the TLP-Sway concept, and it was assumed that only one anchor was required.

To conclude, it seems that different opinions regarding the required dimensions and estimates of the suction anchor are present. Possibly one can explain the numbers given by Equinor (2015) due to high factors of safety given the novel application. Inconsistency among the theoretical mass estimates required is also remarkable. A TLP anchor is subjected to higher forces in the horizontal direction, compared to a spar-buoy using catenary mooring lines, where horizontal forces are limited but also divided on at least two anchors. It is therefore interesting that the TLP-Sway concept requires less anchor capacity. It is however, recognized that the holding capacity of the anchor depends on soil conditions; yet at a high-level study - as carried out by the aforementioned authors - the difference is interesting. For this cost analysis, we assume a design optimization process of the suction anchors' mass given by Equinor (2015) with a reduction in total mass of 50%, where the individual anchor mass is 150 tons and that the WINWIN unit will make use of three suction anchors. The total price for the suction anchors is 5.4M€

7

### 7.3.5. Rotor, turbine and tower

The turbine cost builds upon the estimate performed by (Stehly et al., 2017), where seven offshore wind projects with a total capacity of 1,19 GW, disclosed their financial sheet. The capital cost of a turbine was found to be 1,31M€/MW (1€=0,87\$). The total turbine cost yields 7,86M€. It is assumed that the cost includes the tower, and the required bottom design of the tower to be mated with the substructure.

### 7.3.6. Pump systems and auxiliaries

The pump system is an integral part of the WINWIN concept. The technical aspects of the pumps are given in section 4.2. As stated, the power requirements of the different pump solutions proposed are similar, and we therefore assume a pump rating of 3 MW. The proposed pump systems costs are confidential, and DNV-GL has not declared the costs to the author. Hence, the approximate costs of the system are given by the equation 7.2 as proposed by Almasi (2014).

$$C = A \cdot P + B \quad (7.2)$$

Where factor A accounts for auxiliaries like piping, foundation and steel structures for the pump, and B represents auxiliaries for the whole pump unit, such as

unit electrical facilities, unit protection systems, and P is the pump cost.

For a 3 MW pump package, [Almasi \(2014\)](#) assumed a price of 0.9M€ with an A and B factor corresponding to 1.67 and 1.3M€ respectively. The total cost of the pumps and auxiliaries then amount to 3.9M€. Also, the lift pumps that are responsible for supplying the injection pumps are proposed to add an total cost of 1.5M€.

### 7.3.7. Battery and electrical infrastructure

During low wind periods, the WINWIN system does not inject; however, the system will require energy to ensure the integrity of safety systems, such as communication, lighting, bilge and ballast systems. Heating and ventilation are some of the load the battery must serve during non-generating hours. During non-generating periods it is assumed that the system will require a of capacity 20 kWh/day. Furthermore, during phases of operation, battery power is required to start up the system and close down the system. No detailed assessments of the loads are provided in here. However, it is reasonable to assume an installed battery capacity of 500 kWh, (excluding the required non-generating capacity) that is dependent on the number of non-generating hours, and will depend on the site-specific conditions.

With regards to the type of battery technology required, WINWIN must find the optimum compromise between cost, weight, and space utilization. It is desired to minimize the overall footprint, and also the weight, as this will reduce the required steel for the substructure. For market competitiveness, the cost is of course relevant. Besides, battery technology is subjected to several factors that must be considered. For example, depth of discharge, cycle life, and safety aspects to name but a few. In table 7.4 some specific properties related to lead acid and lithium batteries are listed.

Table 7.4: Properties of Li-ion and Lead acid batteries. Adapted from [IRENA \(2017\)](#)

Parameters	Lead Acid	Li-ion
Energy density [Wh/L]	50-100	200-600
Specific energy [Wh/kg]	33-42	100-265
Cost 2016 [€/kWh]	91-415	175-610
Expected cost 2030 [€/kWh]	50-240	60-261

As can be seen, the cost of Li-ion batteries is likely to undergo a significant reduction in the coming decade. However, the current price of Li-ion batteries, suggest that lead-acid batteries should also be considered, despite the considerable weight difference. In table 7.5 a comparison of the different technologies can be found. As stated above, the energy requirements of the WINWIN unit when it is operational are 500 kWh. This is required to, for instance, start and shut down the pump system, yawing and pitching the turbine and maintaining system readiness; as such the battery should always have 500 kWh available. After the battery has initiated the start up procedures and served the necessary loads, the control logic

should ensure that the battery is re-charged within a reasonable period by the power generated from the wind turbine. When there is no wind, however, we must add additional capacity to ensure that the battery is fully charged (i.e. 500 kWh) to be able to start up the system again. As stated, we assume that the system is consuming 20 kWh/day. We suggest a conservative no-wind period of 96 hrs. Thus the installed battery capacity is 580 kWh.

Table 7.5: Comparison of lead acid and Li-ion batteries.

Parametres	Lead Acid	Li-ion
Installed capacity [kWh]	1160	725
Usable Capacity [kWh]	580	580
Weight [t]	35,2	7,25
Volume[m <sup>3</sup> ]	23,2	3,625
DOD[%]	50	80
Cycles	2400	2400
Cost [€/kWh]	150	400
Round Trip Efficiency [%]	90	96
Total Cost [€]	174000	290000
Cost per cycle [€/kWh/cycle]	0,139	0,2170

From table 7.5, the lead-acid battery proves to be the most cost-effective solution despite its shortcomings concerning cycle efficiency and allowable depth of discharge. The total weight and space required might demand notable adaptations to the spar-buoy structure. Hence the Li-ion battery technology is preferred.

7

To facilitate the battery, the WINWIN requires an electrical system to expedite the energy sources and loads. The electric system is comprised of several components, such as switchboards, converters, dump load facilities, and grid control systems. Without further explanation, it is assumed that this cost amounts to 1,5M€.

### 7.3.8. Control Systems

The autonomous operating mode requires a continuous monitoring and feedback system in order to safely operate the unit. This includes appropriate control systems for the water injection process, micro-grid stability, and in brief, all sensory equipment and control units to allow the unit for autonomous operation, with the possibility of being remote-controlled. According to DNV-GL experts this would amount to 1,5M€.

### 7.3.9. Injection Well and riser

The riser transports the pressurized water down to the injection well. The water depth is assumed to be 200 meters. It is also assumed that the WINWIN platform is situated in close horizontal distance to the injection well. However, the riser must tolerate movement from the platform, hence a safety margin of 1,2 is added to the total length. The cost for the riser is subjected to uncertainty, due to the

novel application of technology and limited available data. Therefore it is proposed a total cost of the riser to 3M€. The estimate is based upon the complexity and level of required safety measures that must be built into the riser. This includes the control mechanism to open and close the flow, and a control umbilical to enable communication with the wellhead.

Lastly, the cost estimate does not include the associated drilling cost and subsequent well. It is assumed that this is already in place. Furthermore, it is also avoided, as estimating well and drilling costs is case-specific. For the two solutions evaluated here namely the conventional way and WINWIN system, the cost of the well is identical.

### 7.3.10. Development cost

The previous subsections have described and estimated typical hardware components. Other costs to consider, are engineering and development. For a floating offshore project, NREL (2018) estimated the cost of engineering and development to 3,3% of total CAPEX. As WINWIN is untested, detailed engineering is required at all interfaces of the project. Varying from a complex microgrid infrastructure, to floating offshore wind in combination with oil and gas requirements. The proposed percentage for development costs will amount to 12,5% of total CAPEX. The cost calculated is then 6,475M€. Assuming a typical rate of an engineer of 180€/hr, yields 36000 hrs in development work.

### 7.3.11. Installation and assembly

The installation and assembly process of the Hywind-Scotland is well documented in online promotional videos. The information obtained from these videos is used as the foundation for the installation and assembly process. The WINWIN assembly dock is located in Kristiansund, Norway. It is assumed that the dock facility has sufficient water depth to accommodate the installation and assembly phase. This is a reasonable assumption, as the port is equipped to facilitate offshore activities. Lastly, it is assumed a 100% weather window for simplicity. The assembly line process is presented as a Gant chart in figure 7.3.

From the Gant chart it is clear that the assembly and installation of a floating turbine unit require assistance from several types of vessels and lifting capabilities. Estimating a vessel's day rate is challenging due to the cyclic nature of this market. Nevertheless, in the following section, an estimate is provided. Assembly and installation is categorized into three phases: transportation, assembly/ float out, and hook up.

**Transportation costs:** Cost of transportation is included in this analysis, as it is assumed that the worked out costs in the sections above, do not include delivery to site. The substructure, the anchors, and the mooring chains are manufactured in Ferrol, Spain. Although a range of possible manufacturers for these components exists, it is favorable to utilize the expertise acquired by the manufacturers from the Hywind-Scotland project. The turbine blades, the tower, and the nacelle, are manufactured in Denmark, and transported from the port of Frederikshavn. The



Figure 7.3: Proposed Gant chart of assembly line process for the WINWIN unit.

cost of transportation is based on an assumed day rate for the vessel required, and the corresponding speed and distance traveled. The costs of transporting the components to the assembly port in Kristiansund are shown in table 7.6

Table 7.6: Expected transportation costs. Day rates include fuel and personnel costs, and are provided by [Fairstar NV \(2011\)](#)

Type of vessel	Component	Speed [km/h]	Distance [km]	Day rate [€/day]	Cost [k€]
Heavy transport Vessel	Susbstructure	24,1	2678	50000	231,73
Heavy transport Vessel	Anchor and mooring	24,1	2678	50000	231,73
Heavy transport Vessel	Blades, nacelle and tower	24,1	1015	50000	87,82

**Assembly:** Once the transported components arrive in Kristiansund, the assembly process can begin. Note that the pumps, battery and microgrid configuration are pre-assembled. The turbine components are assembled in an upright position at the dock. It is assumed that this operation will require two days with a land-based crane arrangement.

The substructure is first ballasted with water before additional ballast is loaded in by a crane vessel. Then the submerged substructure should be anchored to limit movement during the mating process. This operation requires a floating barge, three tugboats to maintain stability, and an anchor-handling vessel. The expected duration for this operation is estimated at four days.

The mating and lifting procedure is a highly complex engineering challenge. This is due to the high center of mass, and also because the center of mass is in front of the vertical lifting direction. The offset provides a horizontal moment when the turbine is lifted and therefore requires substantial crane capacity. Also, the height

of the turbine makes the lift more challenging. In figure 7.4 the magnitude of this operation is illustrated. The picture depicts the mating process of the 6 MW Hywind-Scotland project. The heavy lift vessel acquired in the Hywind-Scotland project was the Saipem 7000, which has a lifting capacity of 14000 tons. Considering that the turbine assembly weighs approximately 1020 tons, it is clear that this is not the optimal vessel for the job. However, due to the challenges mentioned, this is the only vessel that is capable of performing the job securely. The lifting of the turbine and subsequent mating are estimated to require one day in total. We also assume that the heavy lift vessel is in close proximity and that the mobilization time is zero. This can be justified as the port of Kristiansund is home to significant oil and gas activities, where heavy lifting operations are typical, we therefore assume that a heavy lift vessel is readily available. In addition, three tugboats on standby are required. The costs concerning the assembly process are given in table 7.7.

Table 7.7: Cost estimate for for the assembly process.

Vessel type	Day rate[€/day]	Days required	Total cost [k€]
Tugboat (x3)	18000	5	270
Anchor handling	60000	4	240
Barge	35000	7	245
Heavy lift	600000	1	600
Onshore Crane	5000	2	10



Figure 7.4: Mating of the tower-nacelle assembly with floating substructure (Håkonsen, 2017). Day rate for Saipem 7000 is around 630k€ (Bjørheim, 2015)

**Float out and hook up:** After the mating of the substructure and turbine, the WINWIN unit is ready for the final transportation leg. Three tugboats are required

in addition to the towing vessel. This task can be performed by the anchor handling vessel. The route chosen should be carefully assessed with respect to water depths. Furthermore, the towing speed should not exceed 5 knots. The distance from Kristiansund to the chosen area in the North Atlantic sea is 135 nm. Once the WINWIN unit has arrived at the final location, the assistance of the tugboats is no longer required, and the WINWIN is connected to the mooring lines and the injection system. This procedure is estimated to be completed in one week. Costs are presented in table 7.8. Note that the cost of the anchor handling vessel is given for the entire duration. Installation of suction anchors are also estimated to require seven days. Due to the significant weight of the anchors and mooring lines, this procedure requires an installation vessel with lifting capacity. Such a vessel could be the Oleg Stashnov with a typical day rate of 400k€/day (Hoeksema, 2014).

Table 7.8: Float out and hook up costs.

Vessel	Distance-one way[km]	Speed [km/h]	day rate [€/day]	Cost [k€]
Anchor handling	250	9,3	60000	555
Tugboat	250	9,3	18000	121,5
Heavy lift vessel	250	22,2	400000	3175

### 7.3.12. Summary Of CAPEX

In table 7.9 a summary of the CAPEX cost breakdown is outlined.

Table 7.9: Summary of CAPEX costs.

Item	Cost [M€]	Percentage of total cost [%]
Substructure	5,7	9,83
Mooring	2,4	4,11
Anchor	5,4	9,25
Turbine	7,9	13,46
Injection pumps	3,9	6,68
Lift Pumps	1,5	2,57
Microgrid	1,5	2,57
Battery	0,3	0,50
Control System	1,5	2,57
Umbilical and riser	3,0	5,14
Development	6,6	11,33
Installation	5,22	8,93
Contingency	13,5	23,08
Total	58,4	100,00

A contingency clause of 30% is added to account for the uncertainty in the cost estimates. A direct verification of the project cost estimates, to a typical floating offshore wind turbine project, is challenging due to the different applications of the technology. However, on a finance percentage basis, a high level comparison can be made. NREL (2018) estimated the cost of a floating offshore wind park located

in US waters. Here it was found that the expected cost (considering the floating substructure, including mooring and anchors) was higher in relative percentage to the wind turbine cost. This is also found in this thesis. Regarding the other cost components, high levels of uncertainty can be expected. For instance, in estimating the installation costs, downtime due to weather was not accounted for. However, the author has referred to experts in DNV GL when appropriate, and confirmed that the costs are reasonably estimated. Finally, it is expected the CAPEX installments are divided over three years with the following percentage proportions 20%, 45%, and 35% in year one, two and three respectively.

## 7.4. Operation and maintenance

One of the main challenges concerning offshore wind - and therefore the WIN-WIN concept - is related to operation and maintenance. Harsh weather conditions, limited accessibility, and high costs of repairs are some of the concerns for the operators. The operation and maintenance schedule has been reported to account for 25-30 % of the cost of energy for offshore wind turbines (Wiggelinkhuizen et al., 2008). One of the aspects that make maintenance challenging is the sea states. Expected sea states and concerns are addressed in the next section, thereafter follows the maintenance schedules, and a cost appraisal.

### 7.4.1. Sea states

Compared to onshore turbines, offshore turbines are exposed to environmental loads that are challenging to design for. Seawater and humidity could lead to corrosion of vital parts, and weather conditions provide limited accessibility. The accessibility to the turbines is often dictated by the significant wave height ( $H_s$ ). The significant wave height corresponds to the average wave height of the 1/3 highest waves. To enable safe crew transfer and the safety of the marine operations, vessels declare their working capability with respect to the significant wave height ( $H_s$ ). Offshore turbine service vessels can typically operate up to 3m  $H_s$  (ECN, 2016). In table 7.10 the significant wave height in the North Atlantic is shown.

Table 7.10: Seastate and significant wave height ( $H_s$ ) of the North Atlantic ocean. Adapted from Faltinsen (1990).

Sea State	Wave characteristics	% of time	Average $H_s$ [m]
1	Calm	0,7	0,05
2	Smooth	6,8	0,3
3	Slight	23,7	0,88
4	Moderate	27,8	1,88
5	Rough	20,64	3,25
6	Very rough	13,15	5
7	High	6,05	7,5
8	Very High	1,11	11,5
>8	Phenomenal	0,05	>14

For the North Atlantic, where the WINWIN unit is located, it is expected that a  $H_s > 3\text{m}$  around 40% of the time. Which implies that the WINWIN is accessible 60% of the time. The sea state is subjected to seasonal variations, where one can expect more accessibility during the summer months. For the maintenance and operational analysis, the weather window is included, unlike in the CAPEX analysis. This can be justified as the contracts in the CAPEX phase typically are signed on a fixed rate basis.

#### 7.4.2. Maintenance philosophy

The maintenance approach and philosophy can be subdivided into two categories: preventive and corrective maintenance, as proposed by [Wiggelinkhuizen et al. \(2008\)](#). The preventive maintenance approach is based upon fixed time intervals, or dictated by the numbers of hours in operation the component has operated. The corrective maintenance approach evaluates the health condition of the system, and maintenance is undertaken to prevent failures in the system accordingly. Unforeseen failures of components are also considered a subsection of the corrective maintenance approach.

#### 7.4.3. Scheduled maintenance

Due to the variable output of the WINWIN unit, planned maintenance should be scheduled during low wind conditions. Furthermore, the intricate system topology of the WINWIN unit implies that scheduled maintenance should at least be performed every quarter. It is assumed that the preventive maintenance can be carried out with personnel from the mother platform. An appropriate vessel for this operation would be a modified platform supply vessel (PSV). Usually, platforms tend to have PSVs on standby to perform daily routines. However, the PSV should be adapted to allow for crew transfer, to facilitate access to the WINWIN unit. This can be done by installing Ampelmann technology. It is decided to assume a vessel day rate in this analysis, although the vessel is chartered by the platform operator, where in that case, it would be challenging to assign an appropriate monetary term to the scheduled maintenance operation. Lastly, the preventive maintenance scheme will not be subjected to operational weather windows, as the preventive maintenance can be carried out within a certain time frame. It is expected that each trip will take one day.

In addition to the scheme outlined above, the mooring lines and the substructure are required to be inspected every five years according to DNV GL experts. The mooring lines and substructure should be subjected to a visual inspection to assess the integrity of the components. Considering that the lifetime of the WINWIN unit is 20 years, this must be carried out four times during its lifetime. To perform inspections of the mooring lines and substructure, an ROV is required. It is assumed that this operation is not subjected to the weather window, as long as the inspection is carried out within the time frame of five years. Nonetheless, an ROV requires a specialized vessel. The expected inspection rate for the ROV would take two days per mooring line, and two days to inspect the substructure. In addition, two days

are added for the vessel to mobilize, and for unforeseen downtime. Expected costs are listed in table 7.11, and given per trip basis. The total expected maintenance cost per year is 160k€/yr and 770k€ every five years.

Table 7.11: Expected cost for preventive maintenance and the five year scheduled hull and mooring line inspection.

Vessel	Day rate [€/]	Expected duration	Total cost [k€]
PSV	40000	1	40
PSV w/ROV	55000	10	550

#### 7.4.4. Unscheduled maintenance

Despite undertaking a rigorous maintenance schedule with quarterly intervals, failures and breakdowns are expected. Faulstich et al. (2010) summarized the operational data and maintenance reports obtained from 1500 onshore wind turbines in the period from 1989-2006. This is equivalent to 15357 turbine-years. The predicted failure rates and downtime due to the particular failures are shown in table 7.12. It is recognized that the data obtained are subjected to technological improvement. Consequently, operational data concerning technical availability might be higher today. The numbers stated therefore represent a conservative estimate. It is also worth noting that the data is obtained from onshore turbines, and as such may not be directly representative for offshore wind turbines, particularly not for floating wind turbines. Nonetheless, offshore wind turbine technology is similar to onshore wind turbines, and similar failure rates could be expected. The data presented is therefore found adequate to be implemented in the analysis.

Table 7.12: Reliability and expected downtime due to failure for offshore turbines. Adapted from Faulstich et al. (2010). Pump reliability is found in Shao (2009)

System	Failures[p.a.]		Downtime[days]	
	Minor	Major	Minor	Major
El. System	0,45	0,12	0,17	6,55
El. Control	0,34	0,09	0,15	6,87
Sensors	0,2	0,05	0,16	6,41
Hydraulic System	0,18	0,05	0,18	5,93
Yaw system	0,13	0,05	0,16	10,09
Rotor Hub	0,12	0,06	0,18	10,93
Mech. Brake	0,11	0,03	0,16	13,08
Rotor Blades	0,09	0,02	0,18	11,86
Gearbox	0,06	0,03	0,17	18,38
Generator	0,07	0,04	0,15	14,34
Support & housing	0,08	0,02	0,14	28,01
Drive Train	0,03	0,02	0,17	15,47
Pumps	0,85	0,52	3,75	6,4

The failure rates are categorized by the severity of incidence, where minor failures typically correspond to a downtime of less than one day. Major failures are expected to take more than one day to repair. This does not apply to the pumps where Shao (2009) found that the expected downtime for a major and minor failure resulted in a downtime of 6.4 and 3.75 days respectively. In total, the expected major mean failure rate is 1.1 failures per year, with an expected downtime of 9.13 days. For a minor incident, a total of 2.71 failures per year are expected, with a mean downtime of 3.5 days. It is assumed that these failures occur regardless of the preventive maintenance approach outlined in section 7.4.3.

To assess the cost associated with the minor and major incidents, the following approach is used. For the minor incidents, it is believed that this can be handled by the operators on the host platform. This means that in case of a minor failure, the cost is the same as the preventive maintenance schedule multiplied by the probabilistic occurrence. For the major failures, it is assumed that this would require a major component replacement and specialist personnel to be chartered from the home port in Kristiansund. Due to the sudden occurrence of the failure and the immediate required actions, the operational weather window (OW) is included. Downtime due to weather is expected to be 40% to mission length. The results are presented in table 7.13. It is assumed that all the repairs can be undertaken at the WINWIN platform itself.

Table 7.13: Cost breakdown of minor and major failures on a yearly basis.

	Minor failure	Major failure
Failure [p.a]	2,71	1,1
Mean downtime [day]	3,49	9,13
OW [%]	60	60
Total duration [days]	4,9	14,8
Vessel day rate [k€]	40	55
Total cost [k€/yr]	530,0	894,6

#### 7.4.5. Summary of O&M expenses for WINWIN unit

Assessing the anticipated O&M costs for a new concept is challenging. All variables are subject to scrutiny, from expected failure rates to shipping rates and maintenance strategy. However, this O&M breakdown provides a first approach estimate of what could be expected. In table 7.14 the yearly O&M costs are shown. Also, every five years, when hull and mooring line inspections are undertaken, 550k€ will be added in O&M expenses.

Table 7.14: Expected yearly cost of operation and maintenance for the WINWIN unit.

<b>O&amp;M cost per year [k€]</b>	<b>1584,7</b>
-----------------------------------	---------------

#### 7.4.6. Decommissioning of WINWIN

Full decommissioning and well abandonment are required at the end of the expected lifetime of the WINWIN unit. In this analysis, the costs associated with abandoning the injection well are left out, as this will also be required in the comparative case analysis.

Similar to the float out and installation appraisal, different vessels are required depending on the specific task assigned. Crane vessels are required to remove the suction anchor and mooring lines. The rate of removal is assumed to correspond to one anchor/mooring line per day. This gives a total operational time of six days. For the WINWIN unit, an AHTS vessel will be used in the towing operation at 5 knots. Resulting costs are shown in table 7.15.

Table 7.15: Expected decommissioning costs. Note that the towing by the AHTS vessel takes 2.5 days, half a day is added to accommodate for travel to destination.

	Day rate [€/day]	Duration [days]	Cost [k€]
Heavy Lift vessel	400000	6	2400
AHTS	60000	3	180

Depending on the condition of the mooring lines, anchors, and the substructure, these components can either be reused or sold as scrap metal. In this analysis, we consider that the components will be sold as scrap. Like any other commodity, the scrap metal is subjected to the market situation, and the price will vary accordingly. It was decided to use the average value of scrap steel over the year 2018. The price of scrap steel is then 351€/ton ([London Metal Exchange, 2018](#)).

Table 7.16: Value of scrap steel.

Scrap value appraisal	
Substructure [tons]	2329
Anchors [tons]	450
Mooring lines [tons]	1200
Scrap steel value [€/ton]	351
Total [M€]	1,4

Due to the scrap value of the WINWIN unit, then the total cost of decommissioning amounts to 1183k€.

## 7.5. Summary and results of the economic analysis

In figure 7.5 the life cycle cost per barrel injected is presented. Here it is found that the expected cost per barrel of injected water, amounts to 0.42€/BBL. The CAPEX costs account for 72% of the levelized cost. It is therefore likely that the future development and experience acquired whilst developing offshore floating technology, costs could be reduced. As mentioned, this analysis assumes the base

case scenario for the chosen location in the North Sea. Here it was found that the the average daily injection rate was  $49505\text{bbl/day}$ . Unfortunately, the results can not be compared to real numbers experienced in the industry today, as no information was found, however in section 7.6 we undertake a high level costs analysis of conventional water injection solutions found in the industry today.

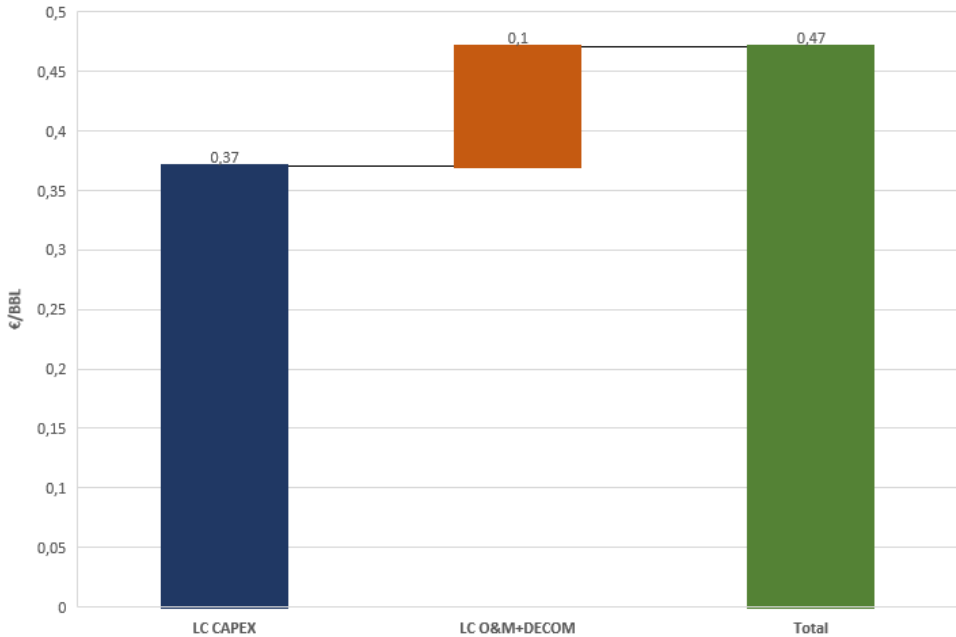


Figure 7.5: Levelized cost per injected barrel

### 7.5.1. Sensitivity analysis

Due to relative uncertainty of the expected costs and the case specific parameters that influence the results, a sensitivity analysis was carried out. In figure 7.6 expected levelized cost per injected barrel is shown together with some variables that were found to influence the result. The respective variables are reviewed whilst keeping all other variables as listed. To understand the figure, for instance when the project lifetime is 10 years, the levelized cost per barrel will be 0.66€ assuming that all other variables are kept constant. Another example would be if the applied discount rate for the project was chosen to be 4%; this would yield an levelized cost of 0.349€/BBL. As can be seen, the project lifetime and the average production rate are the two variables that would influence the levelized cost of the project the most.

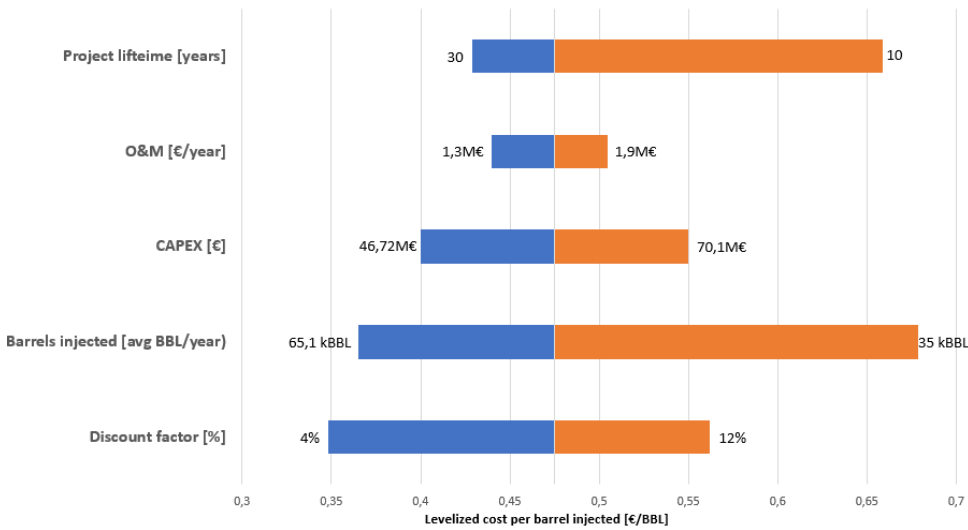


Figure 7.6: Sensitivity analysis of the WINWIN unit

## 7.6. Alternative solution with gas turbines

This section aims to provide an economic analysis for a conventional water injection solution, where gas turbines supply the power on the platform. This is hereafter referred to as the *alternative* method.

Finding the appropriate means of appraisal is challenging as there are numerous solutions that might be possible and should be assessed on a case by case basis. In the following section we therefore try to identify on a high level, the business cases where WINWIN could compete with the alternative solution. The starting point must be that the platform operator has found that additional water injection capacity is required. For comparison reasons we assume that the alternative solution should have the same average injection rate as found for WINWIN, which is 49505BBL/day.

First, we can consider a platform that has sufficient power generating capacities that can accommodate the additional energy requirements imposed by the water injection process. Then the costs of undertaking water injection are associated with the distance to the injection well, required size of pump, fuel cost, and CO<sub>2</sub> tax. Depending on the distance, the operator can choose to have the pumps located on the platform or subsea close to the injection well. The two options have different cost drivers. If the pump is placed "topside", the driving cost is the required subsea flow line to the injection manifold. If the pump is placed on the seafloor next to the injection well, the cost drivers would then be the underwater pump and required power umbilical to the platform. The underwater solution was adapted at the oil

field Tyrihans, described in section 5.1.

Finally, the result presented in the coming section will consider the levelized cost per barrel injected as a function of distance from the platform, found through equation 7.1. The levelized cost for the WINWIN concept was found to be 0.47€/BBL.

## 7.7. Topside alternative:

First we consider the topside solution. In table 7.17 the cost of subsea flowline is shown. The authors do not declare if the costs given also include installation of the flowline. However, Kaiser (2017) estimated the cost of flowline including installation to be 1827€/m. For this analysis, we assume a flowline cost to be 1500€/m.

Table 7.17: Cost of subsea flowline, adapted from OilFieldWiki (2018)

Base Cost [€/m]	187
Coatings [€/m]	391
Pipe Laying cost [€/m]	922
Total [€/m]	1500

### 7.7.1. Pump capacity and cost

The reacquired pump capacity will also be a function of the piping length. The frictional losses increase with length, hence more capacity is required. The pump capacity is estimated by the equation given below.

$$P = \frac{Q\rho gH}{\eta} \quad (7.3)$$

Where  $P$  is the required pump capacity,  $\rho$  is density,  $g$  is gravity, and  $H$  is the required head that is a function of the frictional losses as outlined in section 4.1.9. Lastly, the pump efficiency  $\eta$  is assumed to be 0,7. The required pump power is dictated by the flow rate, which in this case we have kept the same as in the WINWIN case of 49505 BBL/day, which result in an hourly flow rate of 331  $m^3/hr$ . However, as we also analyze the impact of required piping which will influence the head as seen in equation 4.3, the required pump power will increase in accordance with the length of the underwater piping.

For simplicity in this analysis, we assume a cost of pump corresponding to 1€/W, which is below the pump estimate for the WINWIN unit (1.8€/W). This is evaluated to be justified as the pumps on the WINWIN unit are operating autonomously, and therefore more engineering is required.

### 7.7.2. Fuel and emission costs

Fuel costs for the gas turbine are typically stated as 0.24€/m<sup>3</sup>. Moreover, the fuel to electricity conversion is given as 10,8kWh/m<sup>3</sup> at 100% efficiency. Gas turbines

operate in practice with a fuel to electricity efficiency of 30% (Chokhawala, 2008). Lastly, emissions from platforms in Norway are subjected to stringent rules, where the price per ton  $CO_2$  is stated as 58,13€ (Norwegian Petroleum Directorate, 2018). The  $CO_2$  equivalent for a gas turbine is  $0.577\text{kg}/\text{kwh}$  (Lie, 2014). The input values discussed in this section are summarized in table 7.18.

### 7.7.3. Calculation methodology

For clarity, this subsection detail the calculation methodology undertaken, in order to obtain the levelized cost of the topside solution. First we assume a constant injection rate of  $331\text{ m}^3/\text{hr}$  and determine the required head of the system that is dependant of the piping length analyzed. The required power of the pump is found through equation 7.3. Furthermore, the required fuel costs and  $CO_2$  is found through the conversion factors presented in table 7.18. Which in turn represent the annual O&M costs for the topside solution during its 20 year operational lifetime. Furthermore, the levelized cost is found trough equation 7.1, where we also assume the same discount factor as in the WINWIN case. Lastly, a contingency of 30% to the overall cost estimate is added as done in the WINWIN case.

Table 7.18: Summary of input values.

<b>Pump</b>	
Pump Efficiency [%]	70
Flow rate [ $\text{m}^3/\text{hr}$ ]	331
Pump cost [€/W]	1
<b>Gas turbine</b>	
Fuel to electricity at 100% efficiency [ $\text{kwh}/\text{m}^3$ ]	10,8
Gas turbine efficiency [%]	30
Fuel cost [€/m <sup>3</sup> ]	0,24
$CO_2$ emissions [kg/kWh]	0,577
Cost of $CO_2$ [€/ton]	58,1
<b>Flowline [€/m]</b>	<b>1500</b>

### 7.7.4. Results Topside

In figure 7.7 the costs of the alternative topside solution are presented. From the numbers presented above, the major cost driver is the underwater flowlines. However, the costs contributions dictated by the fuel and  $CO_2$  emissions were also significant. For instance, at a required flowline length of 10000 meters, the yearly emissions corresponded to  $12271\text{t}CO_2$  at the cost of  $0.71\text{M€}$ . Fuel cost was calculated to be  $1.47\text{M€}$ . In comparison to the WINWIN unit, the alternative solution has an economic advantage up to approximately  $15\text{km}$ .

The topside cost estimate provides a rough breakdown of the expected cost of a

topside solution. However, a more in depth analysis are required to fully determine the cost of a topside solution. Lastly as previously mentioned, generating capacity on platforms requires space, and space is inherently limited on offshore installations. found in the analysis that the required head of the pump at a flowline length of 15000 meters exceeded commercially available water injection pumps (see Appendix A). This means that the proposed solution is technically not possible without including subsea booster pumps. Which in turn would make the proposed solution more capital intensive. Moreover, the capacity required by the pumps at, for instance, 13000-meter flowline, required 4 MW. It is unlikely that the operator has this amount in spare capacity. As such one can conclude that this solution is only technically and economically feasible when there is a short distance from the host platform to injection well.

## 7.8. Subsea Solution

The topside solution proved to be an inefficient and technically challenging method of pumping water. The subsea solution overcomes the frictional losses by reducing the required flowline to a minimum, by locating the subsea pump close to the injection manifold. The required head of the pump is then found to be 558 meters (the flowline from seabed down to reservoir is 1940 meters). The required capacity of the pump is then estimated from equation 7.3. The capacity of the pump is 0,72MW. The host platform provides the power through a subsea umbilical. The umbilical provides the power and control mechanisms to the subsea pump. Bai and Bai (2010) stated the price of a power umbilical to be 1157,49€/m.

7

Regarding the underwater pump solution, limited public cost data is available. Subsea equipment requires significant engineering in order to operate in harsh conditions. The costs are therefore significant. In the search for possible subsea pump solutions, only one company had declared expected costs. The company Seabox manufactures subsea water injection pumps with water treatment possibilities. The units are ready to be installed offshore and require a power umbilical. The costs of the Seabox solution vary from 7.5M€ to 25M€ depending on water treatment requirements (Haugstad, 2016). As for the base case, we assume that the reservoir will tolerate raw filtered seawater and will, therefore, assume an installed cost of the Seabox unit to be 12M€.

In figure 7.7 the expected cost of the subsea and topside alternative solutions are plotted as a function of distance to the host platform. The levelized cost per barrel is calculated in the same way as stated for the topside solution. For the subsea solotuon, we also assume a cost equal to 1.6M€ for O&M and a contingency of 30%. In comparison to the topside case where the distance has a proportional relationship to fuel and emissions costs, fuel and emissions costs are constant for the subsea case given the case-specific boundaries. The calculated  $CO_2$  emissions costs and fuel cost were 0.16M€ and 0.349M€ respectively. The subsea solution in comparison to the WINWIN system is economically favored where the distance to the host platform is less than 30km.

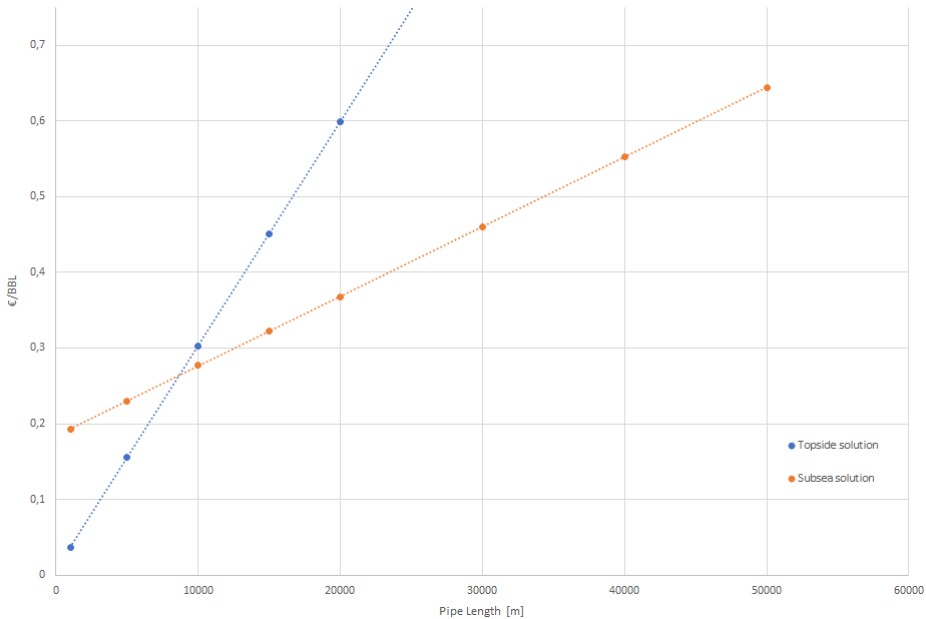


Figure 7.7: Cost of subsea and topside solution

## 7.9. Retrofit case

The topside and subsea solutions were all less expensive than the WINWIN system, up until a distance of approximately 30 km away from the host platform. In both cases, we assumed that the platform had sufficient capacity to accommodate the loads required. In many cases, this might not be the case. Space and weight on platforms come at a premium on offshore installations. With respect to adding generating capacity, it is assumed that a gas turbine with an integrated organic Rankine cycle per  $MW$  weighs  $15 - 20\text{ tons}$  and requires  $30 - 40\text{ m}^3$  of space [Lommasson \(2015\)](#). Thus, when it is found that water injection that was not initially accounted for in the design phase, could increase the recovery factor of the field (as was the case for the Ekofisk field described in section 3.3.1) retrofitting is required. Any attempt at a cost appraisal where retrofitting is required, would be purely based upon speculation, and is therefore not conducted here. Nonetheless, one can easily understand that either retrofitting or building a new platform would require substantial capital where a WINWIN solution might be an option to consider.



# 8

## Conclusion and reflection

This thesis addresses some of the potential synergies in the offshore environment. In a world where the need for sustainable energy solutions is increasing, synergies are a potential solution. We believe synergies could be a part of the future energy scenario. While we acknowledge that the world's energy mix in the coming decades will depend on a significant portion to originate from fossil sources, synergies allow for a more environmentally friendly way of producing hydrocarbons. With this outset, we investigated how synergies can enable a smoother energy transition. In the introduction we outlined the main objectives:

1. What is the potential for successful synergies in the offshore domain between wave and wind energy, and between the oil industry and wind energy.
2. How are the major oil companies implementing renewable solutions in their value chain?
3. Determine the feasibility of the WINWIN system, this shall include a modeling of the injective performance and to perform a cost analysis of the WINWIN concept and benchmark against existing technology.

### 8.1. Objective 1

First, we investigated how synergies in the offshore environment can potentially allow for better usage, improved energy yield and better project economy through sharing of infrastructure. Furthermore, we also noted how the administrative task and required concessions could lower the barrier to entry from new potential stakeholders through synergies. The main synergy that we focused on was the combination of an integrated wind-wave farm. Through qualitative research, potential advantages were identified. The wind-wave farm was found to have better economy compared to two separate floating wind and wave farms. However, it should be acknowledged that still the levelised cost of a stand alone offshore bottom fixed

farm is lower. Furthermore, the better utilization of resources would yield a higher energy density ratio compared to the stand alone solutions separately. This is an important factor as available space for energy technology in the offshore domain is limited. Concerning the technical upsides of the synergy, the integration allows for optimized transmission capacity, as such the sizing of the electrical infrastructure can be reduced, consequently reducing the transmission costs. Perhaps more interesting was the synergy found when integrating floating offshore wind with a wave farm. As both technologies at this point are considered less developed than bottom fixed offshore turbines, the levelised costs of the individual farms alone are higher than for the integrated farm. As when floating wind farms are considered, the developer might benefit from also incorporating a floating wave farm. This will potentially allow both technologies to experience a "pull" towards a faster technology readiness level, and, as a result, a lower barrier for potential developers, which will benefit the society as a whole with regards to the share of sustainably produced energy.

## 8.2. Objective 2

With regards to the likely energy transition, it is believed that the complete abatement of hydrocarbons is yet a distant scenario. However, the way we produce and extract the oil will benefit from a cleaner method. Therefore, a quantitative investigation towards the possible combination of wind powered oil platforms was conducted. During the research, two major oil firms also revealed the planning towards platforms powered by neighbouring wind farms. First, Aker BP announced its plan with the coming development of the NOAKA field, where a significant portion of the energy is thought to originate from a neighbouring wind farm. More lately, Equinor announced the Hywind Tampen project, where ten 8 MW turbines will supply electricity to the platforms Snorre and Gullfaks. It is expected that the turbines will account for 35% of the platforms' energy demand. The resulting  $CO_2$  reduction is predicted to be around 200 000 tons per year. These announcements are encouraging per the subject for this thesis. This topic was also found in literature where [Korpås et al. \(2012\)](#) demonstrated the potential fuel savings and consequently the  $CO_2$  reduction on a platform where wind turbines accounted for 40% of the electricity demand. Furthermore, [Wei et al. \(2013\)](#) further established the business case as the critical grid stability was investigated. Here it was found under different stress scenarios that the internal grid stability maintained within NORSOK requirements. Through the thesis it was also identified that the energy requirements of oil extraction are likely to increase as the the global reserves become more and more depleted, as a consequence the extraction process will have a higher emission intensity compared to today, combined with higher emissions taxation. It is believed that renewables will be more and more incorporated in the oil companies value chain. Thus with reference to the second objective, it is believed that the thesis demonstrated that there is a significant playing field for synergies in the offshore domain, both within the renewable sector and the oil and gas industry. Nonetheless, it is recognized that the quantitative research undertaken is at a high

level, where several other synergies are possible to identify.

### 8.2.1. Objective 3

The main objective of the thesis was to determine the feasibility of the WINWIN concept. The thesis focused on the performance of the WINWIN unit and a cost analysis of the system was undertaken. In order to determine the performance of the WINWIN system, the design and establishment of the components that will directly influence the injection capacity of the WINWIN unit were determined in chapter 4. Here we determined the wind turbine size and associated power curve, the power requirements of the lift pumps, and the power-flow relationship for the respective pump solutions. Furthermore, two pump solutions were evaluated, namely the P1, and P2 configuration. From figure 4.14, we can see that the P2 has a lower power requirement, and a capacity range that is comparably smaller than the P1 configuration, which has a larger power requirement and a larger capacity envelope. Nonetheless, the P2 configuration has a higher average daily injection rate. It should also be noted that both configurations might be suitable, as the P2 configuration might outperform the P1 solution in areas where the wind distribution is relatively small with high wind speeds. Furthermore, for adding value to the WINWIN scenario, four realistic locations were chosen, with associated weather data. The injective performance of the WINWIN was presented in chapter 6. Through our research it was demonstrated that the WINWIN unit could be a potential candidate for water injection purposes, given that the site has sufficient wind resources. On the other hand, locations where the wind resources are low, the potential to integrate the WINWIN solution in the value chain is rather low due to poor injection rates. It should also be mentioned that the analysis performed in the thesis, only assumed a generic design, as such no optimization towards wind turbine size or pump size were considered. Therefore it is possible that a more site specific design could generate a more accurate estimate of the injection rates. Lastly, As available injection numbers from real reservoirs were not attainable it is difficult to evaluate whether the performance of the WINWIN unit could pose as a real scenario. Nonetheless, we believe that the injection capacity demonstrated by the WINWIN should be considered as a real alternative for future water injection projects.

In chapter 7, the cost and levelized cost of the WINWIN unit were determined based on a methodological walk-through of all components that make up the WINWIN unit, also including installation, maintenance and decommissioning. The total cost of the WINWIN system was estimated to be 58.4 M€. Furthermore, through applying the case specific parameters presented in the North Sea case, which allow us to dictate both distance to site and injection levels, a maintenance scheme can be constructed to determine the levelized cost. For the specific North Sea case the cost per barrel injected amounted to 0.47€/BBL. In order to evaluate the levelized cost of the WINWIN unit, we also performed a high level costs analysis of two conventional solutions in chapter 7. This analysis included both a topside and a subsea facilitated water injection system. The topside solution has an economic

advantage up to 15 km, although it was found that the topside solution is only technically feasible when the injection well is located only a few kilometers away from the platform without requiring booster pumps. Unlike the topside case, the subsea solution avoids the need for high pressure underwater flowlines. The subsea solution is powered through an umbilical from the mother-platform that is comparably cheaper than a flowline. The subsea solution proved to be cost effective at a distance up to 30 km away from the platform. Lastly, a retrofit case was considered. Retrofit describes the case where a platform has extended its expected lifetime and requires an upgrade in terms of both available generating capacity and space. It was concluded that any attempt of a cost appraisal would be based on pure speculation and was therefore not undertaken, and the cost is likely to be significantly higher than the WINWIN system. Thus for platforms that do not have available generating capacity onboard to facilitate additional water injection, the WINWIN system could therefore be a solution.

### 8.3. Future Work

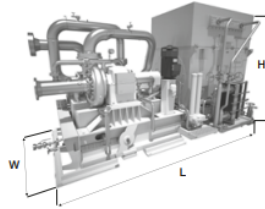
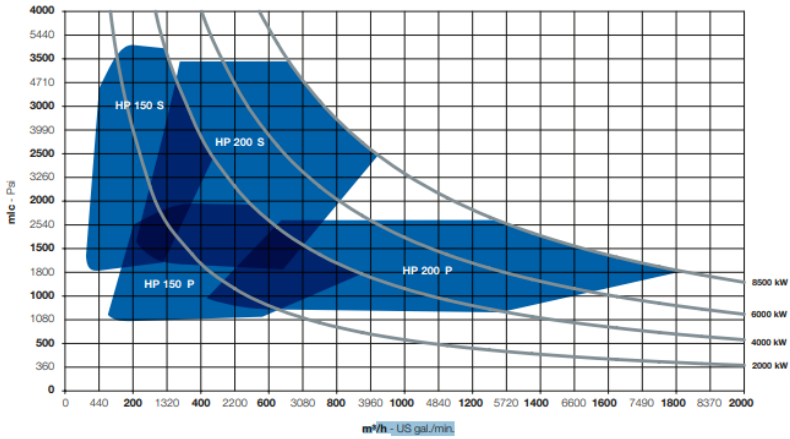
While the main objective of this thesis was to determine the feasibility of the WINWIN concept, it is recognized that several other feasibility studies are required to successfully implement the WINWIN system. One aspect concerns the variations in injection rates. It was identified in our results that the injection process has a significant difference in seasonal and daily injection numbers that might impose a risk to the reservoir. In this context, it would be beneficial to undertake an analysis of potential reservoir characteristics that would tolerate such deviations in injection. Furthermore, studies towards the electrical stability of the micro grid is required. As the power originates from the wind turbine it is of crucial concern that the micro grid is able to maintain a stable grid that ensures the safety and reliability of vital components.

Regarding the methodology to obtain the relationship for the power-flow for the respective pumps, the reader might question why not the straight forward pump equation 7.3 was used and solved for resulting flow when power is available. As we had two pump configurations to evaluate, the rearranged equation 7.3 would simply yield the same result as all other coefficients would have been the same between the two pump configurations. Thus, this thesis followed the proposed method found in literature to estimate the power-flow relationship when appropriate pump diagrams were available (Carlson, 2000, Chantasiriwan, 2013, Zhang et al., 2012). However, it is recognized that a simplification was assumed in determining the pump performance: We assumed the reservoir pressure, and consequently the system's head, to be constant. This assumption might not be true as the internal pressure of the reservoir might increase as a result of the water injected. Thus for future research, the dynamic interaction as a result of the water injection should be accounted for.

# A

## Appendix A

## Technical data



Pump type / Rating	Length [m]	Width [m]	Height [m]	Weight [kg]
HP150/1000	4.6	2.6	2.5	14200
HP150/2000	4.75	2.6	3.3	17200
HP150/3000	4.9	2.6	3.3	18500
HP150/4000	5.1	2.6	3.3	19200
HP200/5000	5.6	2.9	3.7	24900
HP200/6000	5.8	2.9	3.7	29000
HP200/7000	6.0	2.9	3.7	30000
HP200/8500	6.2	2.9	3.7	33000

Figure A.1: Available water injection pumps found in the market today. For the topside water injection solution, the head (mhc) at a pipe-length of 15000 meters was found to be approximately 3800 meters. If the flow rate are kept constant at  $331 \text{ m}^3/\text{hr}$  we are outside the operational envelope of the pump.

## A.1. Intermezzo-Consideration when applying the affinity laws

*This section presents the affinity laws, that are used to deduce pump performance characteristics. Furthermore, wrong use of the affinity laws often occurs and must be avoided to obtain correct performance, this is elaborated in the following section.*

The affinity laws are commonly used in engineering applications, and provides a quick and economical way to deduce the pump characteristics such as flow, head and power predictions. However, the affinity laws are often implemented wrong and such often overestimates the pump characteristics (Carlson, 2000, Chantasiriwan, 2013). Considering that the pump used in the WINWIN project is a variable speed drive centrifugal pump, where the diameter of the impeller remains constant, the affinity laws can be written as follows;

$$\frac{Q_1}{Q_2} = \frac{N_1}{N_2}, \quad \frac{H_1}{H_2} = \left(\frac{N_1}{N_2}\right)^2, \quad \frac{P_1}{P_2} = \left(\frac{N_1}{N_2}\right)^3 \quad (\text{A.1})$$

Here Q is the flow rate, N is speed of pump, P is power and H is head. The subscripts 1 and 2 refers to the operating points of the pump. For instance one can see that if pump speed is halved, flow is reduced with 50%, head is reduced with 75% and 87,5% less power is required. Furthermore, Carlson (2000) exemplified how affinity rules often are wrongly applied. Consider Fig. A.2 that depicts a typical pump performance diagram combined with a system curve and the corresponding pump power, that is the power that corresponds to the pump curve-if operating along this line. Furthermore, it should be noted that the pump and power curve corresponds to a given pump speed  $N$ . From Fig. A.2, assume that the pump is operating at the  $2500 \text{ m}^3/\text{hr}$  represented by the right blue stapled line in Fig. A.2, what would be the pumps operating conditions at  $1000 \text{ m}^3/\text{hr}$ ? From the graph the initial pump conditions are:

- $Q_1 = 2500 \text{ m}^3/\text{hr}$
- $H_1 = 1750 \text{ m}$
- $P_1 = 1000 \text{ kW}$

From equation 4.12 it is clear that the head is proportional to the square of the flow thus we we can obtain  $H_2$ ;

$$H_2 = 1750 \text{ m} \cdot \left(\frac{1000 \text{ m}^3/\text{hr}}{2500 \text{ m}^3/\text{hr}}\right)^2 = 280 \text{ m} \quad (\text{A.2})$$

Subsequently the power pump power required can be calculated as

$$P_2 = 1000 \text{ kW} \left(\frac{1000 \text{ m}^3/\text{hr}}{2500 \text{ m}^3/\text{hr}}\right)^3 = 64 \text{ kW} \quad (\text{A.3})$$

However, this method just outlined clearly gives wrong results. Referring to figure A.2 it can be seen that system head requirement when flow is  $1000\text{m}^3/\text{hr}$  is considerably higher (610 m) than estimated when using the affinity laws in equation A.2. The reason for the wrong results are due to the assumption that the initial conditions were known i.e.  $H_1, Q_1$  and  $P_1$ , this assumption is not true. Moreover of the final conditions only  $H_2$  and  $Q_2$  thus there are four unknowns and three equations. The appropriate method of implementing the affinity laws is to draw the affinity curve to intersect the system curve at desired operating point i.e at  $1000\text{ m}^3/\text{hr}$ . This is illustrated in Fig. A.3, where the affinity curve (grey) is plotted to intersect the system curve at the final operation point. Subsequently, the initial operating conditions can be found, that is where the affinity line crosses the pump curve, furthermore the power can be found by drawing a vertical line from aforementioned intersection point. The initial conditions are then found to be:

- $Q_1 = 1743\text{ m}^3/\text{hr}$
- $H_1 = 1823\text{ m}$
- $P_1 = 820\text{ kW}$

Then the power requirement at  $1000\text{m}^3/\text{hr}$  can be found;

$$P_2 = 820\text{kW} \left( \frac{1000\text{ m}^3/\text{hr}}{1743\text{ m}^3/\text{hr}} \right)^3 = 154\text{ kW} \quad (\text{A.4})$$

The correct result yields a power requirement of  $154\text{ kW}$  as compared to  $64\text{ kW}$  obtained from equation A.3. Generally the affinity laws overestimates the power reduction. Thus as a summary, the affinity laws are an efficient tool that provides pump performance in a simple way. However, careful consideration must be un it dictates the correct initials conditions are found through drawing the affinity curve, as demonstrated above. Moreover, the case presented is rather simple where only two flow conditions are considered, and would prove a rather tedious process when several iterations are required, as such a mathematical modelling of the pump system is required.

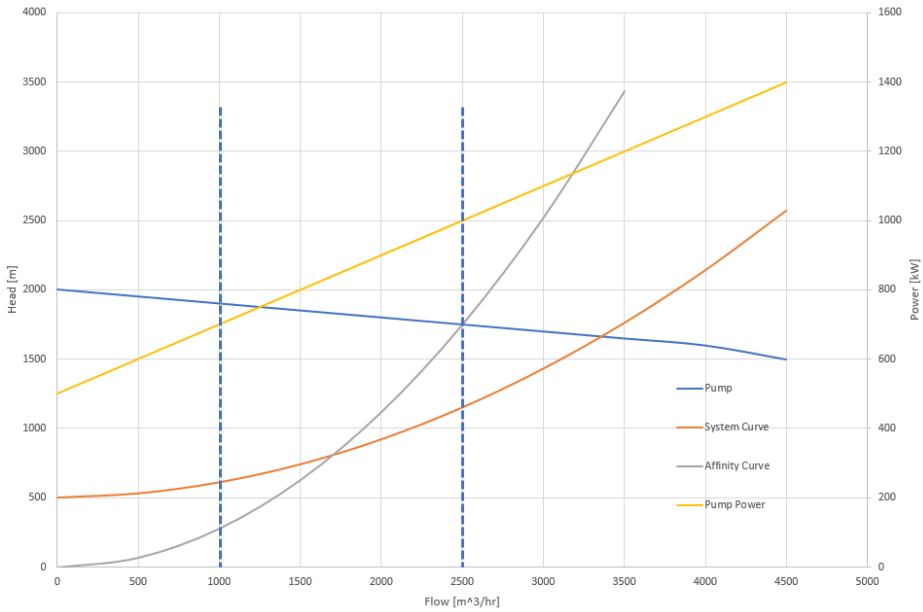


Figure A.2: Figure depicts how wrongful use of the affinity curves underestimates pump performance. Adapted from Carlson (2000)

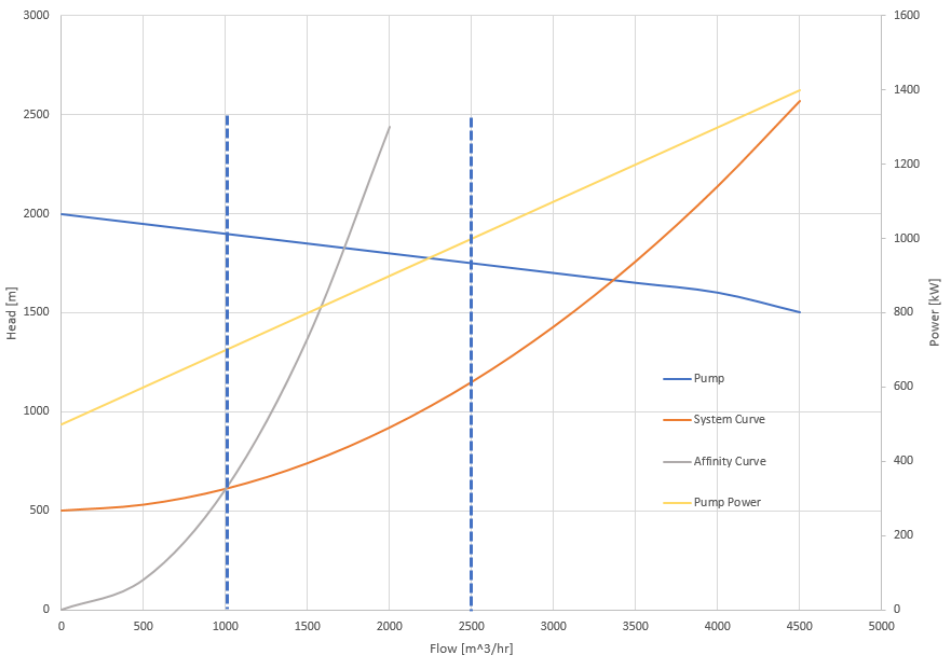


Figure A.3: The correct way of applying the affinity laws. Adapted version from Carlson (2000)

## A.2. Hall-plot equations constants

In table A.1 the values used to obtain the hall plot is listed. Values are worked out with DNV GL experts.

Table A.1: Parameters and values used in equation 4.8

<b>Paramaters</b>	<b>Values</b>	<b>Units</b>
Permiability (k)	400	md
Well radius(Re)	1	m
Reservoir radius (Rw)	3000	m
Skin factor (s)	0,5	
Reseroir pressure (P_avg)	200	bar
Reservoir thickness (h)	400	m
Viscosity	1	cp

# B

## Appendix B

## B.1. WIN WIN performance North Sea, sensitivity analysis

B

Table B.1: Comparison of P1 and P2 in North Sea site, 3 hr operational strategy

<b>Parameters</b>	<b>P1</b>	<b>P2</b>
Total barrels injected [Mbbbl]	16.1	16.2
Av. daily BBL injected	44108.5	44500.1
Non Injecting hours	3001	2782
Longest continuous downtime [hr]	48	47
# of stops	334	323
Ops strategy [hr]	3	3

Table B.2: Comparison of P1 and P2 in North Sea site, 8 hr operational strategy

<b>Parameters</b>	<b>P1</b>	<b>P2</b>
Total barrels injected [Mbbbl]	12,1	12,4
Av. daily BBL injected	33197,3	34057,1
Non Injecting hours	4441,0	4202,0
Longest continuous downtime [hr]	68,0	67,0
# of stops	246,0	243,0
Ops strategy [hr]	8,0	8,0



Figure B.1: WIN-WIN performance 3 hr operational strategy with P1 system



Figure B.2: WIN-WIN performance 3 hr operational strategy with P2 system

B



Figure B.3: WIN-WIN performance 8 hr operational strategy with P1 system



Figure B.4: WIN-WIN performance 8 hr operational strategy with P2 system

## B.2. Brazil

Table B.3: Comparison of P1 and P2 in Brazil, 3 hr operational strategy

<b>Parameters</b>	<b>P1</b>	<b>P2</b>
Total barrels injected [Mbbbl]	10.1	10.7
Av. daily BBL injected	27695.4	29223.4
Non Injecting hours	4848	4596
Longest continuous downtime [hr]	87	70
# of stops	352	346
Ops strategy [hr]	3	3

Table B.4: Comparison of P1 and P2 in Brazil, 8 hr operational strategy

<b>Parameters</b>	<b>P1</b>	<b>P2</b>
Total barrels injected [Mbbbl]	6.4	6.9
Av. daily BBL injected	17423.2	19023.8
Non Injecting hours	6309	6065
Longest continuous downtime [hr]	160	160
# of stops	224	230
Ops strategy [hr]	8	8



Figure B.5: WIN-WIN performance 3 hr operational strategy with P1 system

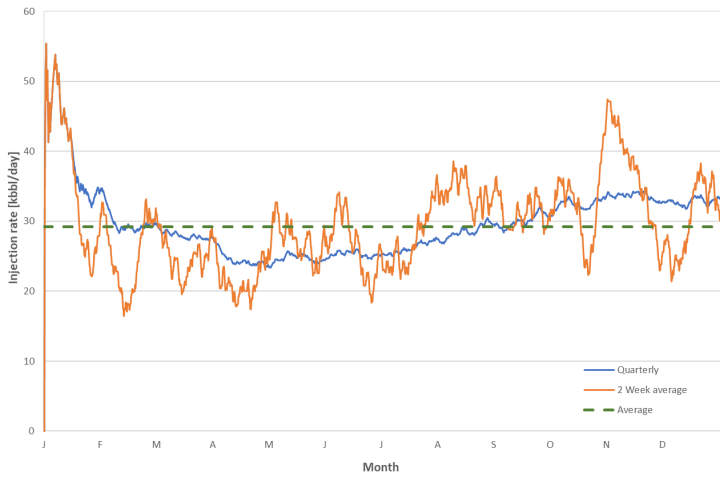


Figure B.6: WIN-WIN performance 3 hr operational strategy with P2 system

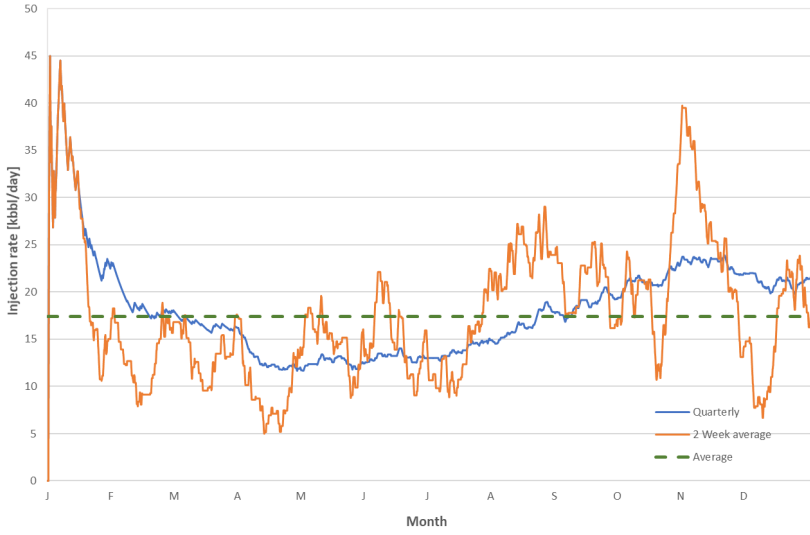


Figure B.7: WIN-WIN performance 8 hr operational strategy with P1 system

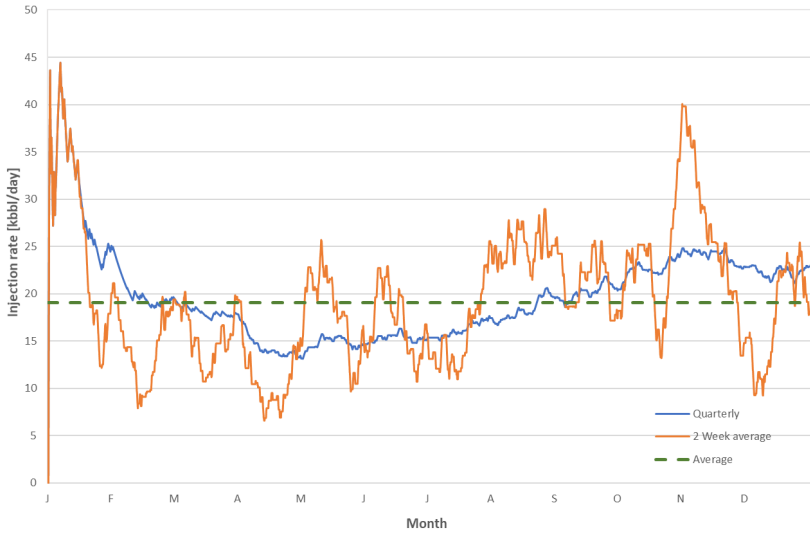


Figure B.8: WIN-WIN performance 8 hr operational strategy with P2 system

### B.3. GoM

Table B.5: Comparison of P1 and P2 in GoM, 3 hr operational strategy, GoM

<b>Parameters</b>	<b>P1</b>	<b>P2</b>
Total barrels injected [Mbbbl]	9.9	10.5
Av. daily BBL injected	27216	28848
Non Injecting hours	5087	4750
Longest continuous downtime [hr]	70	61
# of stops	360	361
Ops strategy [hr]	3	3

Table B.6: Comparison of P1 and P2 in GoM, 8 hr operational strategy

<b>Parameters</b>	<b>P1</b>	<b>P2</b>
Total barrels injected [Mbbbl]	6.2	6.7
Av. daily BBL injected	16914	18485
Non Injecting hours	6490	6208
Longest continuous downtime [hr]	227	189
# of stops	225	231
Ops strategy [hr]	8	8

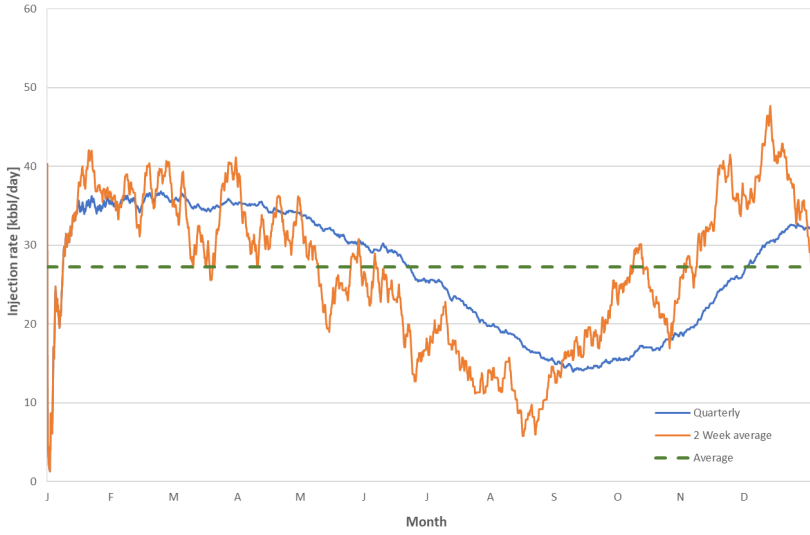


Figure B.9: WIN-WIN performance 3 hr operational strategy with P1 system, GoM



Figure B.10: WIN-WIN performance 3 hr operational strategy with P2 system

B



Figure B.11: WIN-WIN performance 8 hr operational strategy with P1 system, GoM



Figure B.12: WIN-WIN performance 8 hr operational strategy with P2 system, GoM

## B.4. West- Africa

Table B.7: Comparison of P1 and P2 in West-Africa, 3 hr operational strategy

<b>Parameters</b>	<b>P1</b>	<b>P2</b>
Total barrels injected [Mbbbl]	2.3	2.7
Av. daily BBL injected	6236	7407
Non Injecting hours	7804	7598
Longest continuous downtime [hr]	503	503
# of stops	173	191
Ops strategy [hr]	3	3

**B**

Table B.8: Comparison of P1 and P2 in West-Africa, 8 hr operational strategy

<b>Parameters</b>	<b>P1</b>	<b>P2</b>
Total barrels injected [Mbbbl]	1	1.2
Av. daily BBL injected	2667.1	3377.1
Non Injecting hours	8359	8243
Longest continuous downtime [hr]	1746	861
# of stops	71	81
Ops strategy [hr]	8,0	8,0

B

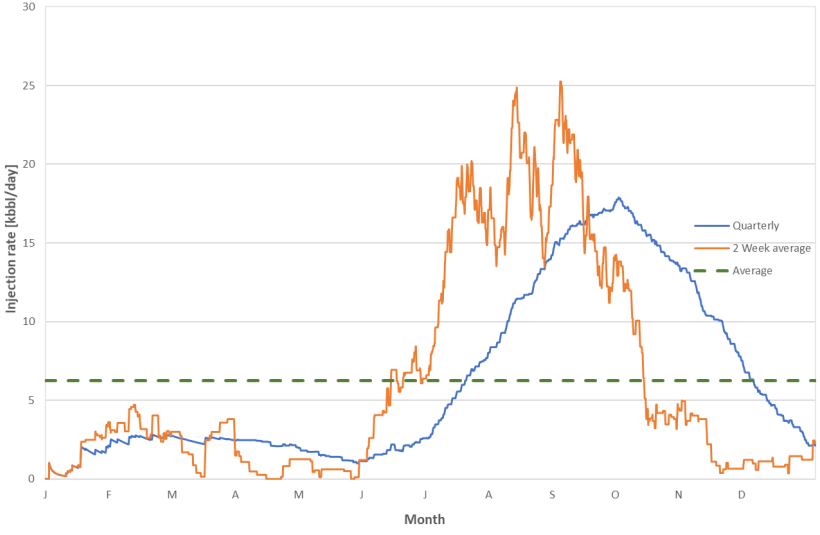


Figure B.13: WIN-WIN performance 3 hr operational strategy with P1 system, West Africa

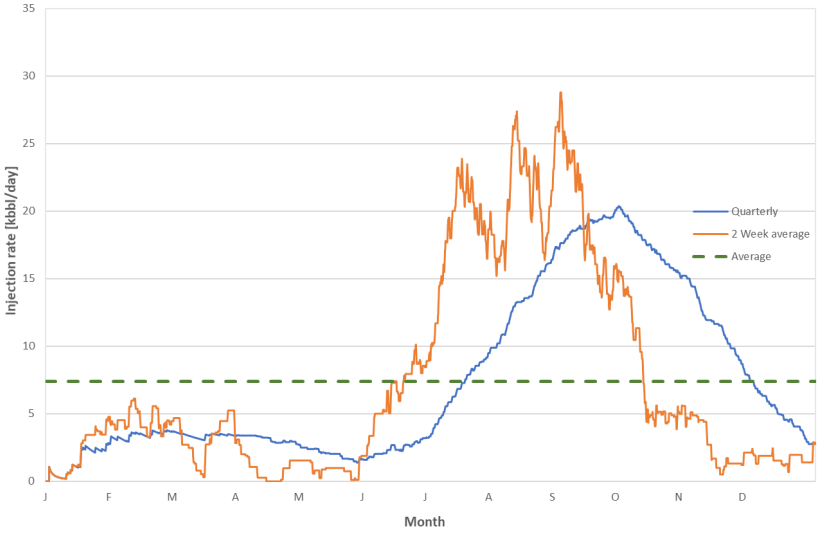


Figure B.14: WIN-WIN performance 3 hr operational strategy with P2 system, West Africa

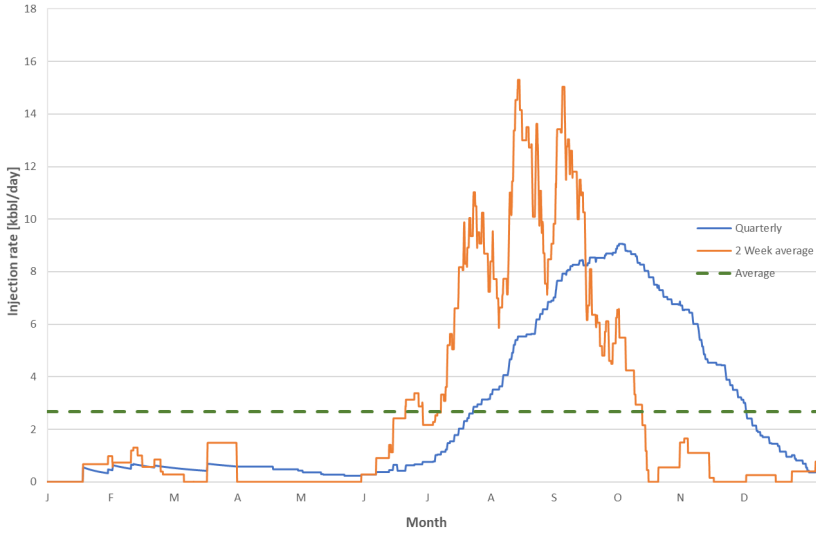


Figure B.15: WIN-WIN performance 8 hr operational strategy with P1 system, West Africa

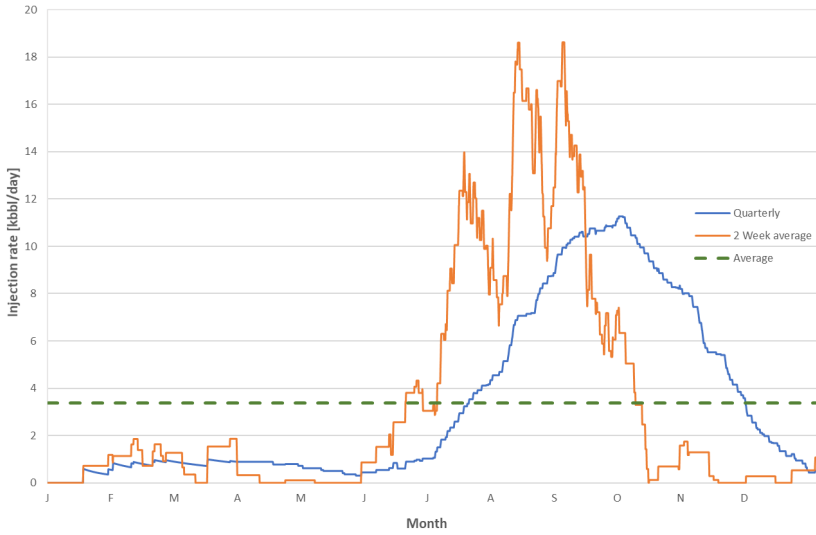


Figure B.16: WIN-WIN performance 8 hr operational strategy with P2 system, West Africa

## References

- 4COffshore (2015). Events on alpha ventus. <https://www.4coffshore.com/windfarms/project-dates-for-alpha-ventus-de01.html>. Accessed 16-01-2019.
- Aabø, A. (2015). Vanninjeksjon i reservoarformasjon. Accessed 02-04-2018.
- ABC-Mooring (2015). Mooring systems. Accessed 1-10-2018.
- AkerBP (2018). Aker bp first quarter 2018 results. Accessed 10-05-2018.
- Almasi, A. (2014). Estimate pump installation costs. Accessed 7-10-2018.
- Alvarado, V. and Manrique, E. (2010). Enhanced oil recovery: An update review. *Energies*, 3(9):1529–1575.
- ANP (2018). Opportunities in the brazilian oil and gas industry. Technical report, National Agency of Petroleum, Natural Gas and Biofuels.
- Arany, L. and Bhattacharya, S. (2018). Simplified load estimation and sizing of suction anchors for spar buoy type floating offshore wind turbines. *Ocean Engineering*, 159:348 – 357.
- Astariz, S. and Iglesias, G. (2017). Enhancing marine energy competitiveness: Co-located offshore wind and wave energy farms. *Coastal Engineering Proceedings*, 3(35).
- Astariz, S., Perez-Collazo, C., Abanades, J., and Iglesias, G. (2015a). Co-located wave-wind farms: Economic assessment as a function of layout. *Renewable Energy*, 83:837 – 849.
- Astariz, S., Vazquez, A., and Iglesias, G. (2015b). Evaluation and comparison of the levelized cost of tidal, wave, and offshore wind energy. *Journal of Renewable and Sustainable Energy*, 7:053112.
- Bai, Y. and Bai, Q. (2010). Chapter 6 - subsea cost estimation. In Bai, Y. and Bai, Q., editors, *Subsea Engineering Handbook*, pages 159 – 192. Gulf Professional Publishing, Boston.
- Becker, R. (1999). Brazils offshore potential extends beyond campos basin. Accessed 28-06-2018.
- Bjørheim, P. (2015). A feasibility study of the Versatruss system. Master's thesis, UIS, Norway.
- Bloomberg (2018). Akerbp stock. Accessed 10-05-2018.
- Boxern, T., Koorneef, J., van Dijk, R., and Halter, M. (2016). System intergration offshore energy: Innovation project north sea energy. Technical report, TNO.

- Bradbury, J. (2007). Debut for downwind. [https://sysla.no/international/debut\\_for\\_downvind/](https://sysla.no/international/debut_for_downvind/). Accessed 25-10-2018.
- BrightSource (2011). Coalinga project facts. Accessed 18-05-2018.
- Brown, D. (1994). Levelized production cost. an alternative form of discounted cash flow analysis.
- Bureau of Safety and Environmental Enforcement (2018). Bsee database-gom platform depth. Accessed 14-06-2018.
- C. Edmondson, J. P., Hall, N., and Deppmann, R. (2016). New pump efficiency standards part 3: Calculating per values. Accessed 24-08-2018.
- Campanile, A., Piscopo, V., and Scamardella, A. (2018). Mooring design and selection for floating offshore wind turbines on intermediate and deep water depths. *Ocean Engineering*, 148:349 – 360.
- Carlson, R. (2000). The correct method of calculating energy savings to justify adjustable-frequency drives on pumps. *IEEE Transactions on Industry Applications*, 36(6):1725–1733.
- Chantasiriwan, S. (2013). Performance of variable-speed centrifugal pump in pump system with static head. 33.
- Chesbrough, H. (2002). Making sense of corporate venture capital. *Harvard Business Review*, 80(3):90–99.
- Chevron (2011). Chevron technology ventures launches world's largest solar enhanced-oil-recovery project. Accessed 18-05-2018.
- Chokhawala, R. (2008). Powering platform- Connecting oil and gas platforms to mainland power grids. Technical report, ABB.
- Clark, C. E., Miller, A., and DuPont, B. (2019). An analytical cost model for co-located floating wind-wave energy arrays. *Renewable Energy*, 132:885 – 897.
- Comello, S., Glenk, G., and Reichelstein, S. (2017). Levelized cost of electricity calculator: A user guide. Technical report.
- Cubitt, J. M., England, W. A., and Larter, S. (2004). *Understanding Petroleum Reservoirs towards an Integrated Reservoir Engineering and Geochemical Approach*. Geological Society.
- de Castro, R. D. and Picolini, J. P. (2016). 1 - main features of the campos basin regional geology. In Kowsmann, R. O., editor, *Geology and Geomorphology*, pages 1 – 12. Campus, Rio de Janeiro.
- d'Emil, B., Jacobsen, M., Jensen, M., Krohn, S., Petersen, C., and Sandstrøm, K. (2001). Wind with miller. Accessed 06-04-2018.

Diepeveen, N. (2004). Seawater-based hydraulics for offshore wind turbines. Technical report, we@sea.

DNV-GL (2018). Energy transition outlook 2018. Technical report, DNV-GL.

DNV GL (2018). Win win joint industry project: Wind-powered water injection. <https://www.dnvgl.com/oilgas/contact/thank-you/win-win-wind-powered-water-injection-joint-industry-project-noindex.html>. Accessed 25-03-2018.

ECN (2016). Reference o&m concepts for near and far offshore wind farms. <https://www.ecn.nl/publications/PdfFetch.aspx?nr=ECN-E--16-055>. Accessed 10-10-2018.

EIA (2015). Offshore production nearly 30% of global crude oil output in 2015. Accessed 10-04-2018.

EIA (2018). U.S. gulf of mexico crude oil production to continue at record highs through 2019. Accessed 18-06-2018.

EngineeringToolbox (2017). Density of crude oil as function of temperature. <https://www.engineeringtoolbox.com/crude-lubricant-lubricating-oil-density-temperature-gravity-volume-1938.html>. Accessed 16-01-2019.

EPA (2018). Light-duty automotive technology, carbon dioxide emissions, and fuel economy trends: 1975 through 2017. Technical report, United States environmental protection Agency.

Equinor (2015). Hywind scotland brochure. Accessed 1-10-2018.

Equinor (2016). Njord a towed to kværner stord. Accessed 07-06-2018.

Equinor (2017). World's first floating wind farm has started production. Accessed 10-05-2018.

Equinor (2018). Campos basin. Accessed 28-06-2018.

Equinor (2018). Wind farm being considered at snorre and gullfaks. <https://www.equinor.com/en/news/27aug2018-hywind-tampen.html>. Accessed 25-10-2018.

Esteban, M. and Leary, D. (2011). Current developments and future prospects of offshore wind and ocean energy. <http://web.mit.edu/12.000/www/m2018/pdfs/japan/offshore-energy.pdf>. Accessed 16-01-2019.

ExxonMobil (2016). Exxonmobil announces significant oil discovery offshore nigeria. Accessed 18-06-2018.

- Fairstar NV (2011). Market segmentation, trends in pricing power and future opportunities in the marine heavy transport industry. <http://www.fairstar.com/media/Fairstar%20presentation%20Oslo%20March%202011.pdf>. Accessed 8-10-2018.
- Faltinsen, O. M. (1990). *Sea loads on ships and offshore structures*. Cambridge University Press Cambridge ; New York.
- Faulstich, S., Hahn, B., and Tavner, P. J. (2010). Wind turbine downtime and its importance for offshore deployment. *Wind Energy*, 14(3):327–337.
- Gavenas, E., Rosendahl, K., and Skjerpen, T. (2015). Co2-emissions from norwegian oil and gas extraction. Technical report, Statistics Norway.
- Gordon, D. (2012). Understanding unconventional oil. Technical report, The Carnegie Papers.
- GrantThornton (2017). Renewable energy discount rate survey results – 2017. Accessed 1-10-2018.
- Grynning, A., Larsen, S., and I, S. (2009). Tyrihans subsea raw seawater injection system. *Offshore Technology Conference*.
- GWEC (2017). Global wind report-annual market update 2017. Technical report, Global Wind Energy Council.
- Haugstad, T. (2016). Denne boksen renser sjøvann på havbunnen - kan spare oljeselskapene for store summer. <https://www.tu.no/artikler/denne-boksen-renser-sjovann-pa-havbunnen-kan-spare-oljeselskapene-for-346694>. Accessed 15-10-2018.
- Haugstad, T. (2018). Tok 15 år: Nå er vannrenseren klar. Accessed 02-04-2018.
- Helman, C. (2015). Ironic or economic? oil giant to build world's largest solar project. Accessed 19-05-2018.
- Hermansen, H., Landa, G., Sylte, J., and Thomas, L. (1999). Experiences after 10 years of waterflooding the ekofisk field, norway. *Journal of Petroleum Science and Engineering*, 26(1-4):11–18.
- HIenergy (n.d.). Beatrice talisman project. <http://www.hi-energy.org.uk/Hi-energy-Explore/talisman-beatrice-project.htm>. Accessed 25-10-2018.
- Hirtenstein, A. (2017). Big oil is investing billions to gain a foothold in clean energy. Accessed 10-05-2018.
- Hoeksema, W. (2014). Innovative Solution for Seafastening Offshore Wind Turbine Transition Pieces during transport . Master's thesis, TU Delft, The Netherlands.
- Hovland, K. (2017). Statoil leverer plan for njord. Accessed 07-06-2018.

- Hundleby, G. (2016). Lcoe – weighted average cost of capital (wacc). Accessed 1-10-2018.
- Håkonsen, P. (2017). Møllemontering stord hywind hywind park statoil saipem 7000 sunnhordland. <https://www.youtube.com/watch?v=DkMTBvyfz4o>. Accessed 7-10-2018.
- IOCE (2010). Oceans of energy- european ocean energy roadmap 2010-2050. Technical report, International Conference on Ocean Energy.
- IEA (2018). Solar energy. <https://www.iea.org/topics/renewables/solar/>. Accessed 26-10-2018.
- IHS Inc. (2014). Surveillance analysis theory. Technical report, IHS.
- IOGP (2017). Environmental performance indicators – 2016 data. Technical report, International Association of Oil and Gas Producers.
- IPCC (2018). Global warming of 1.5 °c an ipcc special report on the impacts of global warming of 1.5 °c above pre-industrial levels and related global greenhouse gas emission pathways, in the context of strengthening the global response to the threat of climate change, sustainable development, and efforts to eradicate poverty. Technical report, Intergovernmental Panel on Climate Change.
- IRENA (2016). Floating foundations: a game changer for offshore wind power. Technical report, International Renewable Energy Agency.
- IRENA (2017). Electricity storage and renewables: Costs and markets to 2030. Technical report, International Renewable Energy Agency.
- IRENA (2018). Renewable power generation costs in 2017. Technical report, The International Renewable Energy Agency.
- Johnson, R. (1998). *The Handbook of Fluid Dynamics*. CRC Press.
- Kaiser, M. J. (2017). Offshore pipeline construction cost in the u.s. gulf of mexico. *Marine Policy*, 82:147 – 166.
- Kjelstad, E. (2018). En komparativ kostnadsanalyse av forankringsssystemer for flytende vindturbiner. Master's thesis, NMBU, Norway.
- Knight, R. and Westwood, J. (1999). West african deep water, development prospects in a global context. Technical report, Ocean Docs.
- Korpås, M., Warland, L., He, W., and Tande, J. O. G. (2012). A case-study on offshore wind power supply to oil and gas rigs. *Energy Procedia*, 24:18 – 26. Selected papers from Deep Sea Offshore Wind R&D Conference, Trondheim, Norway, 19-20 January 2012.

- Kovscek, A. (2012). Emerging challenges and potential futures for thermally enhanced oil recovery. *Journal of Petroleum Science and Engineering*, 98-99:130 – 143.
- Li, X., Beadall, K., Duan, S., and Lach, J. (2013). Water injection in deepwater, over-pressured turbidites in the gulf of mexico: Past, present and future. *Offshore Technology Conference*.
- Lie, O. (2014). Her er regnestykket som viser at elektrifisering er et klimatiltak. <https://www.tu.no/artikler/her-er-regnestykket-som-viser-at-elektrifisering-er-et-klimatiltak/225709>. Accessed 13-10-2018.
- Liu, F., Guthrie, C. F., and Shipley, D. (2012). Optimizing water injection rates for a water-flooding field. *Society of Petroleum Engineers*, 12.
- Lommasson, T. C. (2015). Optimization of electrical energy production in offshore installations. [file:///C:/Users/MAGIO/Downloads/SESJON2-DEL2Dr.TimothyC.LommassonTEKNOVA%20\(2\).pdf](file:///C:/Users/MAGIO/Downloads/SESJON2-DEL2Dr.TimothyC.LommassonTEKNOVA%20(2).pdf). Accessed 15-10-2018.
- London Metal Exchange (2018). Lme steel scrap. <https://www.lme.com/Metals/Ferrous/Steel-Scrap#tabIndex=0>. Accessed 11-10-2018.
- MacKay, D. (2007). *Sustainable energy without the hot air*. UIT Cambridge Ltd., Cambridge.
- Molde, A. (2015). Puslepillet maria. Accessed 12-06-2018.
- Mooney, C. (2011). One of the country's biggest oil fields just turned to an unexpected power source: Solar. Accessed 18-05-2018.
- Muggeridge, A., Cockin, A., Webb, K., Frampton, H., Collins, I., Moulds, T., and Salino, P. (2014). Recovery rates, enhanced oil recovery and technological limits. *Philosophical Transactions. Series A, Mathematical, Physical, and Engineering Sciences*, 3(2006).
- Myhr, A., Bjerkseter, C., Ågotnes, A., and Nygaard, T. A. (2014). Levelised cost of energy for offshore floating wind turbines in a lifecycle perspective. *Renewable Energy*, 66:714 – 728.
- NDP (2018). Ekofisk factpage. <http://factpages.npd.no/ReportServer?/FactPages/PageView/field&rs:Command=Render&rc:Toolbar=false&rc:Parameters=f&NpdId=43506&IpAddress=80.213.85.220&CultureCode=en>. Accessed 25-09-2018.
- NDP (2018). Factpages-ekofisk. Accessed 07-04-2018.
- Nixon, L., Kazanis, E., and Alonso, S. (2016). Deepwater gulf of mexico. Technical report, U.S. Department of the interior Bureau of Ocean Energy Management.

Norsk Petroleum (2018). Factsheet norwegian oil fields. Accessed 14-06-2018.

Norwegian Petroleum Directorate (2018). Emission to air. <https://www.norskpetroleum.no/miljo-og-teknologi/utslipp-til-luft/>. Accessed 13-10-2018.

NPD (2018). Factsheet norne. Accessed 07-06-2018.

NREL (2014). Reference manual for the system advisor model's wind power performance model. <https://www.nrel.gov/docs/fy14osti/60570.pdf>. Accessed 11-01-2019.

NREL (2018). Homer.

NREL (2018). Wind resources us. Accessed 18-06-2018.

Offshore Energy Today (2018a). Aker bp: Noaka platform could be powered by offshore wind. <https://www.offshoreenergytoday.com/aker-bp-noaka-platform-could-be-powered-by-offshore-wind/>. Accessed 25-10-2018.

Offshore Energy Today (2018b). Aker bp: Noaka platform could be powered by offshore wind. Accessed 13-05-2018.

Offshore Energy Today (2018c). Co2 european emission allowances. <https://markets.businessinsider.com/commodities/co2-emissionsrechte>. Accessed 25-09-2018.

Offshore Technology (2018). Barracuda and caratinga fields. Accessed 28-06-2018.

OGJ (1990). Phillips steps up ekofisk water injection. Accessed 24-08-2018.

OilFieldWiki (2018). Subsea equipment costs. [http://www.oilfieldwiki.com/wiki/Subsea\\_Equipment\\_Costs](http://www.oilfieldwiki.com/wiki/Subsea_Equipment_Costs). Accessed 13-10-2018.

Petersen, J. and Jacoby, R. (2007). Selecting a positive displacement pump. *Chemical Engineering*, 114(8):42–46. Copyright - Copyright Chemical Week Associates Aug 2007; Document feature - Graphs; Photographs; Illustrations; Last updated - 2016-11-19; SubjectsTermNotLitGenreText - United States–US.

Petro (2009). Rått løp på tyrihans. <https://petro.no/ratt-lop-pa-tyrihans/14594>. Accessed 13-10-2018.

Petro Industry News (2018). What is the difference between primary, secondary & enhanced recovery for oil extraction? <https://www.petro-online.com/news/fuel-for-thought/13/breaking-news/what-is-the-difference-between-primary-secondary-amp-enhanced-reco-31405>. Accessed 25-09-2018.

Petrobras (2017). Investment opportunities in shallow water fields in brazil. Accessed 28-06-2018.

- PetroWiki (2015). Ekofisk field. Accessed 07-09-2018.
- PowerTechnology (2018). Belridge solar thermal power plant, california. Accessed 19-05-2018.
- Principle Power (2016). Principle power's windfloat prototype celebrates its 5-year anniversary and the final stage of technology demonstration. <http://principlepowerinc.com/en/news-press/press-archive/2016/06/02/principle-powers-windfloat-prototype-celebrates-its-5-year-anniversary> Accessed 15-10-2018.
- Pérez-Collazo, C., Greaves, D., and Iglesias, G. (2015). A review of combined wave and offshore wind energy. *Renewable and Sustainable Energy Reviews*, 42:141 – 153.
- Ragheb, M. (2014). Optimal rotor tip speed. <http://mragheb.com/NPRE%20475\%20Wind%20Power%20Systems/Optimal%20Rotor%20Tip%20Speed%20Ratio.pdf>. Accessed 11-01-2019.
- Reichelstein, S. and Rohlfing-Bastian, A. (2015). Levelized product cost: Concept and decision relevance. *The Accounting Review*, 90(4):1653–1682.
- Reuters (2017). Shell sells stake in dutch wind farm to switzerland's partners group. Accessed 10-05-2018.
- RIVM (2018). Greenhouse gas emissions in the netherlands 1990-2015. : National inventory report 2017. Technical report, Netherlands National Institute for Public Health and the Environment.
- Rodriguez, D. (2018). Brazil enhanced oil recovery success tied to petrobras divestments. Accessed 27-06-2018.
- Rystad Energy (2018). Rystad energy ranks. Accessed 27-06-2018.
- S. Kempenaar, A., Diepeveen, N., and Jarquin, A. (2011). Microdot: Design of a 10kw prototype of the delft offshore turbine.
- Sandler, J., Fowler, G., Cheng, K., and Kavscek, A. R. (2014). Solar-generated steam for oil recovery: Reservoir simulation, economic analysis, and life cycle assessment. *Energy Conversion and Management*, 77:721 – 732.
- Schlumberger (2018). Oil glossary - brownfields. Accessed 06-06-2018.
- Shah, A., Fishwick, R., Wood, J., Leeke, G., Rigby, S., and Greaves, M. (2010). A review of novel techniques for heavy oil and bitumen extraction and upgrading. *Energy and Environmental Science*, 3(6):700–714.
- Shao, H. (2009). Use risk-based method to develop a foundation for quantitatively assessing the contribution of maintenance activities in offshore petroleum oil and gas industry. Master's thesis, UIS, Norway.

- Slätte, J., Sandberg, J., Flach, T., Dekker, G., and Sixtensson, C. (2014). Wind-powered subsea water injection pumping: Technical and economic feasibility. *Offshore Technology Conference*.
- Stangeland, G. (2017). Kværner og aker solutions skal oppgradere njord for fem milliarder kroner. Accessed 07-06-2018.
- Stehly, T. J., Heimiller, D. M., and Scott, G. N. (2017). 2016 cost of wind energy review. Technical report, NREL.
- Stoutenberg, E. (2012). *Intergrating Wind and Wave in California*. Phd thesis, Stanford University.
- Taber, J., Martin, F., and Seright, R. (1997). Eor screening criteria revisited part 1 : Introduction to screening criteria and enhanced recovery field projects. *Society of Petroleum Engineers*, 12.
- Udy, J., Hansen, B., Maddux, S., Petersen, D., Heilner, S., Stevens, K., Lignell, D., and Hedengren, J. (2017). Review of field development optimization of water-flooding, eor, and well placement focusing on history matching and optimization algorithms. *Processes*.
- Vaughan, A. (2018). Bp aims to invest more in renewables and clean energy. Accessed 10-05-2018.
- Vryhof (2015). Vryhof manual the guide to anchoring. Technical report, Vryhof Anchors B.V.
- Wei, H., Uhlen, K., Hadiya, M., Chen, Z., Shi, G., and del Rio, E. (2013). Case study of integrating an offshore wind farm with offshore oil and gas platforms and with an onshore electrical grid. *Journal of Renewable Energy*, 2013(2):10.
- Wiggelinkhuizen, E., Verbruggen, T., Braam, H., and J. Xiang, L. R., and Watson, S. (2008). Assessment of condition monitoring techniques for offshore wind farms. *Journal of Solar Energy Engineering*, 130.
- Wintershall (2015). Wintershall tildeler undervannskontrakt for maria-feltet. Accessed 14-06-2018.
- Zhang, H., Xia, X., and Zhang, J. (2012). Optimal sizing and operation of pumping systems to achieve energy efficiency and load shifting. *Electric Power Systems Research*, 86:41 – 50.
- Zhong, M. and Bazilian, M. (2018). Contours of the energy transition: investments by international oil and gas companies in renewable energy. *The Electricity Journal*, 31.